Improving the GPS Data Processing Algorithm for Precise Static Relative Positioning

by

Chalermchon Satirapod

B.Eng., Chulalongkorn University, Bangkok, Thailand, 1994

M.Eng., Chulalongkorn University, Bangkok, Thailand, 1997

A thesis submitted to The University of New South Wales
in partial fulfilment of the requirements for the degree of
Doctor of Philosophy

School of Surveying and Spatial Information Systems

The University of New South Wales

Sydney NSW 2052, Australia

January, 2002

ABSTRACT

Since its introduction in the early 1980's, the Global Positioning System (GPS) has become an important tool for high-precision surveying and geodetic applications. Carrier phase measurements are the key to achieving high accuracy positioning results. This research addresses one of the most challenging aspects in the GPS data processing algorithm, especially for precise GPS static positioning, namely the definition of a realistic stochastic model. Major contributions of this research are:

(a) A comparison of the two data quality indicators, which are widely used to assist in the definition of the stochastic model for GPS observations, has been carried out. Based on the results obtained from a series of tests, both the satellite elevation angle and the signal-to-noise ratio information do not always reflect the reality.

(b) A simplified MINQUE procedure for the estimation of the variance-covariance components of GPS observations has been proposed. The proposed procedure has been shown to produce similar results to those from the standard MINQUE procedure. However, the computational load and time are significantly reduced, and in addition the effect of a changing number of satellites on the computations is effectively dealt with.

(c) An iterative stochastic modelling procedure has been developed in which all error features in the GPS observations are taken into account. Experimental results show that by applying the proposed procedure, both the certainty and the accuracy of the positioning results are improved. In addition, the quality of ambiguity resolution can be more realistically evaluated.

(d) A segmented stochastic modelling procedure has been developed to effectively deal with long observation period data sets, and to reduce the computational load. This procedure will also take into account the temporal correlations in the GPS measurements. Test results obtained from both simulated and real data sets indicate that the proposed procedure can improve the accuracy of the positioning results to the millimetre level.

(e) A novel approach to GPS analysis based on a combination of the wavelet decomposition technique and the simplified MINQUE procedure has been proposed. With this new approach, the certainty of ambiguity resolution and the accuracy of the positioning results are improved.

ACKNOWLEDGMENTS

TABLE OF CONTENTS

3. A SIMPLIFIED MINQUE PROCEDURE FOR THE ESTIMATION OF VARIANCE-COVARIANCE COMPONENTS OF GPS OBSERVABLES

4. AN ITERATIVE STOCHASTIC MODELLING PROCEDURE

Figures

LIST OF TABLES

Tables

1.1   Global Positioning System (GPS) Background

The NAVSTAR GPS (NAVigation System with Time and Ranging Global Positioning System) is a satellite-based radio-positioning and time-transfer system. The GPS system has been developed by the U.S. Department of Defense since 1973. The motivation was to develop an all-weather, 24-hour, global positioning system to support the positioning requirements for the U.S. military and its allies (see Parkinson, 1994, for a background to the development of the GPS system). Thus, there are limited opportunities for managing the system for civilian users. The system can provide precise three-dimensional position, velocity and time in a common reference system, anywhere on or near the surface of the earth, on a continuous basis (e.g. Lamons, 1990; Parkinson, 1979; Wooden, 1985).

Due to the recently developed technology and procedures to overcome some of the constraints to GPS performance, there is a growing community that utilises the GPS for a variety of civilian applications. A huge and rapid-growing quantity of literature relating to GPS, and the geodetic use of GPS, can be found in monographs and text books (e.g. Clarke, 1994; Hofmann-Wellenhof et al., 1997; Kaplan, 1996; King et al., 1987; Leick, 1995; Parkinson & Spilker 1996; Rizos, 1997; Seeber, 1993; Teunissen & Kleusberg, 1998; Wells et al., 1987).

The GPS system consists of three segments, namely the Space Segment, the Control Segment and the User Segment. A brief description of these components is given.

The Space Segment comprises the constellation of spacecraft and the transmitted signals. The system nominally consists of 21 satellites and three active spares, deployed

in six orbital planes of about 20,200 km altitude above the earth's surface with an orbital inclination of 55 degrees, and with four satellites in each orbital plane. The satellite orbits are almost circular and the orbital period is approximately 11 hours and 58 minutes (or half a sidereal day). The arrangement of satellites within the full constellation is such that at least four satellites are simultaneously visible above the horizon anywhere on the earth, or near the earth's surface, 24 hours a day.

Each GPS satellite continuously transmits a unique navigational signal centred on two L-band frequencies of the electromagnetic spectrum, L1 at 1575.42 MHz and L2 at 1227.60 MHz, which are generated by an onboard atomic oscillators (Spilker, 1978). The satellite signals basically consist of three main components, the two L-band carrier waves, the navigation message and the ranging codes (Figure 1.1).
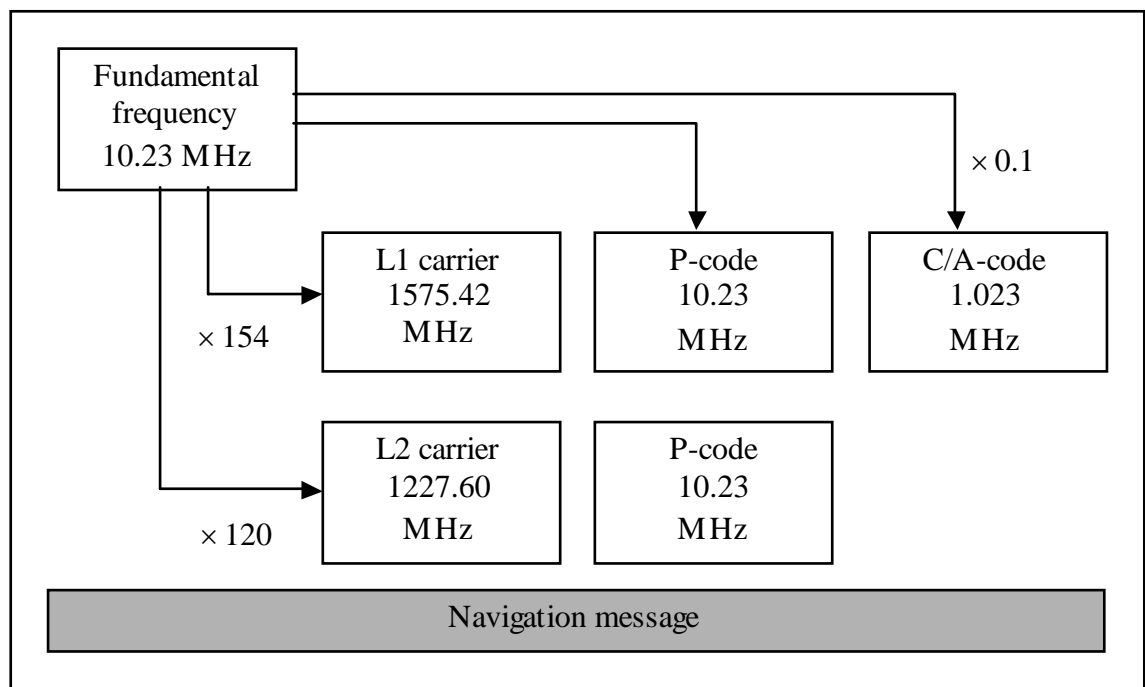
Figure 1.1 GPS satellite signal components (Rizos, 1997)

The navigation message contains information such as satellite orbits (ephemerides), satellite clock corrections, and satellite status. The ranging codes and the navigation message are modulated on the carrier waves. The Coarse/Acquisition code (C/A-code) is modulated only on the L1 carrier, while the Precise code (P-code) is modulated on both the L1 and L2 carriers. The P-code has higher measurement resolution and is

therefore more precise than the C/A-code. In general, there are two levels of service in Single Point Positioning (SPP) mode. The first one is called "Standard Positioning Service" (SPS) and the second one is called "Precise Positioning Service" (PPS) (Seeber, 1993). The SPS is intended for civilian use and uses only the C/A-code. Unlike the SPS, the PPS accesses both codes (C/A-code and P-code), but is generally reserved for U.S. military use. Due to the surprisingly good Standard Positioning Service accuracy for SPP, the policy of Selective Availability (SA) was endorsed on 25 March 1990 in order to artificially widen the gap between the SPS and PPS (Georgiadou & Doucet, 1990). As a result of SA, the accuracy of SPS had been degraded to about 100 metres in the horizontal components and 156 metres in the vertical component (at the 95% confidence level). Fortunately, the former U.S. President Bill Clinton made a decision to turn off SA on 1 May 2000. According to Rizos & Satirapod (2001) the accuracy of SPS without SA is significantly improved to about 6.8 metres in the horizontal components and approximately 12.3 metres in the vertical component (at the 95% confidence level).

The Control Segment consists of the ground facilities carrying out the task of satellite tracking, orbit computations, telemetry and supervision necessary for the daily control of the Space Segment. There are five ground facility stations located around the world. The U.S. Department of Defense owns and operates all stations. The Master Control Station is located in Colorado Springs, and the processing of the tracking data in order to generate the satellite orbits and satellite clock corrections is performed at this station. The other three stations, located at Ascension Island, Diego Garcia and Kwajalein, are upload stations, and hence the uplink of data to the GPS satellites is carried out at these stations.

In short, the most important task of the Control Segment is to compute the satellite orbits (or ephemerides) and to determine the satellite clock biases. The ephemerides are expressed in the ECEF (earth-centred, earth-fixed) World Geodetic System 1984, known as WGS84. The WGS84 is maintained by the U.S. National Imagery and Mapping Agency (NIMA, 1997). The characteristic of each GPS satellite clock is monitored against GPS Time, as maintained by a set of atomic clocks at the Master Control Station.

The User Segment is the entire spectrum of applications equipment and computational techniques that are available to the users. GPS user equipment and computational techniques have undergone a huge program of development both in the military and civilian spheres. The military research and development programs have concentrated on accomplishing a high degree of miniaturisation, modularisation and reliability, while the civilian user equipment manufacturers have, in addition, sought to bring down costs and to develop features that enhance the capabilities of the positioning system. Initially, GPS was designed for navigation applications. However, with the appropriate receiver technology and data reduction procedures it is possible to achieve a high relative accuracy, at the centimetre level, in the so-called precise GPS positioning mode.

1.2   Fundamental GPS Measurements

There are two types of fundamental measurements used in position determination, namely *pseudorange measurements* and *carrier phase measurements*.

1.2.1   Pseudorange Measurement

A pseudorange is the measurement of the time shift between the code generated by a receiver and the code transmitted from a GPS satellite. If the receiver and satellite clocks are synchronised with the GPS time, the travel time of the satellite signal will be equal to the difference between the transmission time and the reception time. The range between the satellite and the receiver can be calculated by multiplying the travel time with the speed of light. In practice, the satellite and receiver clocks are not synchronised with the GPS Time. Moreover, there are some errors or biases when the satellite signal propagates from the satellite to the receiver. The pseudorange measurement can be expressed as (Erickson, 1992; Langley, 1993):

$$R = \rho + \Delta r + d_{ion} + d_{trop} + c \bullet (\Delta \delta_i - \Delta \delta^j) + dm_R + \varepsilon_R \qquad (1.1)$$

where

R is the measured pseudorange

ρ is true range or geometric range

Δr is the orbit bias

d_{ion} is the ionospheric bias

d_{trop} is the tropospheric bias

$\Delta\delta_i$ is the receiver clock error

$\Delta\delta^j$ is the satellite clock error

dm_R is the multipath error on the pseudorange

ε_R is the pseudorange measurement noise

c   is the speed of light

The true range or geometric range can be represented by:

$$\rho = \sqrt{(X^j - x_i)^2 + (Y^j - y_i)^2 + (Z^j - z_i)^2} \tag{1.2}$$

where

X^j, Y^j and Z^j are the satellite coordinates

x_i, y_i and z_i are the receiver coordinates

The pseudorange measurement is generally used in applications where the accuracy is not high (few metre level), as is typical for single-epoch navigation applications.

1.2.2   Carrier Phase Measurement

Carrier phase is the measurement of the phase *difference* between the carrier signal generated by a receiver's internal oscillator and the carrier signal transmitted from a satellite. In order to convert the carrier phase to a range between the satellite and the receiver, the number of full cycles and the fractional cycle must be known. However, at the first time that the satellite signal is locked on to by the receiver, only the fractional phase can be measured. If the satellite signal is assumed to be continuously locked, the

receiver will keep track of *changes* to the phase. Therefore, the initial phase cycle is still *ambiguous* by a number of full cycles. To use the carrier phase as a measurement for positioning, this initially unknown number of cycles (or the phase ambiguity) must be resolved or accounted for in some way (Counselman & Shapiro, 1979; Wells et al., 1987). The basic equation for the carrier phase measurement is:

$$\phi = \rho + \Delta r \ - d_{ion} + d_{trop} + c \bullet (\Delta\delta_i - \Delta\delta^j) + dm_\phi + \varepsilon_\phi + \lambda \bullet N \qquad\qquad (1.3)$$

where

ϕ is the carrier phase measurement in unit of metres

dm_ϕ is the multipath error on the carrier phase

ε_ϕ is the carrier phase measurement noise

λ is the wavelength of the carrier phase

N is the integer carrier phase ambiguity

The definition of the remaining terms (ρ, Δr, d_{ion}, d_{trop}, c, $\Delta\delta_I$ and $\Delta\delta^j$) is the same as in Equation (1.1). It can be seen that there are similarities between Equations (1.1) and (1.3). However, the major differences are the presence of the integer carrier phase ambiguity term ($\lambda \bullet N$), and the reversal of sign for the ionospheric bias term (d_{ion}). In addition, the level of the carrier phase measurement noise (at the mm level) is much smaller than the level of the pseudorange measurement noise (typically at the metre level). Therefore, the carrier phase is extensively used as the primary measurement in precise (cm level) GPS positioning applications.

With regard to Equations (1.1) and (1.3), both the pseudorange and carrier phase measurements are contaminated by many errors or biases that affect the positioning accuracy. A brief discussion of the error sources in GPS positioning is given in the next section.

1.3   Error Sources in GPS Positioning

In general, the errors or biases associated with GPS positioning can be conveniently classified into three classes, satellite-dependent biases, receiver-dependent biases and signal propagation biases.

1.3.1   Satellite-Dependent Biases

The satellite-dependent biases include satellite orbit bias and satellite clock bias. The satellite orbit information is generated from the tracking data collected by the monitor stations. The Master Control Station processes the tracking data, and the other three monitor stations (Section 1.1) upload the navigation message to every satellite so that the user can navigate. In reality, it is impossible to perfectly model the satellite orbit. Hence, the satellite orbit information calculated by the master control station would be different from the true position of a satellite, and this discrepancy is the *satellite orbit bias*.

Since 1 January 1994 the International GPS Service (IGS) has carried out routine operations necessary to generate precise GPS orbits. An international network of nearly 200 continuously operating GPS stations is used to track the satellites. The satellite orbit bias can therefore be mitigated by using the precise orbits obtained from the IGS in place of the broadcast orbits. Table 1.1 is an example of the estimated quality of the IGS products (IGS, 2001).

Table 1.1 Estimated quality of the IGS products (GPS broadcast values included for comparison)

Orbit Type	Accuracy	Latency
Broadcast Orbits	~260 cm	Real time
Predicted Orbits	~25 cm	Real time
Rapid Orbits	~5 cm	After 17 hours
Final Orbits	<5 cm	After 13 days

The *satellite clock bias* is the difference between the satellite clock time and the true GPS time. Despite the fact that high quality cesium, or rubidium, atomic clocks are used in the GPS satellites, the satellite clock bias is still unavoidable. In the case of SPP, a typical way to account for the satellite clock bias is to use the broadcast clock error model defined by the polynomial coefficients. This broadcast clock error model is generated by the Control Segment and transmitted as part of the navigation message. Even with the best efforts in monitoring the behaviour of each satellite clock, their behaviour can not be precisely modelled (JPS, 1998). As a result, there is a residual error after applying the broadcast clock error model. In the case of relative positioning, the satellite clock bias can be eliminated by differencing the measurements obtained from two receivers (Section 1.4.2), since the satellite clock bias is the same for two receivers observing the same satellite, at the same time.

1.3.2   Receiver-Dependent Biases

The receiver-dependent biases include the receiver clock bias, inter-channel bias, antenna phase centre variation and receiver noise. Similar to the satellite clock bias, the receiver clock bias is an offset between the receiver clock time and the true GPS time. Due to the fact that GPS receivers are usually equipped with relatively inexpensive clocks, the receiver clock bias is very large compared to the satellite clock bias. In the case of SPP, a typical way to account for the receiver clock bias is to treat the receiver clock bias as an additional unknown parameter in the estimation procedure. In the case of relative positioning, the receiver clock bias can be eliminated by differencing the measurements made at the same receiver (Section 1.4.2), since the receiver clock bias would be the same for all measurements made at the same receiver, at the same time.

The inter-channel bias arises because a multi-channel receiver takes the measurements to different satellites, using different hardware tracking channels. However, multiplexing and sequential single-channel receivers were generally free of the inter-channel bias (Seeber, 1993). With modern GPS receiver technology, the inter-channel bias can be calibrated at the sub-millimetre level or better (Hofmann-Wellenhof et al., 1997).

In GPS positioning, the measurements taken by the GPS receiver are usually referred to the distance between the electrical centre of the satellite's transmitter and the electrical centre of the receiving antenna. The discrepancy between the electrical centre and the physical centre is called *phase centre variation*. The electrical centre tends to vary with the direction and strength of the incoming signal. In addition, the phase centre variations for the L1 and L2 carriers may have different properties (Leick, 1995; Rothacher et al., 1990). For most antenna types, the antenna phase variation is usually calibrated by the manufacturers. In addition, the antenna phase centre models for various antennas can be obtained from the National Geodetic Survey (NGS, 2001). These models can subsequently be applied to mitigate the antenna phase variations. It is however recommended that for high-precision applications care has to be taken not to mix antenna types, or to swap antennas between sites and receivers during a survey (Rizos, 1997).

The magnitude of the receiver noise is dependent on parameters such as signal-to-noise ratio and tracking bandwidth. According to a rule of thumb for classical receivers the measurement noise is approximately 1% of the signal wavelength. Therefore, the level of noise in pseudorange measurements is about 3 metres (~300 m wavelength) for C/A-code and 0.3 metres (~30 m wavelength) for P-code, while the level of noise in carrier phase is a few millimetres for L1 (~ 19 cm wavelength) and L2 (~ 24 cm wavelength). Modern receiver technology tends to bring the internal phase noise below 1 millimetre, and to reduce the C/A-code noise to the decimetre level (JPS, 1998; Qiu, 1993; Seeber, 1993).

1.3.3   Signal Propagation Biases

When the satellite signals travel from the satellite to the receiver, the signals may be contaminated by the atmospheric delay and multipath error. The atmosphere causing the delay in GPS signals consists of two main layers, *ionosphere* and *troposphere*. Thus, the atmospheric signal propagation biases include the ionospheric and tropospheric delays.

The ionosphere is the band of the atmosphere from around 50km to 1000km above the earth's surface (Hofmann-Wellenhof et al., 1997; Seeber, 1993). Because of free electrons in this layer, the GPS signals do not travel at the speed of light as they transit this region (Parkinson, 1996). As a result, the measured pseudoranges become too long (Equation (1.1)), and on the other hand the measured phase ranges become too short (Equation (1.3)). The ionospheric delay is a function of the Total Electron Content (TEC) along the signal path, and the frequency of the propagated signal (Lin, 1997). The TEC depends on time, season and geographic location, with major influencing factors being the solar activity and the geomagnetic field (Klobuchar, 1991; Leick, 1995; Seeber 1993). In extreme cases, the ionospheric delay can range from about 50m for signals at the zenith to as much as 150m for measurements made at the receiver's horizon.

The simple broadcast ionosphere model transmitted within the navigation message is generally used to reduce this effect for single-frequency users (see Klobuchar, 1987, for details of the model). With regard to the dual-frequency user, the ionospheric delay is frequency-dependent and the ionosphere-free combination (L3) can be formed in order to eliminate this delay (Hofmann-Wellenhof et al., 1997; Leick, 1995; Rizos, 1997). However, the disadvantage of using the ionosphere-free combination is that it increases the noise to approximately three times that of the original L1 signal. Due to the fact that the ionospheric delays are highly correlated over distances of approximately 10km to 20km, the impact of ionospheric delays can be largely reduced by forming a difference between the measurements made by two receivers on short baselines.

The troposphere is the band of the atmosphere from the earth's surface to about 50km (Spilker, 1996a). The tropospheric delay is a function of elevation and altitude of the receiver, and is dependent on many factors such as the atmospheric pressure, temperature and water vapour content. The tropospheric delay ranges from approximately 2m for signals at the zenith to about 20m for signals at an elevation angle of 10 degrees (Brunner & Welsch, 1993). Unlike the ionospheric delay, the tropospheric delay is not frequency-dependent. It cannot therefore be eliminated through linear combinations of L1 and L2 observations.

Several 'standard' troposphere models can be used to estimate the tropospheric delay (e.g. Saastamoinen model, Hopfield model, Black model, etc.). The signal refraction due to the troposphere is separated into two components, the dry component and the wet component. Due to the high variation in the wet component, it is difficult to predict or model this component. As a result, the standard models can account for about 90% of the total delay. Similar to the ionospheric delay, the tropospheric delay can be largely eliminated by forming a difference between the measurements made by two receivers on short baselines. For high-precision static applications, the residual tropospheric delays in the measurements may be treated as additional unknown parameters in the baseline estimation procedure (e.g. Dodson et al. 1996; Roberts & Rizos, 2001; Rothacher et al., 1990; Tralli & Lichten, 1990).

Multipath is the error caused by nearby reflecting surfaces. GPS signals can arrive at the receiver via multiple paths due to reflections from nearby objects such as trees, buildings, the ground, water surfaces, vehicles, etc. Theoretically, the maximum pseudorange multipath error is approximately one chip length of the code (that is, about 300m for the C/A-code, and approximately 30m for the P-code), while the maximum carrier phase multipath error is about a quarter of the wavelength (that is, about 5cm for the L1 carrier, and 6 cm for the L2 carrier) (Georgiadou & Kleusberg, 1989; Lachapelle, 1990; Wells et al., 1987). Since the multipath error depends on the receiver's environment, it cannot be reduced by using the data differencing technique. In the case of static positioning, averaging the computed results over a period of time will reduce the contribution of multipath errors. However, some options for reducing the effect of multipath have been suggested by Rizos (1997):

- Make a careful selection of antenna site in order to avoid reflective environments.
- Use a good quality antenna that is multipath-resistant.
- Use an antenna groundplane or choke-ring assembly.
- Use a receiver that can internally digitally filter out the effect of multipath signal disturbance.
- Do not observe low elevation satellites (signals are more susceptible to multipath).

1.4   GPS Positioning Methods

Based on the available measurements made on the GPS signals, the determination of the receiver's position can be conveniently classified into two techniques, *Absolute Positioning* and *Relative Positioning*.

1.4.1   Absolute Positioning

The absolute positioning technique, also known as *the single point positioning (SPP) technique*, permits one receiver to determine the 'absolute' coordinates (X, Y, Z) of a point with respect to a coordinate system such as WGS84. This technique can be further divided into two classes depending on the measurements used, namely *pseudorange-based point positioning* and *carrier phase-based point positioning*.

1.4.1.1   Pseudorange-based point positioning

For navigation applications, pseudoranges are widely used as the fundamental measurements. The basic principle of the absolute positioning technique is to use simple resection by distances to determine the receiver's coordinates. If the satellite coordinates are assumed to be known (as they can be computed from the navigation message), the receiver's coordinates can be computed from the resection using the measured pseudoranges. If it is assumed that there is no error in the pseudoranges, the absolute coordinates are considered as the only unknown parameters. Therefore, at least three pseudoranges need to be measured in order to solve for three coordinate components. As a matter of fact, there are many errors in measuring pseudoranges, especially in measuring the travel time. This is due to the use of an inexpensive clock in the receiver. Hence, the receiver clock bias is considered as an additional parameter, and a minimum of four pseudoranges are then needed to solve for four unknown parameters, three coordinates and the receiver clock offset. As mentioned in Section 1.1, the accuracy of SPP is currently about 7 metres in the horizontal component and 12 metres in the vertical component (at the 95% confidence level) for civilian users.

1.4.1.2   Carrier phase-based point positioning

With the availability of precise GPS orbits and satellite clock corrections, the precise point positioning technique has recently been proposed by the Jet Propulsion Laboratory (JPL) (Zumberge et al., 1997; Zumberge, 1999). Since this technique mainly uses the carrier phase measurements from both frequencies (L1 and L2), with the post-mission information in the estimation procedure, it can produce high-precision positioning results. Nevertheless, this technique requires a reasonably large amount of data, implying that *instantaneous* solutions are not possible, and this technique can only be used when the receiver is stationary. As stated in Zumberge et al. (1997), the users could expect daily repeatabilities of a few mm in the horizontal components, and about a cm in the vertical component, for data from a static site occupied by a geodetic-quality receiver.

1.4.2   Relative Positioning

The relative positioning technique, sometimes also called the *differential positioning technique*, requires the use of two receivers, one as a *reference station* and the other one as a *user station*, in order to determine the coordinates of the user with respect to the reference station. This technique is very effective if the measurements are simultaneously made at both receivers. Many biases (e.g. satellite orbit bias, satellite clock bias, ionospheric and tropospheric delays) can be largely reduced by forming the difference between the measurements made at both stations. For this reason, the relative positioning technique is extensively used for applications that require high accuracy (cm level). However, the effectiveness of the relative positioning technique is largely dependent on the distance between the two receivers. If the distance between the receivers becomes large, the residual errors will become larger. Consequently, the positioning results become degraded. This is a limitation of the relative positioning technique. Similar to the case of absolute positioning technique, the relative positioning technique can be divided into two classes depending on the measurements used, *pseudorange-based differential GPS* and *carrier phase-based differential GPS*.

1.4.2.1 Pseudorange-based differential GPS

As previously discussed, both the accuracy and integrity of GPS solutions can be improved by the Differential GPS (DGPS) technique. The estimation of the range error for each satellite is carried out at the reference station and the estimated range errors (or corrections) are broadcast to the users by an appropriate communication link. With differential corrections, the SPS navigation accuracy can be improved down to the 1m level, provided the correction data age is less than 10 seconds, and the user is within 50km of the reference station (Parkinson & Enge, 1996). Note that the accuracy of DGPS will be degraded if the distance from the reference station or the age of the correction data increases. If only one reference station is employed, this DGPS technique is generally referred to as *Local Area Differential GPS* (LADGPS). LADGPS is suitable for operations over a small area.

If a network of reference stations is employed to generate a correction for each satellite, the correction data is valid over a much larger area, for example, regional or continental extent. This concept is referred to as *Wide Area Differential GPS* (WADGPS). The accuracy of WADGPS is independent of the geographical location of the user relative to the nearest reference station, though the validity of the correction still decreases with an increase in the age of the correction data (Kee, 1996).

The *Wide Area Augmentation System* (WAAS) is a space-based augmentation system, which employs geostationary satellites to transmit to users the DGPS corrections for each satellite, together with additional GPS-like ranging signals and an integrity message, hence improving availability and reliability (Enge & Van Dierendonck, 1996). The processing of WAAS data begins at the master stations. Subsequently, all data are packed into WAAS messages and sent to Navigation Earth Stations (NES). The NES uplinks the WAAS messages to the geostationary satellites, which broadcast the messages, together with the GPS-like ranging signals, to WAAS-capable receivers.

In summary, the pseudorange-based DGPS techniques can achieve accuracies in the range 0.5m and 5m. However, for some applications with very stringent accuracy requirements, carrier phase-based GPS techniques have to be used.

1.4.2.2   Carrier phase-based differential GPS

The basis of high precision relative positioning is the use of carrier phase measurements (Section 1.3.2). Data differencing techniques are one of the keys to achieving high precision positioning results as they can significantly reduce a variety of errors or biases in the measurements and models. For example, by differencing the measurements made to the same satellite by two receivers, at the same time, the spatially correlated atmospheric delays and satellite-dependent biases are largely eliminated. This is referred to as *single-differencing between receivers*. Similarly, by differencing the measurements to two satellites made by the same receiver, at the same time, the receiver clock bias cancels. This is referred to as *single-differencing between satellites*. If the difference between the above single-differenced observations is formed, this procedure is called *double-differencing*, and the resultant double-differenced observable is the standard input for carrier phase-based processing. Another key to achieving high precision positioning results is to 'fix' the initial carrier phase ambiguities (Section 1.2.2) to their (theoretically) integer values. This procedure is commonly referred to as *Ambiguity Resolution*.

Carrier phase-based DGPS techniques can be further categorised as *static positioning* and *kinematic positioning*.

Static positioning implies that both receivers are stationary during the entire period of data collection. The length of the observation period is dependent on parameters such as the number of observed satellites, the satellite geometry, the distance between two receivers (i.e. baseline length), the receiver type and the accuracy requirement. Since the late 1980's, rapid static positioning modes have been introduced, by which the observation period can be significantly reduced, to only a few minutes or less, yet ensuring centimetre positioning accuracy over baseline lengths below 20km or so (Blewitt et al., 1989; Euler et al., 1990; Frei & Beulter, 1990). It should be noted that the baseline lengths may be varied from 10km to 20km depending on the similarity of biases between two stations. However, the 20km baseline length is typically used as the standard practice in relative positioning.

Kinematic positioning implies that either (or both) the reference and user receivers are in motion. The concept of kinematic positioning was first introduced by Remondi (1985). With recent receiver technology and data processing procedures, it is possible to obtain the positioning results in 'real time'. This technique is referred to as *real-time kinematic (RTK) positioning*. In the standard RTK positioning, the reference receiver transmits the data via a radio link to the user receiver, where the data obtained from both receivers are processed in the field to obtain immediate positioning results (Langley, 1998; Talbot 1993).

In short, the carrier phase-based DGPS can deliver accuracies in the range sub-cm to sub-dm, depending on the baseline length and other factors (Hatch, 1986; Goad, 1987).

1.5   Previous Research on Stochastic Modelling for GPS Positioning

Since its introduction to civilian users in the early 1980's, GPS has been playing an increasingly important role in high-precision surveying and geodetic applications. As with traditional geodetic network adjustment, data processing for precise GPS static positioning is invariably performed using the least-squares method. To employ the least-squares method, both the functional and stochastic models of the GPS measurements need to be defined. The *functional model*, also called the mathematical model, describes the mathematical relationships between the GPS measurements and the unknown parameters, such as the ambiguity terms and the baseline components. The *stochastic model* describes the statistical properties of the measurements, which are mainly defined by an appropriate covariance matrix. In order to ensure high accuracy, both the functional model and the stochastic model must be correctly defined. If the function model is adequate, the residuals obtained from the least-squares solution should be randomly distributed (e.g. Tiberius & Kenselaar, 2000; Satirapod et al., 2001a). Over the last two decades the functional models for GPS carrier phases have been investigated in considerable detail, and are well documented in the literature (e.g. in such texts as Hofmann-Wellenhof et al., 1997; Leick, 1995; Rizos, 1997; Seeber, 1993; Teunissen & Kleusberg, 1998). Since GPS measurements are contaminated by many errors such as the atmospheric biases, the receiver clock bias, the satellite clock

bias, and so on, it is impossible to model all systematic errors in the functional model without some understanding, or prior knowledge, of the physical phenomena which underpin these errors. Although the data differencing techniques are extensively used for constructing the functional model, some unmodelled (or 'residual') biases still remain in the GPS observables following such differencing. As a result, the residuals obtained from a least-squares static solution would normally represent both unmodelled systematic errors and noise. In principle it is possible to further improve the accuracy and certainty of GPS results through an enhancement of the stochastic model. Many researchers have emphasised the importance of the stochastic model, especially for high-accuracy applications (e.g. Barnes et al., 1998; Han, 1997; Satirapod, 1999; Wang, 1999). Furthermore, an accurate stochastic model is the key to obtaining a better covariance matrix of the parameters (e.g. El-Rabbany, 1994; Han & Rizos, 1995). The challenge is to find a way to realistically incorporate information on such unmodelled biases into the stochastic model. Therefore, accurate stochastic modelling for the GPS measurements is still both a controversial topic and a difficult task to implement in practice (Cross et al., 1994; Wang et al., 2001).

In practice, the stochastic models of GPS measurements are mainly based on considerable *simplifications*. In current stochastic models it is usually assumed that all carrier phase or pseudorange measurements have the same variance, and that they are statistically independent. The time-invariant covariance matrix of the double-differenced (DD) measurements is then constructed using the error propagation law. In this covariance matrix the correlation coefficient between any two DD measurements is +0.5. This so-called 'mathematical correlation' is introduced by the double-differencing process. To set up a simple stochastic model for DD measurements, it is further assumed that temporal correlations are absent. However, these assumptions are not realistic. As commented in, for example, Goad (1987), Gourevitch (1996), and Langley (1997), the GPS measurement errors are dominated by the systematic errors caused by the orbit, atmospheric and multipath effects, which are quite different for each satellite. Therefore the measurements obtained from different satellites cannot have the same accuracy. On the other hand, the raw measurements are spatially correlated due to similar observing conditions for these measurements (it is this fact that makes the double-differencing procedure effective in mitigating measurement biases). Moreover,

the time correlations may exist in the measurements because the residual systematic errors change slowly over time.

To model the *heteroscedasticity*, many researchers have recently used two types of external information, the signal-to-noise ratio (SNR) and the satellite elevation angle, to calculate the accuracy of the one-way GPS measurements (Satirapod & Wang, 2000). This is done by employing an approximate formula using the satellite elevation angle (e.g. Euler & Goad, 1991; Gerdan, 1995; Han, 1997; Jin, 1996; Rizos et al., 1997), or SNRs (e.g. Barnes et al., 1998; Brunner et al., 1999; Gianniou & Groten, 1996; Hartinger & Brunner, 1998; Langley, 1997; Talbot, 1988) as input. Given the variances of the one-way measurements, the covariance matrix for the DD measurements is constructed using the error propagation law. Furthermore, a rigorous statistical method, known as MINQUE (*Minimum Norm Quadratic Unbiased Estimation,* Rao, 1971), can be employed to estimate the stochastic model for the GPS DD measurements (Wang et al., 1998a).

The impact of *temporal correlations* on GPS baseline determination has been investigated in, for example, Vanicek et al. (1985), El-Rabbany (1994), Han & Rizos (1995) and Howind et al. (1999). In these studies all one-way measurements are considered to be independent and having the same variance and same temporal correlation. It has been noted that the GPS measurement may have a heteroscedastic, space- and time-correlated error structure (Satirapod et al., 2000; Wang, 1998). Any mis-specifications in the stochastic model may lead to inaccurate results (e.g. Cannon & Lachapelle, 1995; Chen, 1994; Hatch & Euler, 1994; Kim & Langley, 2001; Sauer et al., 1992; Teunissen, 1998; Wang, 1998). Hence, stochastic modelling is still a challenging research topic for precise GPS positioning.

1.6   Outline of Thesis

This thesis consists of eight chapters and one appendix.

Chapter 1 – Introduction. This chapter gives some background on GPS, fundamental GPS measurements, error sources in GPS positioning, GPS positioning methods, an outline of previous studies on stochastic modelling procedures, the outline of the thesis and the contributions of this research work.

Chapter 2 – Quality Indicators for GPS Carrier Phase Observations. This chapter reviews and compares two quality indicators commonly used in constructing the stochastic model for GPS carrier phase observations, namely *satellite elevation angle* and *signal-to-noise ratio*. Single-differenced residuals are used to analyse the validity of the quality indicators, on a satellite-by-satellite basis. The results from a series of tests are presented and discussed.

Chapter 3 – A Simplified MINQUE Procedure for Estimation of Variance-Covariance Components of GPS Observables. Here, the standard MINQUE method used for estimation of variance-covariance components of GPS observations is first reviewed. A simplified MINQUE procedure is then proposed in which the computational load and time are significantly reduced. Experimental results are presented and discussed.

Chapter 4 – An Iterative Stochastic Modelling Procedure. This chapter first briefly describes the mathematical equations used in static GPS baseline data processing, and then discusses the estimation of variance-covariance components and the treatment of temporal correlations. Then, an iterative stochastic modelling procedure is proposed in which the heteroscedastic, space- and time-correlated error structure of GPS measurements are taken into account. Details of the iterative stochastic modelling method are presented. Applications of the proposed method are also demonstrated using a variety of GPS data sets.

Chapter 5 – A Segmented Stochastic Modelling Procedure. This chapter presents a new stochastic modelling procedure, known as *a segmented stochastic modelling procedure*. The new procedure is proposed to deal with long observation period data sets, and in order to reduce the computational load. The effectiveness of the new procedure is tested using both real data and simulated data sets for short to medium length baselines.

Chapter 6 – GPS Analysis with the Aid of Wavelets. This chapter presents the theory of wavelet decomposition and its application to GPS data processing. A new method based on a *wavelet decomposition technique* and a robust estimation of the variance-covariance matrix is proposed to improve the certainty of ambiguity resolution and the accuracy of estimated baseline components. A discussion of the experimental results and analysis is presented.

Chapter 7 – An Implementation of Segmented Stochastic Modelling Procedure and Some Considerations. This chapter describes detailed procedures for implementing the segmented stochastic modelling procedure in software. A discussion on some considerations in utilising this procedure is also given.

Chapter 8 – Conclusions and Recommendations. This chapter summarises findings, draws conclusions, and makes recommendations for future investigations.

Appendix A gives some details of the accompanying matrices described in Chapter 3.

1.7   Contributions of this Research

In this study, the challenging stochastic modelling issues outlined in Section 1.5, suitable for use in the GPS relative static positioning mode, have been investigated. The contributions of this research can be summarised as follows:

- The two commonly used quality indicators for constructing a stochastic model of GPS carrier phase observations have been compared and validated using the single-differenced residuals. It is recommended that a more rigorous method for constructing a realistic stochastic model needs to be developed.

- A simplified MINQUE procedure has been developed, in which the computational time and the memory requirements of the simplified procedure are much less than those in the case of the rigorous MIQNUE procedure. In addition, the effect of a change in the number of satellites on the computation is effectively dealt with.

- An iterative stochastic modelling procedure has been proposed, in which all of the error features of GPS measurements are taken into account. With the new stochastic procedure developed here, the certainty of the estimated positioning results is improved and the quality of ambiguity resolution can be more realistically evaluated.

- A segmented stochastic modelling procedure has been proposed to deal with long observation period data sets, and in order to reduce computational load. The proposed procedure can be implemented with any long observation period data sets with no significant increase in processing time.

- A new method based on a wavelet decomposition technique, and a robust estimation of the variance-covariance matrix, has been proposed to improve the certainty of ambiguity resolution and the accuracy of estimated baseline components.

QUALITY INDICATORS FOR GPS CARRIER PHASE OBSERVATIONS

2.1 Introduction

To achieve accurate GPS positioning results, a realistic stochastic model for GPS carrier phase observations has to be specified. However, the correct stochastic model for the GPS measurements is a difficult task to define. In order to develop such a stochastic model, the quality characteristics of GPS carrier phase measurements made by a receiver must be well understood. Recently there has been interest in using two types of information, signal-to-noise ratio (SNR) and satellite elevation angle, as quality indicators for GPS observations. It is important that a better understanding of these quality indicators is gained in order that they may be used appropriately.

In this chapter the quality indicators for GPS carrier phase observations are described, as well as the methodology used to assess them. A series of tests are described and some conclusions are drawn based on the analysis of the GPS data.

2.2 Quality Indicators

2.2.1 Signal-to-Noise-Ratio (SNR)

The SNR is the ratio of a GPS signal power and the noise level that contaminates a GPS observation. The SNR value can be affected by several factors (i.e. antenna gain pattern, receiver type, space loss, multipath etc.). Most SNR models were designed to mitigate the multipath effect, as multipath is a major concern in GPS positioning, especially in urban areas. For instance, the relationship between multipath and SNR, or Carrier-to-

Noise density ratio (C/No), has been investigated by many authors (e.g. Brunner et al., 1999; Comp & Axelrad, 1996; Lau & Mok, 1999; Sleewaegen, 1997; Talbot, 1988). More recently SNR has been introduced as a quality indicator for GPS observations and used to construct the stochastic model. In Spilker (1996b), the relationship between the RMS phase noise (σ_ϕ) and the SNR_L is given as:

$$\sigma_\phi^2 \cong \frac{1}{SNR_L} \tag{2.1}$$

Langley (1997) claims that C/No is the key parameter in analysing GPS receiver performance and that it directly impacts the precision of GPS observations. Hartinger & Brunner (1998) also state that the SNR information indicates the quality of the individual GPS phase values, and the performance of their SIGMA-ε model is based on the following assumption:

$$\sigma_1^2 = S_1 \bullet 10^{\frac{-C/No}{10}} \tag{2.2}$$

where the subscript indicates the L1 signal and S_1 consists of the carrier loop noise bandwidth and a conversion term from cycle^2 to mm^2. From an analysis of many data sets the value of S_1 was estimated to be about 1.6×10^4. Lau & Mok (1999) described the performance of the Signal-to-noise ratio Weighted Ambiguity function Technique (SWAT), where they emphasised the close relationship between the SNR cofactor matrix and the elevation angle (as SNR is almost directly proportional to the elevation angle in 'not-too-noisy environments').

2.2.2   Satellite Elevation Angle

Satellite elevation angle information is often used to construct a simplified stochastic model. Jin (1996) stated that the precision of GPS code observations at comparatively low satellite elevation angles decreases with decreasing elevation, and that the relationship can be modelled quite well by an exponential function:

$$y = a_0 + a_1 \bullet \exp\{-x/x_0\} \tag{2.3}$$

where y is the RMS error, a_0, a_1 and x_0 are coefficients dependent on the receiver brand and the observation type, and x is the satellite elevation angle in degrees. This relationship has been used by many researchers in various GPS data processing schemes (e.g. Euler & Goad, 1991; Gerdan, 1995; Han, 1997; Jin, 1996; Rizos et al., 1997).

2.2.3   Single-Differenced Model

The single-differenced model (between receivers) is chosen as the method of analysis for this study since the validity of the two above-mentioned quality indicators can then be assessed on a satellite-by-satellite basis. For short baselines, the single-differenced model can be expressed as (Hofmann-Wellenhof et al., 1998; Leick, 1995; Rizos, 1997; Teunissen & Kleusberg, 1998):

$$\Phi^j_{AB}(t) = \frac{1}{\lambda} Z^j_{AB}(t) + N^j_{AB} - f\delta_{AB}(t) + e^j_{AB}(t) \tag{2.4}$$

where the superscript j denotes the satellite, the subscripts A and B indicate the two receivers, the index t denotes the epoch at which the data were collected, Φ is the measured carrier phase, λ is the wavelength of carrier phase, Z is the distance to the satellite, N is the single-differenced integer ambiguity, f denotes the frequency of the satellite signal and δ is the relative receiver clock bias. The term e represents all remaining errors, including random noises of receivers and systematic errors, such as unmodelled multipath effects, atmospheric delay, etc.

In order to compute the single-differenced residuals, the double-differenced ambiguities have to be resolved to their integer values. This procedure is performed by the standard GPS ambiguity resolution algorithm. Then these double-differenced ambiguity values are introduced as known parameters into the single-differenced model by subtracting them from Equation (2.4). Therefore, the unknown parameters remaining in the GPS observation model are the relative receiver clock bias, the integer ambiguity of the base

satellite and the errors. From Equation (2.4), the single-differenced model can be written as (assuming that there are four satellites (j, k, l, m) available at epoch t and satellite k is chosen as the base satellite):

$$\Phi_{AB}^{j}(t) = \frac{1}{\lambda} Z_{AB}^{j}(t) + N_{AB}^{k} - f\delta_{AB}(t) + e_{AB}^{j}(t)$$

$$\Phi_{AB}^{k}(t) = \frac{1}{\lambda} Z_{AB}^{k}(t) + N_{AB}^{k} - f\delta_{AB}(t) + e_{AB}^{k}(t)$$

$$\Phi_{AB}^{l}(t) = \frac{1}{\lambda} Z_{AB}^{l}(t) + N_{AB}^{k} - f\delta_{AB}(t) + e_{AB}^{l}(t)$$ (2.5)

$$\Phi_{AB}^{m}(t) = \frac{1}{\lambda} Z_{AB}^{m}(t) + N_{AB}^{k} - f\delta_{AB}(t) + e_{AB}^{m}(t)$$

A 'reverse engineering' process is applied to this model in order to produce a reliable estimate of true errors for each satellite. Barnes et al. (1998) and Satirapod (1999) demonstrated the use of this process with the double-differenced model. If the epoch-by-epoch solution is computed, the relative receiver clock bias and the single-differenced integer ambiguity of the base satellite can be eliminated from Equation (2.5) by subtracting the mean value from the residuals. Hence, the single-differenced error (e) for each satellite can be derived and used for a comparison with the two quality indicators.

2.3   Test Results and Analysis

The following series of tests were carried out using data collected on the Mather Pillar a top the Geography and Surveying building, at The University of New South Wales campus, Sydney, Australia. The photograph in Figure 2.1 shows the GPS receiver set up on the Mather Pillar station. This station is a GPS permanent station, and has a good observing environment. There are no tall buildings in the vicinity of the site, and phase diffraction effects are largely eliminated. Test 1 was carried out to investigate the characteristics of SNR. The relationship between SNR and satellite elevation angle information is discussed in the context of Test 2, while a comparative analysis of the two quality indicators is presented in the discussion of Test 3.

Figure 2.1   The Mather Pillar station at GAS, UNSW.

2.3.1   Test 1 – SNR Characteristics

A zero baseline test was used for this investigation since it was necessary to eliminate any uncertainty due to the use of different antenna types. Three types of receivers were used in the experiment: the Canadian Marconi Corporation Allstar (CMC), the Leica CRS1000 and the NovAtel Millennium. In order to investigate the SNR characteristics for the same receiver type, data were collected by connecting each pair of receivers (of the same type) to the same antenna. Data were collected in static mode for three hours, for each pair of receivers, at a 5-second data rate. C/No values obtained for each receiver type were recorded and converted into the RINEX file using their propriety software. C/No values are presented for the case of two satellites only as the results for the other satellites displayed similar trends. These results are presented in Figures 2.2 to 2.4, which show the time series of the differenced C/No values obtained for the CMC, CRS1000 and NovAtel receivers, respectively.
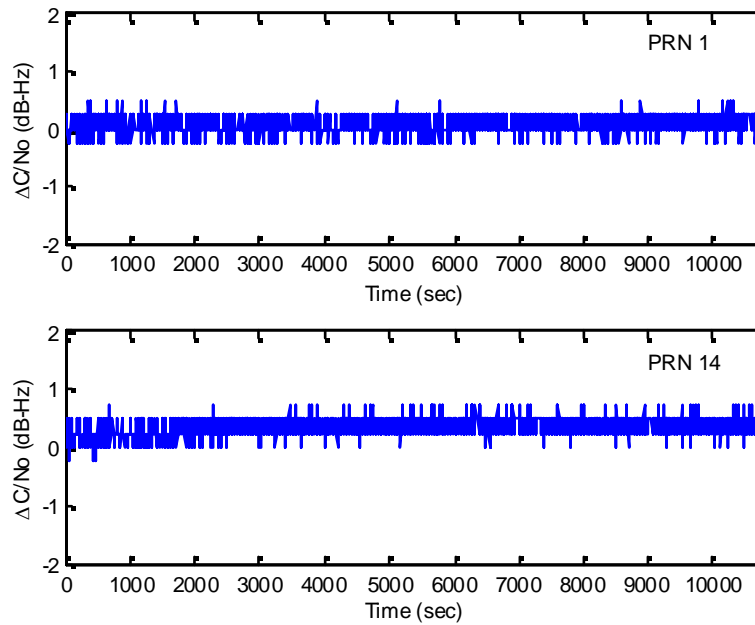
Figure 2.2   ΔC/No values between two CMC receivers for PRN 1 (top), ΔC/No values between two CMC receivers for PRN 14 (bottom).
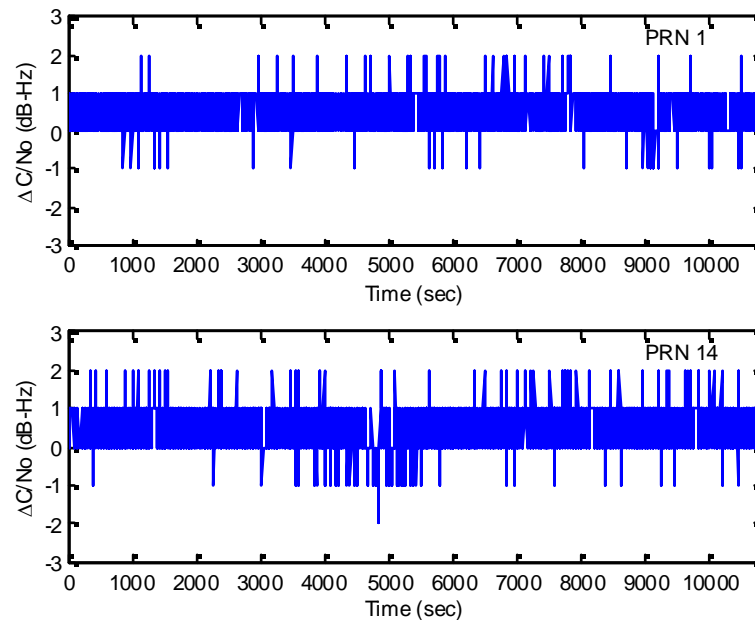
Figure 2.3   ΔC/No values between two CRS1000 receivers for PRN1 (top), ΔC/No values between two CRS1000 receivers for PRN 14 (bottom).
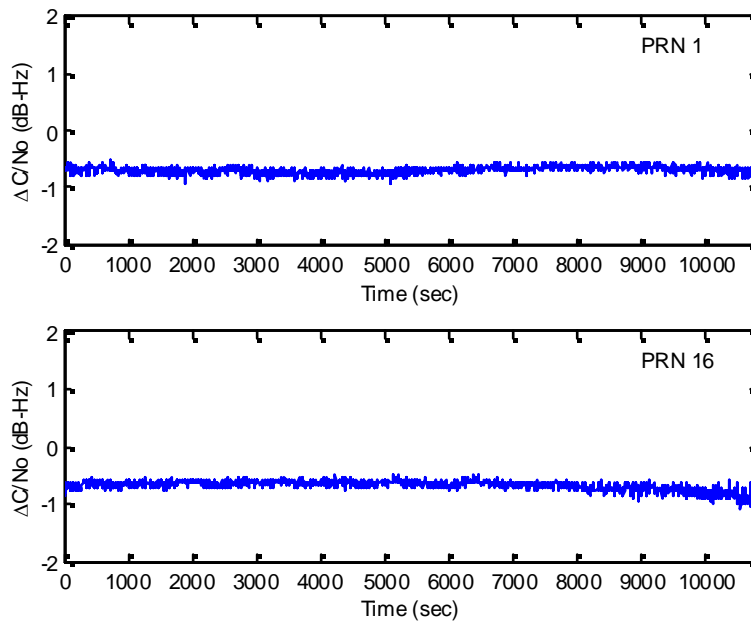
Figure 2.4   ΔC/No values between two NovAtel receivers for PRN 1 (top), ΔC/No
             values between two NovAtel receivers for PRN 16 (bottom).

With reference to Figures 2.2 to 2.4, it is evident that, although the same receiver type
was used, there is a non-zero difference in C/No values, indicating that receivers of the
same type nevertheless have different outputs of C/No. It can also be seen from Figures
2.2 to 2.4 that the different receiver types output the different resolution in the C/No
values.

Next, an investigation of the SNR characteristics of the different receiver types was
carried out by connecting three types of receivers to the same antenna. The same cable
type was also used in this session. Data were collected in static mode for 3 hours at a
1Hz rate. However, the data were sampled every 5 seconds and the results obtained
from three satellites are presented for comparison. The C/No values obtained from the
three receivers for three satellites are plotted in Figure 2.5.
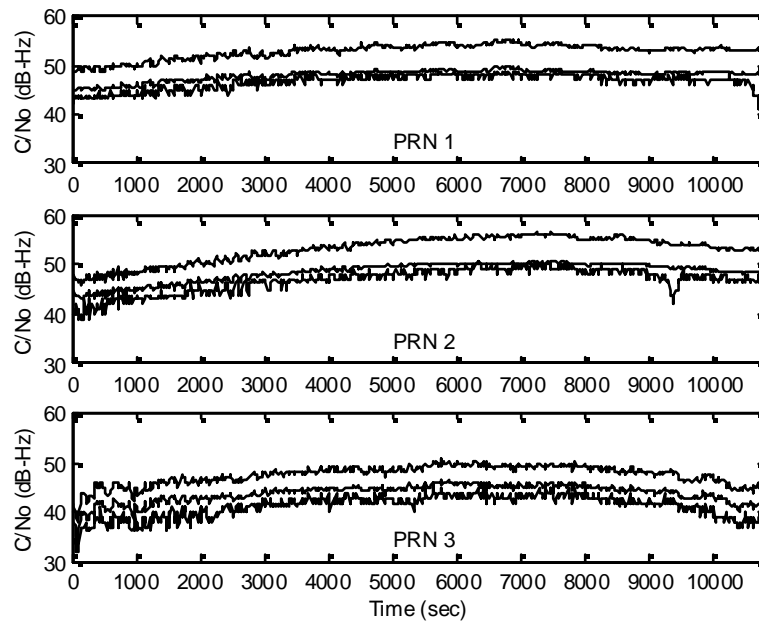
Figure 2.5   C/No values obtained from three receivers (CMC, CRS1000 and NovAtel)
for PRN 1 (top), PRN 2 (middle), and PRN 3 (bottom).

Figure 2.5 shows the time series of the C/No values obtained from the three different
receivers (CMC, CRS1000 and NovAtel). Top, middle and bottom lines represent the
C/No values obtained from CMC, NovAtel and CRS1000 receivers respectively. The
results indicate that there is a difference in C/No values when different receiver types
were used. However, the C/No values show a similar trend for all receivers. This trend
may be caused by an antenna gain pattern effect. Sudden drops in the C/No values are
clearly noticeable for satellites PRN1 and PRN2 at different times for the case of the
CRS1000 receiver. Similar phenomena were also noted by Hartinger & Brunner (1998).
In order to further investigate this phenomenon it was decided to collect some zero
baseline data with the CRS1000 receivers at a 1Hz rate for 2 hours. Selected results for
PRNs 3, 29 and 31 are presented in Figure 2.6.
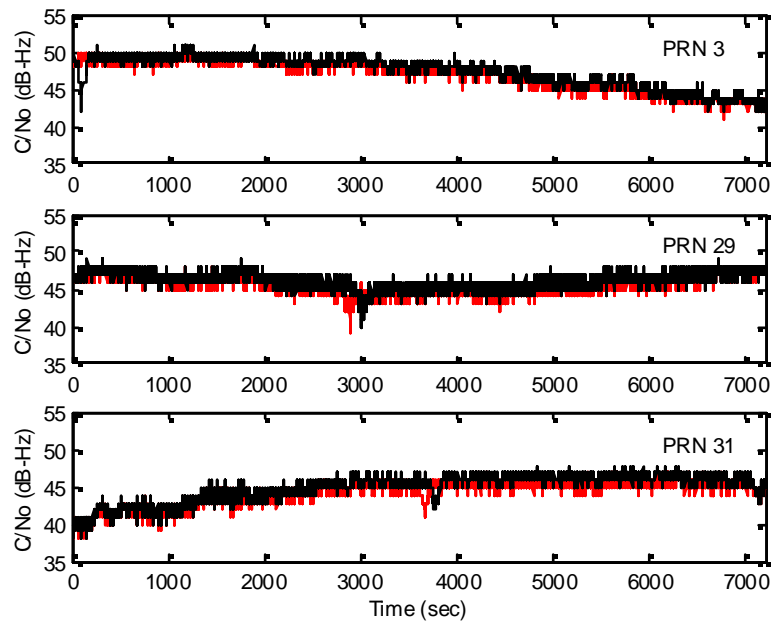
Figure 2.6   C/No values obtained from the CRS1000 receivers for PRN 1 (top),
PRN 29 (middle), and PRN 31 (bottom) (Two subplots for each of the three plots
indicate the C/No values for each of the two CRS1000 receivers).

From Figure 2.6 it appears that these sudden drops are caused by a firmware problem in
an individual receiver, as they occur at different times, even in the case of the same
receiver types. Figures 2.7(a) and 2.7(b) show the C/No values against the true errors
obtained for the single-differenced data for the case of PRN 3. It can be seen that this
sudden drop does not reflect any change in the true errors (note different C/No values
for the two receivers in Figure 2.7(a)).
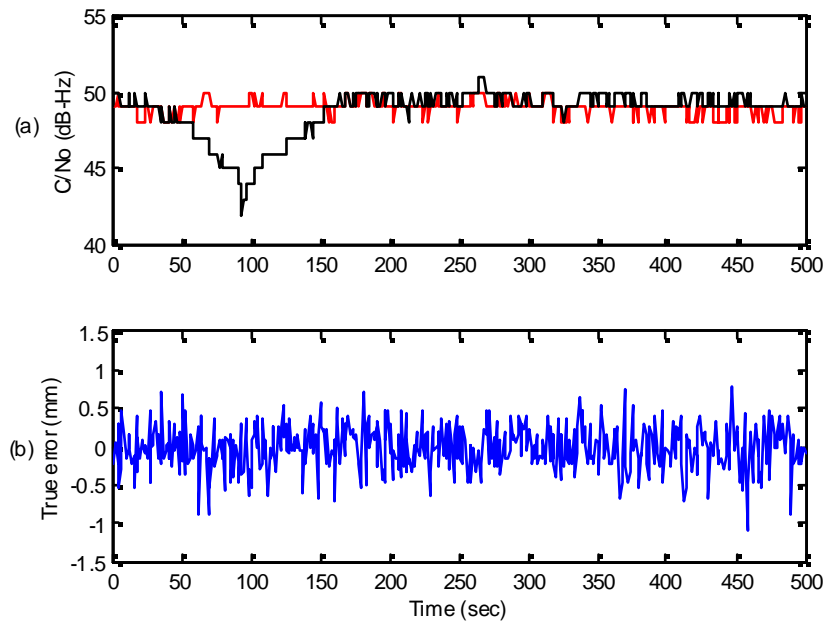
Figure 2.7   Time series of the C/No values and true errors obtained from the CRS1000 receivers, (a) C/No values for PRN 3, (b) true errors for PRN 3.

2.3.2   Test 2 – SNR & Satellite Elevation

The relationship between SNR and satellite elevation angle data has been mentioned by several authors (e.g. Hartinger & Brunner, 1998; Lau & Mok, 1999), and it is often assumed that SNR is directly proportional to satellite elevation. However, it is necessary to examine this relationship more closely before advocating the use of these quality indicators. An experiment was therefore carried out in which several zero baseline data sets were collected in static mode for over 16 hours. The data set obtained from the CMC receiver was selected for the analysis. From this data set, four satellites were selected to study this relationship. The TEQC software was then used to check for the presence of any multipath disturbance, and it was found that there was no significant multipath effect on the satellite signals (Estey & Meertens, 1999). The time series of the C/No values and the satellite elevation angle values are plotted in Figures 2.8 and 2.9. Figure 2.8 shows that the relationship between SNR and satellite elevation is indeed as established by previous studies. However, Figure 2.9 shows that this relationship may not be true for high satellite elevation angles.
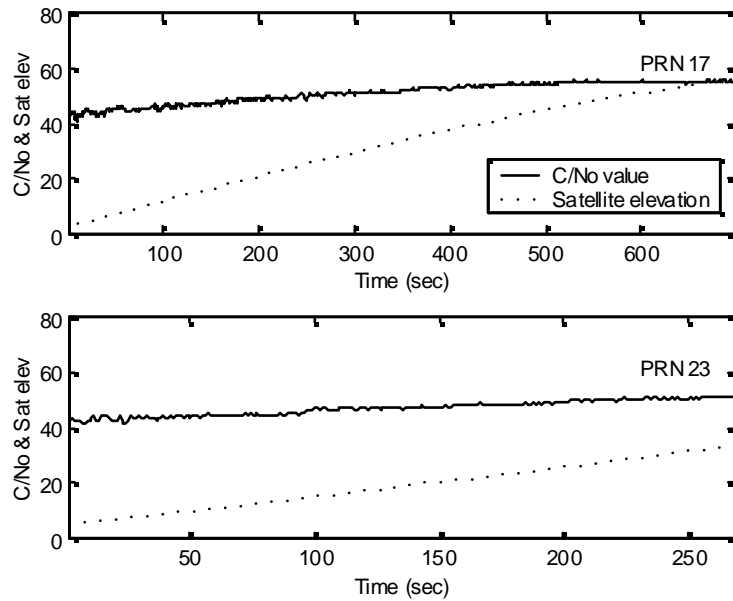
Figure 2.8   Time series of the C/No values and satellite elevation data obtained from

the CMC receiver, (a) C/No values and satellite elevation data for PRN 17,

(b) C/No values and satellite elevation data for PRN 23.

It is also evident that the C/No value for low satellite elevation angles in some instances is higher than the C/No value for high satellite elevation angles (see the two peaks in Figure 2.9(a) and 2.9(b)). It can be seen that the C/No value is not directly proportional to the satellite elevation angle. The C/No value can be affected by many factors, not just an elevation angle. Thus, the two standard quality indicators do not always follow the same trend. Further comparative analysis of these two quality indicators therefore was necessary, and the results are presented in the following section.
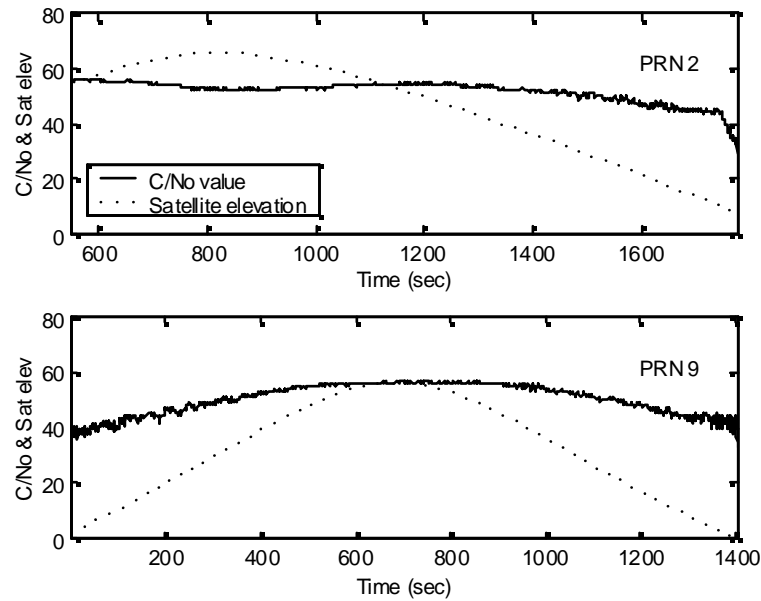
Figure 2.9   Time series of the C/No values and satellite elevation data obtained from

the CMC receiver, (a) C/No values and satellite elevation data for PRN 2,

(b) C/No values and satellite elevation data for PRN 9.

2.3.3   Test 3 – The Comparative Analysis

The aim of this experiment was to compare the two measurement quality indicators with the estimated true errors through the use of single-differenced observables. Single-differenced observables were chosen as both the SNR and satellite elevation angle data are 'one-way observations'. Therefore, the validity of these quality indicators should be assessed on a satellite-by-satellite basis. A previous investigation on the relationship between phase noise and satellite elevation angles based on double-differenced residuals was reported in Cannon (1998). For this experiment, zero baseline data were collected for a variety of receiver types. Each of the data sets was divided into 0.5-hour sessions, and then processed using the single-differenced model described in section 2.2.3. The standard deviation of the estimated true errors and the mean values of C/No and satellite elevation are the quantities of interest in this analysis. The results from the different receivers show similar trends, and selected results from the experiments are plotted in Figures 2.10 and 2.11.

Figures 2.10 and 2.11 show the relationship between the two measurement quality indicators and the standard deviation of the estimated true errors for the CRS1000 and NovAtel receiver observations, respectively. For each of the Figures the top chart shows the relationship between the mean C/No values and the standard deviation of the estimated true errors, while the bottom chart shows the relationship between the mean satellite elevation values and the standard deviation of the estimated true errors.

From these Figures it can be seen that the C/No values reflect a more realistic trend than those based on satellite elevation data, which show a larger discrepancy. However, it can also be seen that in some cases both of these indicators fail to reflect reality, as they do not match the standard deviation of the estimated true errors. Moreover, SNR and satellite elevation data are dependent upon the receiver type, therefore in order to use these data appropriately further investigations will be necessary.
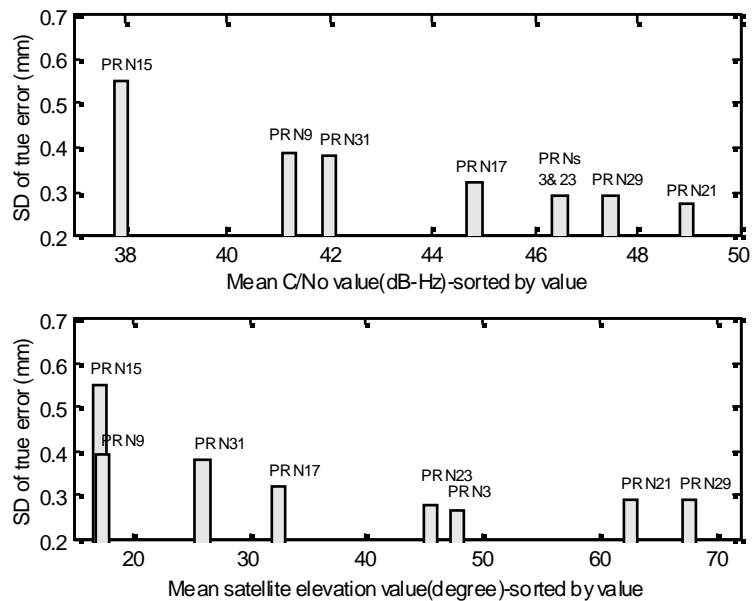
Figure 2.10 Comparison of the two quality indicators for CRS1000 receivers (zero baseline), mean C/No values and standard deviation of the estimated true errors (top), mean satellite elevation values and standard deviation of the estimated true errors (bottom).
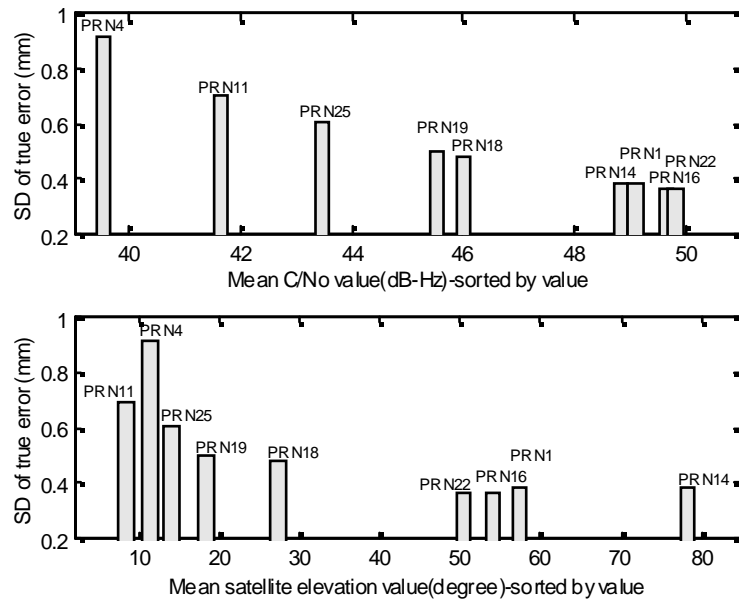
Figure 2.11 Comparison of the two quality indicators for NovAtel receivers (zero baseline), mean C/No values and standard deviation of the estimated true errors (top), mean satellite elevation values and standard deviation of the estimated true errors (bottom).

2.4   Concluding Remarks

It is necessary that one develops a better understanding of quality indicators for GPS measurements. In this chapter, the standard quality indicators for GPS measurements, SNR and satellite elevation angle information, have been reviewed and investigated. A comparative analysis was carried out in an attempt to verify the previously established relations between these indicators. Based on the results obtained, the following comments can be made:

- There is a variation in the C/No values for the same receiver types, as well as for different receiver types.
- It was found that sudden drops do occur in the C/No values for a specific receiver type, even in the case of high elevation satellites. These sudden drops may result in a misrepresentation of the quality of the measurements if the C/No values are used as a quality indicator.

- The two standard measurement quality indicators do not always follow the same trend.

- C/No values reflect a more realistic trend than satellite elevation angle data.

- In general, both C/No values and satellite elevation angle information can be used as quality indicators, but they do not always reflect reality. More rigorous quality indicators therefore need to be developed.

In rapid static and kinematic GPS positioning, the issue of the appropriateness of the stochastic model becomes critical. A realistic stochastic model will lead to an improvement in the accuracy and certainty of GPS results. In such 'high productivity' GPS techniques many researchers have extensively used the two standard quality indicators to refine the stochastic model, hoping to obtain a more accurate solution. However, from these admittedly limited investigations, both quality indicators did not always reflect reality as far as data quality is concerned. This can be partially attributed to the fact that although the relationships defined by Equations (2.2) and (2.3) are empirically derived from extensive data sets, they are still largely dependent on the data originally used for their derivation. In Wang et al. (1998a), a rigorous statistical method known as MINQUE (Minimum Norm Quadratic Unbiased Estimation -- Rao, 1971) is used to construct a more realistic stochastic model. However, this method has the drawback of being computationally intensive. In order to reduce the computational load and computer memory requirements of the MINQUE procedure a simplification of the MINQUE procedure will be proposed in the next chapter.

Chapter 3
A SIMPLIFIED MINQUE PROCEDURE FOR THE ESTIMATION OF VARIANCE-COVARIANCE COMPONENTS OF GPS OBSERVABLES

3.1   Introduction

As pointed out in Chapter 2, two commonly used GPS measurement quality indicators, namely the Signal-to-Noise Ratio (SNR) and the satellite elevation angle, fail to reliably reflect the reality of data quality. In addition, the relationship between these quality indicators and the standard deviations of the GPS observations are largely dependent on the data used in for their derivation, and hence the statistical properties of the estimations are still ambiguous. It is therefore appropriate to investigate a rigorous method for constructing variance-covariance matrices of GPS observations.

Fortunately, in the case of static and rapid static GPS relative positioning, redundant observations are available, from which realistic variance-covariance matrices can be estimated using modern statistical methods. A comprehensive review of some methods for estimating the variance components can be found in Crocetto et al. (2000). The MINQUE procedure is one of those most commonly used, and was successfully applied by Wang et al. (1998a) to estimate the variance-covariance components of GPS observations. Moreover, the certainty of the resolved ambiguities and the relative efficiency of baseline estimation were shown to have been significantly improved through the use of the MINQUE approach. However, the computational burden of this technique was still a significant limitation, as was the requirement to have an equal number of variance-covariance components in the estimation step. In this Chapter, a simplified MINQUE procedure is proposed in which the computational load and time are significantly reduced.

In the following sections, the standard MINQUE method is first reviewed, the simplified procedure is then derived and discussed. Finally, experimental results are presented and discussed, followed by some concluding remarks.

3.2   MINQUE Procedure

Assume the following Gauss-Markov model with n measurements and t unknowns:

$$l = Ax + v \tag{3.1}$$

$$C = P^{-1} = \sum_{i=1}^{k} \theta_i T_i \tag{3.2}$$

where

l	is the $n \times 1$ vector of the measurements
v	is the $n \times 1$ vector of the residuals
A	is the $n \times t$ design matrix
x	is the $t \times 1$ vector of unknown parameters
$\theta_1, \theta_2, \dots, \theta_k$	are the variance-covariance components of the measurements to be estimated
k	is the number of variance-covariance components
$T_1, T_2, \dots, T_k$	are the so-called accompanying matrices (see Appendix for more details)
P	is the weight matrix of the observations
C	is the variance-covariance matrix of the observations

According to Rao (1970, 1971), a minimum norm quadratic unbiased estimation of the linear function of θ_i ($i = 1, 2, \dots, k$), i.e., $g_1\theta_1 + g_2\theta_2 + \dots + g_k\theta_k$, is the quadratic function $l^T M l$, if the matrix M is determined by solving the following matrix trace minimum problem:

$$Tr\{MCMC\} = \min \tag{3.3}$$

Subject to:

$$MA = 0, \tag{3.4}$$

$$Tr\{MT_i\} = g_i \tag{3.5}$$

where $Tr\{\ \}$ is the trace operator of a matrix. Based on Equations (3.3), (3.4) and (3.5), the variance-covariance components can be estimated as (Rao, 1979):

$$\hat{\theta} = (\hat{\theta}_1, \hat{\theta}_2, ..., \hat{\theta}_k)^T = S^{-1}q \tag{3.6}$$

where the matrix $S = \{s_{ij}\}$ with

$$s_{ij} = Tr\{RT_iRT_j\} \tag{3.7}$$

and the vector $q = \{q_i\}$ with

$$q_i = l^T RT_i Rl \tag{3.8}$$

and

$$R = PQ_vP \tag{3.9}$$

with $Q_v = [P^{-1} - A(A^TPA)^{-1}A^T]$ being the adjusted residuals cofactor matrix.

R can also be expressed by a partitioned matrix:

$$R = \begin{bmatrix} R_{11} & R_{12} & \cdots & R_{1m} \\ R_{21} & R_{22} & \cdots & R_{2m} \\ \cdots & \cdots & \cdots & \cdots \\ R_{m1} & R_{m2} & \cdots & R_{mm} \end{bmatrix} \tag{3.10}$$

where m is the number of the observation epoch in a session.

Since the relationships between v and l are:

$$v = -Q_v Pl \tag{3.11}$$

$$PQ_v Pv = -PQ_v Pl = Pv \tag{3.12}$$

then according to Equations (3.11) and (3.12), Equation (3.8) can be further written as:

$$q_i = l^T RT_i Rl = v^T RT_i Rv = v^T PT_i Pv \tag{3.13}$$

It is noted from Equations (3.6), (3.7), (3.8) and (3.9) that the estimated variance-covariance components depend on matrix C, which includes the variance-covariance components themselves. Therefore, an iterative process must be performed. Initially, an *a priori* value of θ_i is given by θ_i^0. With Equation (3.6), the initial estimate $\hat{\theta}^1$ is then obtained. In the $(j+1)^{th}$ iteration, using the previous estimate $\hat{\theta}^j$ as the *a priori* value, the new estimate is:

$$\hat{\theta}^{j+1} = S^{-1}(\hat{\theta}^j)q(\hat{\theta}^j) \quad (j = 0,1,2,\ldots) \tag{3.14}$$

which is called the iterated MINQUE. If $\hat{\theta}$ converges, the limiting value of $\hat{\theta}$ will satisfy the following equation:

$$S(\hat{\theta})\hat{\theta} = q(\hat{\theta}) \tag{3.15}$$

which can be further expressed as (Rao, 1979):

$$Tr\{R(\hat{\theta})T_i\} = l^T R(\hat{\theta})T_i R(\hat{\theta})l, \quad (i = 1,2,\ldots,k) \tag{3.16}$$

3.3   Simplified MINQUE Procedure

It is noted from the above procedure that when the MINQUE method is used in GPS data processing, the storage of the matrix R may require a huge computer memory. In addition, the computational procedure relating to this matrix is extensive.

A simplification of the MINQUE procedure can be obtained by assuming temporal correlations between epochs are absent. In this case the matrix R in Equation (3.10) is replaced by a diagonal matrix R^*. The matrix R^* has a block-diagonal structure and can be defined as:

$$R^* = \begin{bmatrix} R_{11} & 0 & \cdots & 0 \\ 0 & R_{22} & \cdots & 0 \\ \cdots & \cdots & \cdots & \cdots \\ 0 & 0 & \cdots & R_{mm} \end{bmatrix} \tag{3.17}$$

Assuming that the temporal correlations between epochs are absent, the weight matrix P and the accompanying matrices T_i have the following structures:

$$P = diag(P_k), \quad (k = 1,2,...,m) \tag{3.18}$$

$$T_i = diag(T_{ik}), \quad (k = 1,2,...,m) \tag{3.19}$$

where $P_u = P_v$ and $T_{iu} = T_{jv}$, with $u,v = 1, 2...., m$. Then, Equations (3.7) and (3.13) can be simplified as:

$$s_{ij} = Tr\{RT_iRT_j\} = \sum_{k=1}^{m} Tr(R_{kk}T_{ik}R_{kk}T_{jk}) \tag{3.20}$$

$$q_i = v^T PT_i Pv = \sum_{k=1}^{m} Tr(v_k^T P_k T_{ik} P_k v_k) \tag{3.21}$$

Table 3.1 illustrates the advantage of using the matrix R^* in the computation in terms of computer memory usage. It is assumed that 6 satellites are tracked during the observation period, and a 15-second sampling interval is used.

Table 3.1 Comparison of memory usage

Session length (minutes)	Memory usage (kilobytes)	
	MINQUE procedure	Simplified procedure
5	78.1	3.9
10	312.5	7.8
15	703.1	11.7
20	1250.0	15.6
25	1953.1	19.5
30	2812.5	23.4
35	3828.1	27.3
40	5000.0	31.3
45	6328.1	35.2
50	7812.5	39.1
55	9453.1	43.0
60	11250.0	46.9

Clearly, from Table 3.1, the memory usage is substantially reduced with the implementation of the simplified procedure. In addition, it is possible to easily handle the change in the number of satellites during an observation session since the computation of Equation (3.20) can be performed on an epoch-by-epoch basis. The reduction in the computation time will be discussed in a subsequent section.

Matlab-based GPS baseline processing software developed for the purpose, was used to process the data. The original Matlab code was downloaded from the Website given of Strang & Borre (1997). The Matlab code for the implementation of the MINQUE and simplified MINQUE procedures can be found in SNAP (2001).

3.4   Experimental Data

To demonstrate the efficiency of the simplified MINQUE procedure, four GPS static
baseline data sets have been analysed. The details of the four data sets are presented in
Table 3.2.

Table 3.2 Details of the four experimental data sets

Receivers	Ashtech Z-XII	NovAtel Millennium	Leica system 300	Trimble 4000SSE
Baseline length (m)	215	15	870	13,300
Survey date	June 7, 1999	July 10, 2000	Nov 18, 1996	Dec 18, 1996
Satellites	02,07,10,13,19,27	02,08,11,13,27	04,14,18,19,24,27,29	07,14,15,16,18,29
Elevation angle (°)	83,15,52,71,19,53	63,68,16,54,49	41,25,61,71,26,36,30	19,53,82,24,18,78
Data interval (sec)	15	15	15	15
Data span (min)	30	30	30	30

All data sets were first processed using the whole data span to estimate the true
ambiguity values, which were then used to verify the correctness of the resolved
ambiguities from subsequent data processing. Each data set was divided into three sets
of ten minutes. Three solutions for each data set were computed by applying the
standard stochastic modelling procedure (assuming that all observations have the same
weight and only mathematical correlation is taken into account in this stochastic model),
the rigorous MINQUE procedure and the simplified MINQUE procedure.

3.5   Analysis of Results

In the process of ambiguity resolution, the difference between the best and second best
ambiguity candidate set is crucial for the ambiguity discrimination step. The F-ratio is
commonly used as the ambiguity discrimination statistic, and hence the larger the F-
ratio value, the more reliable the ambiguity resolution. The critical value of the F-ratio
is normally chosen to be 2.0 (e.g. Euler & Landau, 1992). The ambiguity validation test
can also be based on the alternative statistic W-ratio (Wang et al., 1998b). Similarly,
the larger the W-ratio value, the more reliable the ambiguity resolution. The statistics,

F-ratio and W-ratio, obtained from the data processing are shown in Figures 3.1 and 3.2. In both Figures, each subplot represents a receiver type, and each group of columns (I, II, III) represents the solution obtained from an individual session. More details of the results obtained from the MINQUE procedure can be found in Wang et al. (1998a).
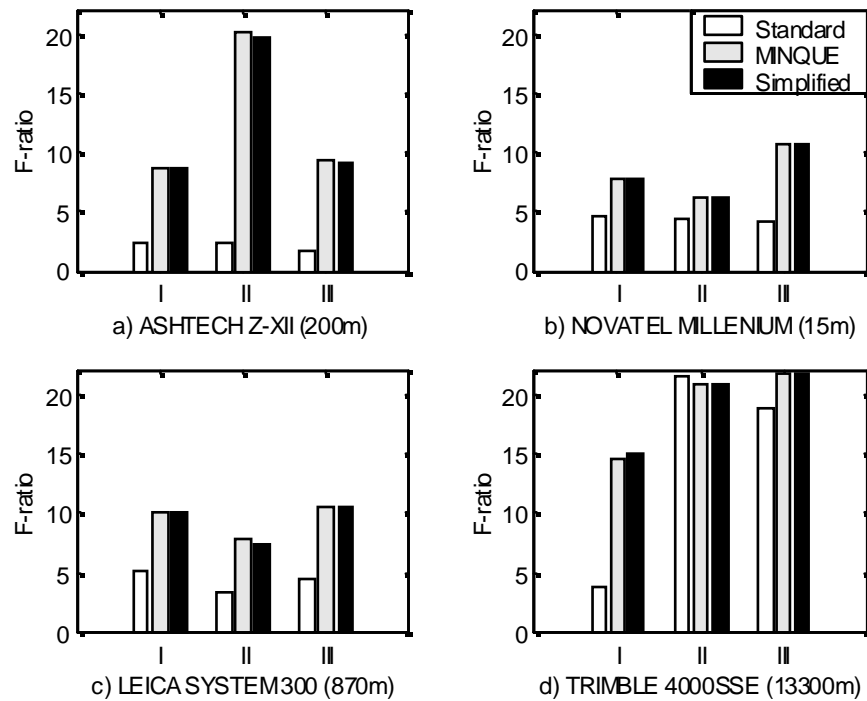
Figure 3.1 F-ratio value in the ambiguity validation tests.
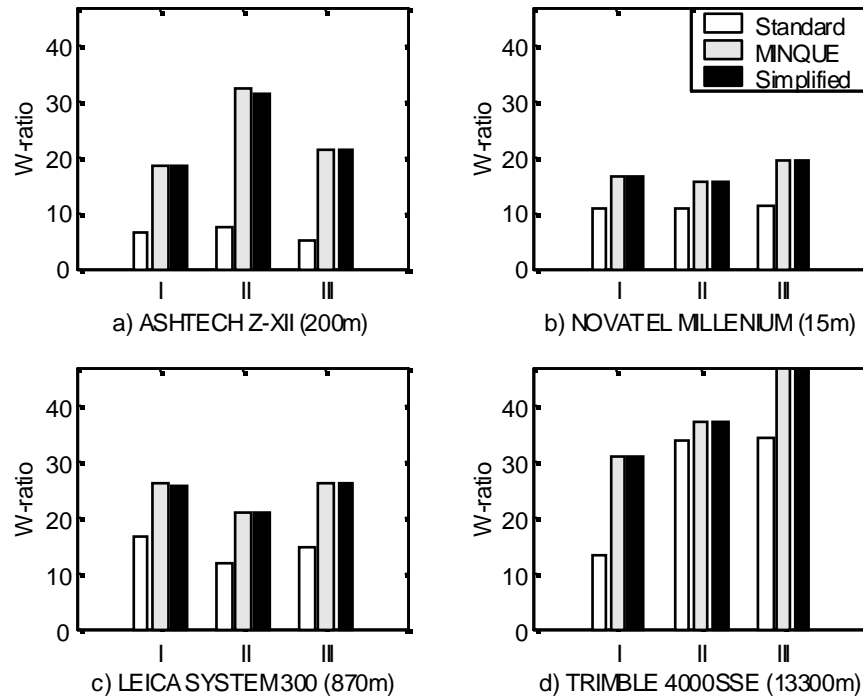
Figure 3.2 W-ratio value in the ambiguity validation tests.

From Figures 3.1 and 3.2, the F-ratio and W-ratio values obtained from the rigorous
MINQUE and the simplified MINQUE procedures are larger compared to those from
the standard procedure. Clearly, the certainty of the resolved ambiguity set is improved.
It can also be seen that both the rigorous and the simplified procedures yield very
similar numerical results. In the case of the simplified procedure, a larger number of
iterations is required but the computational time is significantly reduced. This is due to
there not being a need to compute the non-diagonal elements of the matrix R in
Equations (3.7) and (3.8). Table 3.3 summarises the performance of these procedures in
terms of computational time. It is also important to note that when the number of
observations is increased, the computational time is dramatically increased. This is more
so in the case of the rigorous MINQUE procedure.

Table 3.3 Comparison of computational time

Receiver and batch solution	Computational time (seconds)	
	MINQUE procedure	Simplified procedure
Ashtech (1) – 6 sats	511.37	28.00
Ashtech (2) – 6 sats	932.35	39.00
Ashtech (3) – 6 sats	887.59	36.46
NovAtel (1) –5 sats	152.30	5.13
NovAtel (2) –5 sats	194.27	6.34
NovAtel (3) –5 sats	114.65	3.91
Leica (1) – 7 sats	664.73	27.30
Leica (2) – 7 sats	1338.04	73.31
Leica (3) – 7 sats	514.18	18.75
Trimble (1) – 6 sats	871.47	39.28
Trimble (2) – 6 sats	518.16	21.03
Trimble (3) – 6 sats	346.08	10.08

*All solutions are computed using Matlab GPS baseline processing software running on
a PentiumII- 366MHz processor.*

It should be noted that in the case of the estimated baseline components and the
positional standard deviations, the results obtained from both the standard and
simplified MINQUE procedures are exactly the same.

3.6   Concluding Remarks

In this Chapter, the standard MINQUE procedure has been reviewed, and the simplified
procedure has been derived and discussed. The simplified procedure is shown to
produce results that are close in quality to those of the rigorous MINQUE procedure.
However, the computational time and the memory requirements of the simplified
procedure are much less than those in the case of the rigorous MINQUE procedure.
Furthermore, the effect of a change in the number of tracked satellites on the
computation is effectively dealt with.

The simplified procedure assumes that there are no large systematic errors in the
observations. If large systematic errors exist in the measurements (i.e. $E(v) \neq 0$),
temporal correlation will need to be taken into account before the simplified procedure

is applied. In addition, given a small number of observations, the variance-covariance components may not be reliably estimated and it may consequently lead to biased solutions. Hence, it is recommended that this procedure should be implemented only with a large-redundancy data set (at least 10 minutes of data for short baseline case) and if there is an absence of large systematic errors in the observations. In order to utilise this procedure efficiently the temporal correlation should be taken into account. Therefore, an appropriate method to cope with the temporal correlation is required. A new method for dealing with this problem is discussed in the next Chapter.

4.1   Introduction

The rigorous MINQUE procedure has been reviewed, and a simplification of the MINQUE procedure has been proposed in Chapter 3. In these procedures temporal correlations are assumed to be absent in the GPS measurements. However, temporal correlations may exist in the GPS measurements because the residual systematic errors change slowly over time. Previous studies have shown that GPS measurements have a heteroscedastic, space- and time-correlated error structure (Wang, 1998; Wang et al., 1998a), and hence any misspecification in the stochastic models will result in inaccurate positioning results. Recently, some effort has been made to include the temporal correlations in the stochastic model (e.g. El-Rabbany, 1994; Han & Rizos, 1995; Howind et al., 1999). In these studies all one-way measurements are considered to be independent, and having the same variance and same temporal correlation. Since it has been shown that different satellites have different temporal correlation coefficients (Satirapod et al., 2000; Wang, 1998), it is not appropriate to make such assumptions. Therefore, a stochastic modelling procedure which realistically takes into account all error features needs to be developed.

In this Chapter, an iterative stochastic assessment procedure is proposed, in which all of the aforementioned error features of GPS measurements are taken into account. In the following sections first the mathematical equations used in static GPS baseline data processing are briefly reviewed, and then the procedure for the estimation of variance-covariance components and the treatment of temporal correlations is presented. Finally, details of the iterative stochastic modelling method will be presented. Applications of the proposed procedure will be demonstrated using a variety of GPS data sets.

4.2   Basic Equations for Processing GPS Carrier Phase Measurements

In precise GPS positioning, double-differenced (DD) carrier phase observables are usually formed because many systematic errors existing in the GPS measurements cancel, and the resultant DD observables have a simplified functional model. For short baselines, the DD carrier phase observables (in cycles) can be expressed as (Hofmann-Wellenhof et al., 1997; Leick, 1995; Rizos, 1997):

$$\varphi_{uv}^{pq}(t) = \frac{1}{\lambda} Z_{uv}^{pq}(t) + N_{uv}^{pq} + e_{uv}^{pq}(t) \tag{4.1}$$

where the superscripts p and q denote satellites, and the subscripts u and v specify the receivers, and the indices t denote the epoch at which the measurement data were collected. Z is the topocentric distance to the satellites, λ is the wavelength of the carrier wave, and N is the DD integer ambiguity. The term e represents all possible errors, including random noises of receivers, and residual systematic errors such as unmodelled multipath effects, ionospheric and tropospheric delays, etc.

Assuming that the vector x contains all the unknown parameters necessary for baseline parameter estimation, a set of linearized DD measurement equations for the *ith* satellite pair can be formed:

$$l_i = A_i x + e_i, \qquad i = 1, 2, \ldots, n \tag{4.2}$$

with

$$l_i = \begin{bmatrix} l_i(1), & l_i(2), & . & . & ., & l_i(s) \end{bmatrix}^T ;$$

$$A_i = \begin{bmatrix} A_i(1) & A_i(2) & . & . & ., & A_i(s) \end{bmatrix}^T ; \text{ and}$$

$$e_i = \begin{bmatrix} e_i(1), & e_i(2), & . & . & ., & e_i(s) \end{bmatrix}^T .$$

In Equation (4.2), l_i is an $s \times 1$ vector of the observed-minus-computed DD carrier phase values; A_i is the design matrix corresponding to the measurements l_i; e_i is an $s \times 1$ vector of the error terms for the measurement l_i; n is the number of satellite pairs forming the DD observables; and s is the number of observation epochs.

By collecting all the linear(ized) DD carrier phase observable equations from the entire observation session, the functional (mathematical) model is then constructed:

$$l = Ax + e \tag{4.3}$$

with

$$l = [l_1^T, l_2^T, ..., l_n^T]^T \; ;$$

$$A = [A_1^T, A_2^T, ..., A_n^T]^T \; ; \text{ and}$$

$$e = [e_1^T, e_2^T, ..., e_n^T]^T \; .$$

In practice, GPS measurements are usually assumed to have the same precision, and to be statistically independent in time and space, that is, satisfy the conditions:

$$E[e_i(t)] = 0 \tag{4.4}$$

$$E[e_i(t) \cdot e_j(v)] = 0 \quad (t \neq v) \tag{4.5}$$

$$E[e_i(t) \cdot e_j(t)] = \sigma_{ij}^2 = \begin{cases} 4\sigma^2 \, (i \equiv j) \\ 2\sigma^2 (i \neq j) \end{cases} \tag{4.6}$$

where $i = 1, 2, ..., n$; $t, v = 1, 2, ..., s$; and σ is the standard deviation of the one-way measurements. Then, a covariance matrix for all the DD observables l is constructed (for the case that all epochs have measurements to the same satellites):

$$C = \Sigma \otimes I_s = \sigma^2 \cdot Q \otimes I_s \qquad (4.7)$$

with

$$\Sigma = \begin{bmatrix} \sigma_{11}^2 & \sigma_{12}^2 & . & . & . & \sigma_{1n}^2 \\ \sigma_{21}^2 & \sigma_{22}^2 & . & . & . & \sigma_{2n}^2 \\ . & . & & & & . \\ . & . & & & & . \\ . & . & & & & . \\ \sigma_{n1}^2 & \sigma_{n2}^2 & . & . & . & \sigma_{nn}^2 \end{bmatrix} = \begin{bmatrix} 4\sigma^2 & 2\sigma^2 & . & . & . & 2\sigma^2 \\ 2\sigma^2 & 4\sigma^2 & . & . & . & 2\sigma^2 \\ . & . & & & & . \\ . & . & & & & . \\ . & . & & & & . \\ 2\sigma^2 & 2\sigma^2 & . & . & . & 4\sigma^2 \end{bmatrix} = \sigma^2 Q,$$

where I_s is the $s \times s$ Identity matrix, and Q is a co-factor matrix. With the mathematical and stochastic models expressed by Equations (4.3) and (4.7), the least-squares estimator of the unknowns, and the residuals of the measurements, can be obtained:

$$\hat{x} = [A^T(\Sigma^{-1} \otimes I_s)A]^{-1} A^T(\Sigma^{-1} \otimes I_s)l = [A^T(Q^{-1} \otimes I_s)A]^{-1} A^T(Q^{-1} \otimes I_s)l \qquad (4.8)$$

$$\hat{e} = l - A\hat{x} \qquad (4.9)$$

The optimal estimate of this variance factor is given by:

$$\hat{\sigma}^2 = \frac{\hat{e}^T(Q^{-1} \otimes I_s)\hat{e}}{f} \qquad (4.10)$$

where f is the degree of freedom (Leick, 1995). Clearly, the estimate $\hat{x}$ is independent of the variance factor. The estimated variance factor $\hat{\sigma}^2$ is an indicator of the internal precision of the measurements in general. By substituting the unknown variance factor σ^2 by the estimated one $\hat{\sigma}^2$, the covariance matrix Σ of the measurements is replaced by a similar matrix $\hat{\Sigma}$. The covariance matrix for the estimate $\hat{x}$ is then written as:

$$C_{\hat{x}} = \hat{\sigma}^2 [A^T (Q^{-1} \otimes I_s) A]^{-1} = [A^T (\hat{\Sigma}^{-1} \otimes I_s) A]^{-1} \qquad (4.11)$$

It can be seen that the estimator $\hat{x}$ and its covariance matrix $C_{\hat{x}}$ are dependent on the stochastic model adopted for the measurements. Any misspecification of the stochastic model will lead to inaccurate results, contrary to the optimality property of the least-squares solution. By using a misspecified stochastic model, the least-squares computations will produce unrealistic statistics, subsequently used in ambiguity resolution and in the final baseline determination. Therefore, a realistic stochastic model for GPS baseline processing is critical and is discussed in detail in the next section.

4.3   Stochastic Assessment of Carrier Phase Measurements

From the data processing point of view, the stochastic model is essentially a fully distributed covariance matrix for all the measurements used in the least-squares estimation procedure. Generally, the magnitude of the elements of such a covariance matrix are unknown. Consequently, similar to the situation with the functional model, there are also unknown parameters in the stochastic model. A rigorous estimation procedure should therefore include the estimation of all the unknown parameters in both the functional and stochastic models. A general procedure for the parameterization and estimation of the elements of a complex stochastic model is described below.

4.3.1   Estimating Variance-Covariance Components

An estimation of variance-covariance matrices of GPS measurements can be performed using the rigorous MINQUE procedure discussed in Chapter 3.

It should be noted, however, that because of the lack of enough geometric information contained within the measurements, not all the unknown parameters in the stochastic model can be feasibly estimated. In practice it is very common to use a simplified stochastic model, which is assumed to be completely known, or may just include a few

unknown parameters. For instance, the stochastic model described by Equation (4.7) actually contains one unknown parameter, hence the whole structure of the model is assumed to be based on a simple form. This makes for efficient data processing. Under such circumstances, the estimation of the unknown parameter in the stochastic model is straightforward, and doesn't even need any iteration (see Equation (4.10)). With the assumption that the temporal correlations between epochs are absent, all the elements of the matrix $\sum$ could be estimated. However, a simultaneous estimation of both the matrix $\sum$ and the temporal correlations is still a challenge.

4.3.2   Treatment of Temporal Correlations

In order to obtain a more realistic stochastic model, the covariance matrix for the measurements should be designed in such a way as to adequately reflect the error structure, and should include a reasonable number of unknown parameters (that can be feasibly estimated).

It has been long recognised that the GPS measurements are temporally correlated (e.g. Vanicek et al. 1985; El-Rabbany, 1994; Wang, 1998; Howind et al., 1999; Borre & Tiberius, 2000). To take such temporal correlations into account, the error specification represented by Equation (4.5) is replaced by:

$$
\begin{bmatrix} e_1(t) \\ e_2(t) \\ . \\ . \\ . \\ e_n(t) \end{bmatrix} = \begin{bmatrix} \rho_{11} & \rho_{12} & . & . & . & \rho_{1n} \\ \rho_{21} & \rho_{22} & . & . & . & \rho_{2n} \\ . & . & & & & . \\ . & . & & & & . \\ . & . & & & & . \\ \rho_{n1} & \rho_{n2} & . & . & . & \rho_{nn} \end{bmatrix} \cdot \begin{bmatrix} e_1(t-1) \\ e_2(t-1) \\ . \\ . \\ . \\ e_n(t-1) \end{bmatrix} + \begin{bmatrix} u_1(t) \\ u_2(t) \\ . \\ . \\ . \\ u_n(t) \end{bmatrix} \qquad (4.12a)
$$

or

$$
e(t) = R \cdot e(t-1) + u(t) \qquad (4.12b)
$$

where *u(t)* are random variables; ρ_{ii} describes the so-called temporal correlation within the DD observables of the *ith* satellite pair; and ρ_{ij} presents the inter-temporal correlation between the measurements of the *ith* and *jth* satellite pairs. Equation (4.12) is called a *first-order vector auto-regressive model*, as discussed by Sargan (1961). If all the inter-temporal correlations are assumed to be absent, i.e., $\rho_{ij} = 0$, Equation (4.12) is reduced to a *first-order scalar auto-regressive model*. In most of the previous investigations concerning temporal correlations of GPS measurements, it has been assumed that all inter-temporal correlations (between the measurements from different satellite pairs and at different epochs) are absent, and that the temporal correlations for all the satellite pairs are the same. Therefore, Equation (4.12) represents a more general error specification.

In Equation (4.12), the error terms $u(t)$ are temporally independent, that is, satisfy the conditions:

$$E[u(t) \cdot u(v)^T] = 0, \tag{4.13}$$

$$E[u(t) \cdot u(t)^T] = \Omega \tag{4.14}$$

where $t, v = 2, ..., s$. Therefore, the whole covariance matrix for the error term vector *u* is:

$$E(u \cdot u^T) = \Omega \otimes I_s \tag{4.15}$$

However, due to the temporal and inter-temporal correlations, the derivation of the covariance matrix $C = E(e \cdot e^T)$ in Equation (4.7) is complicated. Even though such a covariance matrix is available, it is difficult, if not impossible, to estimate the variance and covariance components and the (inter-) temporal correlation coefficients simultaneously. So, a two-stage estimation procedure is necessary, in which the estimation of the matrices Ω and R is essentially separated. To achieve this a matrix

G is so determined that the error term vector e can be transformed, as Equation (4.3) is transformed into the error term vector u , that is:

$$Ge = u \qquad\qquad (4.16)$$

and therefore, Equation (4.3) is transformed to:

$$\bar{l} = \overline{A}x + u \qquad\qquad (4.17)$$

where $\bar{l} = Gl$, $\overline{A} = GA$.   The structure of the matrix G has been derived (Guilkey & Schmidt, 1973):

$$G = \begin{bmatrix} G_{11} & G_{12} & . & . & . & G_{1n} \\ G_{21} & G_{22} & . & . & . & G_{2n} \\ . & . & & & & . \\ . & . & & & & . \\ . & . & & & & . \\ G_{n1} & G_{n2} & . & . & . & G_{nn} \end{bmatrix}, (ns \times ns) \qquad\qquad (4.18)$$

with

$$G_{ii} = \begin{bmatrix} \beta_{ii} & 0 & 0 & . & . & . & 0 & 0 \\ -\rho_{ii} & 1 & 0 & . & . & . & 0 & 0 \\ 0 & -\rho_{ii} & 1 & . & . & . & 0 & 0 \\ . & . & . & & & & . & . \\ . & . & . & & & & . & . \\ . & . & . & & & & . & . \\ 0 & 0 & 0 & . & . & . & -\rho_{ii} & 1 \end{bmatrix}, (s \times s) \qquad\qquad (4.19)$$

$$
G_{ij} = \begin{bmatrix} \beta_{ij} & 0 & 0 & . & . & . & 0 & 0 \\ -\rho_{ij} & 0 & 0 & . & . & . & 0 & 0 \\ 0 & -\rho_{ij} & 0 & . & . & . & 0 & 0 \\ . & . & . & & & & . & . \\ . & . & . & & & & . & . \\ . & . & . & & & & . & . \\ 0 & 0 & 0 & . & . & . & -\rho_{ij} & 0 \end{bmatrix} \quad (i \neq j) , (s \times s) \tag{4.20}
$$

and

$$
B = \begin{bmatrix} \beta_{11} & 0 & . & . & . & 0 \\ \beta_{21} & \beta_{22} & . & . & . & 0 \\ . & . & & & & . \\ . & . & & & & . \\ . & . & & & & . \\ \beta_{n1} & \beta_{n2} & . & . & . & \beta_{nn} \end{bmatrix} , (n \times n) \tag{4.21}
$$

The elements of B can be found via triangular or Cholesky decomposition of Ω and Σ. The matrix B satisfies $B \Sigma B^T = \Omega$. For instance, B can be chosen as $H_1 H_2^{-1}$, where H_1 and H_2 are lower triangular matrices satisfying the conditions $\Omega = H_1 H_1^T$ and $\Sigma = H_2 H_2^T$. By using the relationship $\Sigma = R \Sigma R^T + \Omega$ (Guilkey & Schmidt, 1973), the matrix Σ can be determined:

$$
Vector(\Sigma) = (I - R \otimes R)^{-1} Vector(\Omega) \tag{4.22}
$$

where the $Vector(\bullet)$ is constructed by stacking the rows of a matrix.

It is noted that the transformed measurements $\bar{l}$ are temporally independent and have a simple stochastic model defined by Equation (4.15). A MINQUE procedure, as discussed in Section 3.2, could be used to estimate the unknown elements of the matrix Ω. However, the determination of the transformation matrix G relies on the elements (ρ_{ij}) of R, which are unknown and need to be estimated separately.

Since the true values of the measurement errors are unknown, the estimation of (inter-) temporal correlation coefficients, or the elements (ρ_{ij}) of R, has to be based on the residuals ($\hat{e}$) of the original DD observables l. Based on Equation (4.12), one obtains:

$$
\begin{bmatrix}
\hat{e}_i(2) \\
\hat{e}_i(3) \\
. \\
. \\
. \\
\hat{e}_i(s)
\end{bmatrix}
=
\begin{bmatrix}
\hat{e}(1)^T \\
\hat{e}(2)^T \\
. \\
. \\
. \\
\hat{e}(s-1)^T
\end{bmatrix}
r_i +
\begin{bmatrix}
u_i(2) \\
u_i(3) \\
. \\
. \\
. \\
u_i(s)
\end{bmatrix}
\qquad i = 1, 2,..., n
\tag{4.23a}
$$

or

$$
E_{2i} = E_1 r_i + u_i
\tag{4.23b}
$$

where E_{2i} is an $(s-1) \times 1$ vector; E_1 is an $(s-1) \times n$ matrix; and r_i is an $n \times 1$ vector representing the *ith* row of matrix R. The unknown vector r_i can therefore be estimated by applying the least-squares principle to Equation (4.23), or all the elements of R are estimated together as:

$$
Vector(\hat{R}) = [E_a^T (\Omega^{-1} \otimes I_{s-1}) E_a]^{-1} E_a^T (\Omega^{-1} \otimes I_{s-1}) E_b
\tag{4.24}
$$

with

$$
E_a =
\begin{bmatrix}
E_1 \\
E_1 \\
. \\
. \\
. \\
E_1
\end{bmatrix}
\quad \text{and} \quad
E_b =
\begin{bmatrix}
E_{21} \\
E_{22} \\
. \\
. \\
. \\
E_{2n}
\end{bmatrix}
$$

Because the estimation of the residuals depends on the covariance matrix, an iterative estimation procedure is required.

4.3.3   An Iterative Stochastic Modelling Procedure

Based on the above theoretical analysis, an iterative procedure for the estimation of the (inter-) temporal correlation matrix R and the covariance matrix Ω is summarised below.

Preparatory steps:

(1)   use the standard stochastic model represented by Equation (4.7)

(2)   to obtain estimates of the unknown parameters and residuals using Equations (4.8) and (4.9);

(3)   then estimate the covariance matrix ($\hat{\Sigma} = \hat{\Omega}$) using Equation (4.10).

Iterative steps:

(4)   estimate the temporal correlation matrix $\hat{R}$ using Equation (4.24);

(5)   then construct the transform matrix G using Equations (4.18), (4.19), (4.20) and (4.21) with the matrices $\hat{R}$ and $\hat{\Omega}$;

(6)   then estimate the covariance matrix ($\hat{\Omega}$) for the transformed measurements $\bar{l}$ using the MINQUE procedure;

(7)   to obtain estimates of the unknown parameters from

$$\hat{x} = [\bar{A}^T(\hat{\Omega}^{-1} \otimes I_s)\bar{A}]^{-1}\bar{A}^T(\hat{\Omega}^{-1} \otimes I_s)\bar{l};$$

(8)   then obtain the residuals $\hat{e}$ from Equation (4.9) using the estimated unknown parameters $\hat{x}$;

(9)   then check the variations of the estimated elements of the matrices $\hat{R}$ and $\hat{\Omega}$; and

(10)   stop iteration if sufficient accuracy (say, 0.001mm in the baseline components) is achieved, otherwise go back to Step (4).

This iterative stochastic modelling procedure can also be represented by the flow diagram in Figure 4.1.
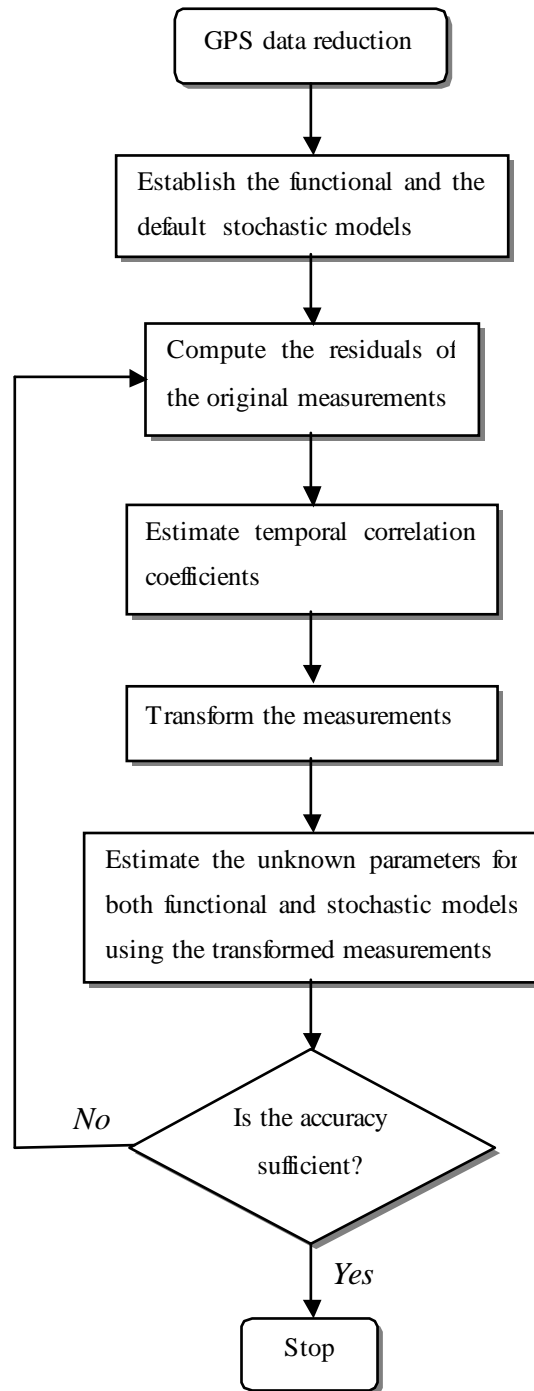
Figure 4.1 The proposed iterative stochastic modelling procedure.

4.4   Experimental Results and Analysis

4.4.1   Description of the Data Sets

To demonstrate the impact of various stochastic modelling procedures on GPS relative positioning, three static GPS baseline data sets were analysed (Table 4.1). For all the data sets, the data interval is 15 second and the session length is 30 minutes. In the data processing, only L1 frequency data were used.

Table 4.1 Details of the experimental data sets.

Baseline names	Receivers	Baseline length (m)	Survey dates
B15M	NovAtel Millennium	15	July 10, 2000
B215M	Ashtech Z-XII	215	June 7, 1999
B13KM	Trimble 4000SSE	13,300	Dec 18, 1996

It should be noted that in the case of the Ashtech data set, two receivers were mounted on pillars that are part of a first-order terrestrial survey network. The known baseline length between the two pillars is 215.929 ± 0.001 m, which will be used as a ground truth to check the results obtained using the various stochastic modelling procedures. Both the B15M and B13KM baseline data sets were collected under a good environment (no reflection surface nearby). Therefore, the main error source of the B15M baseline data would be only the receiver noise while the main error source of the B13KM baseline was expected to be the atmospheric delays. In the case of the B215M baseline, the data were collected under the multipath environment, and hence multipath was the dominant error source in this data set.

4.4.2   Data Processing Methods

All the data sets were processed using the following stochastic modelling options:

A. The standard procedure with the stochastic model expressed by Equation (4.7), assuming that temporal correlations are absent ($R = 0$).

B. A modified standard procedure with $R_{ij} = 0$ and $R_{ii} = R_{jj}$ $(i \neq j)$, that is, assuming that R_{ii} is the same for every satellite pair and follows an exponential function defined by El-Rabbany (1994).

C. A two-stage procedure with $R_{ij} = 0$ and $R_{ii} \neq R_{jj}$ $(i \neq j)$ *(a first-order scalar auto-regressive model)*, and applying the MINQUE procedure to estimate a variance-covariance matrix for the transformed measurements.

D. A two-stage procedure with $R_{ij} \neq 0$ $(i \neq j)$ *(a first-order vector auto-regressive model)*, applying the MINQUE procedure to estimate a variance-covariance matrix for the transformed measurements.

Due to the more unknown parameters to be estimated by methods C and D, the 30-min data span was processed in this Chapter.

4.4.3   Analysis of Results

The resulting DD residuals for each data set are in Figures 4.2 to 4.4. These show the time series of the DD residuals obtained from the baselines B15M, B215M and B13KM respectively. Because the residuals obtained by methods B, C and D showed similar trends, for clarity only the residuals obtained by method D are compared with those obtained from method A. The 'heavy' lines represent the residuals obtained from method A, while the 'light' lines are the residuals obtained from method D. Among these stochastic models, the preferred one will produce the most randomized residuals.

It can be seen from these Figures that, for most of the satellite pairs, the standard processing results in residuals that exhibit significant systematic errors. This is further confirmed by the temporal correlation coefficients listed in Table 4.2, computed by applying the Durbin-Watson statistic (Durbin & Watson, 1950 – see Equations (5.2) and (5.3)) to the DD residuals. The time series of DD residuals in Figure 4.3 show some significant multipath errors for satellite pairs PRN 2-7 and 2-19 (PRNs 7 and 19 have elevation angles of 15 and 19 degrees, respectively). With reference to Figures 4.2 to 4.4, it is evident that the systematic errors of the transformed measurements are much

61

smaller than those of the original measurements. Hence the residuals for the transformed measurements are more random than those of the original measurements.
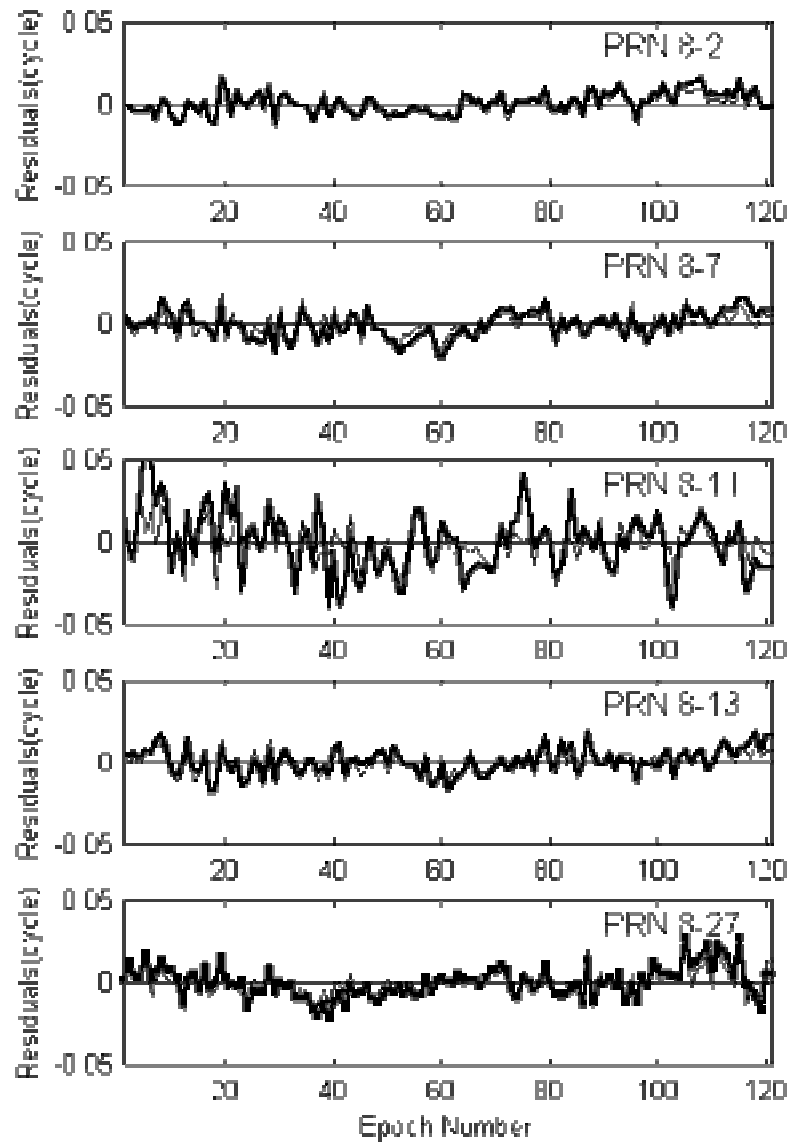
Figure 4.2 DD residuals obtained from baseline B15M for various satellite pairs.
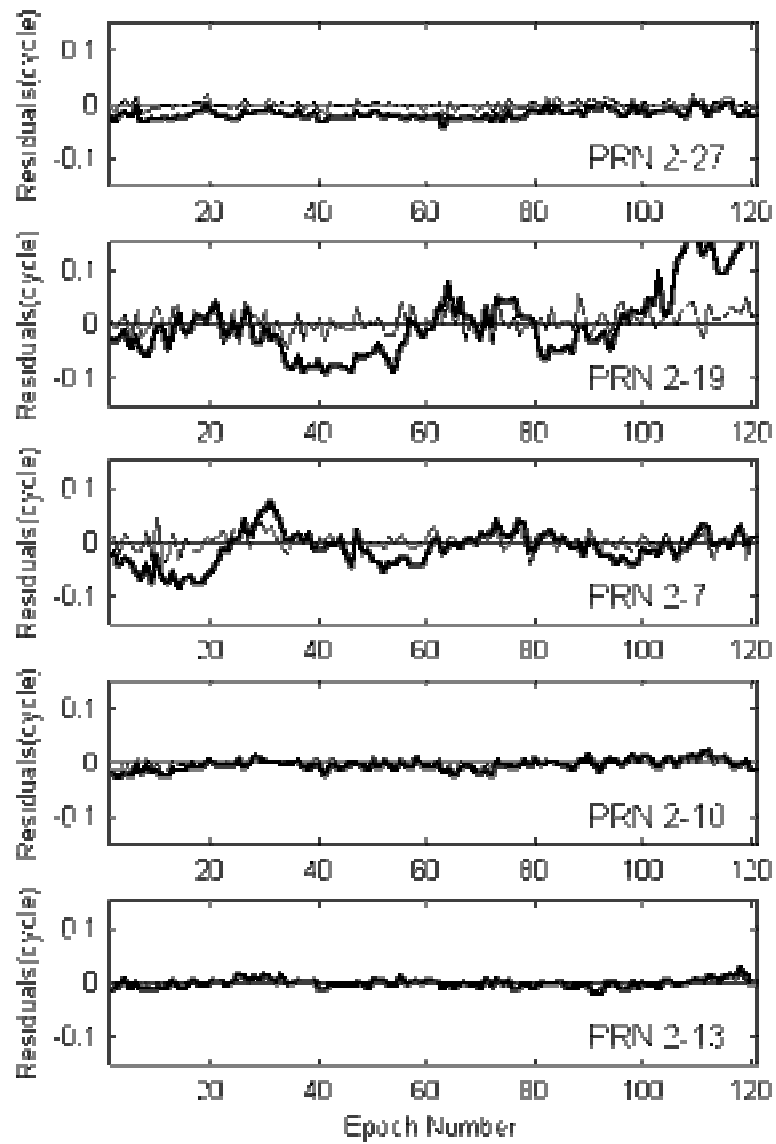
Figure 4.3 DD residuals obtained from baseline B215M for various satellite pairs.
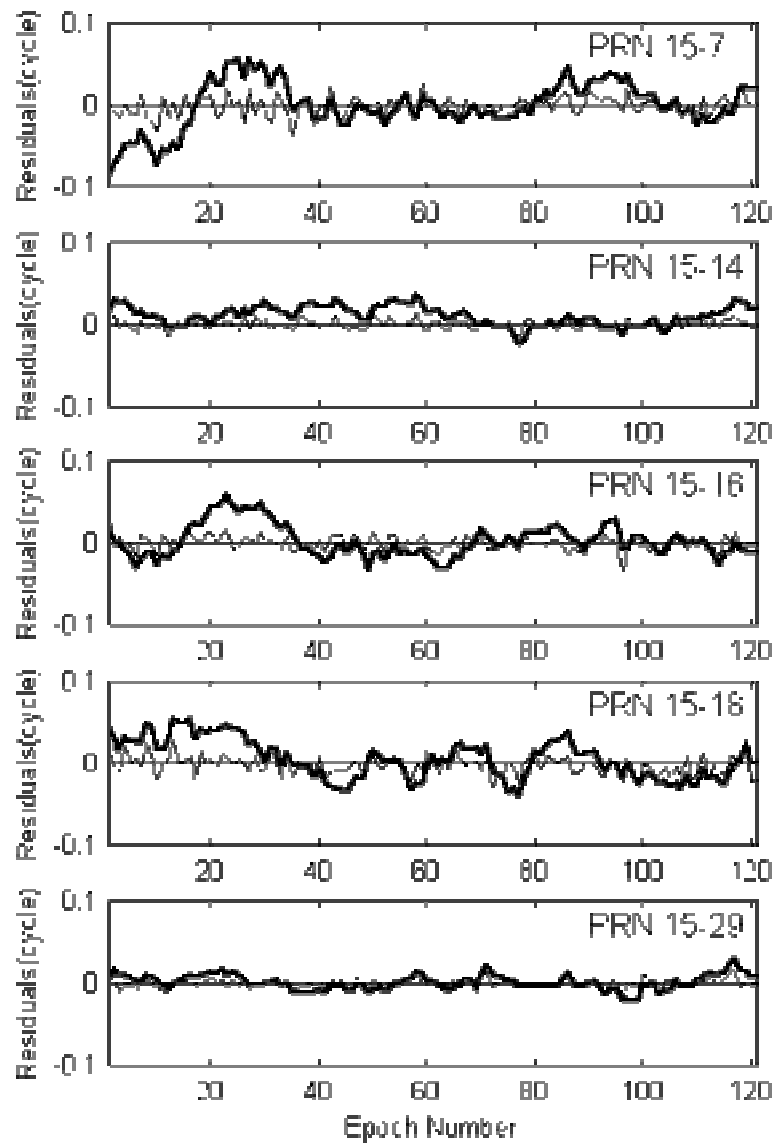
Figure 4.4 DD residuals obtained from baseline B13KM for various satellite pairs.

It should be noted that the temporal correlation coefficients from method B are large and negative. Table 4.2 indicates that fixing the temporal correlation coefficients to the same value for all the satellite pairs might be inappropriate in reality. As expected, from Table 4.2, the estimated temporal coefficients obtained by methods C and D are closer to zero than those obtained from methods A and B. The residuals obtained by methods C and D are therefore essentially random, which indicates that the temporal correlations have been taken into account in the measurement transformation step.

Table 4.2 Comparison of temporal coefficients.

Baselines	Sat pairs	Temporal coefficients			
		Method A	Method B	Method C	Method D
B15M	8-02	0.38	-0.41	0.10	0.06
	8-07	0.49	-0.47	-0.17	-0.14
	8-11	0.43	-0.28	-0.02	0.02
	8-13	0.30	-0.39	-0.03	0.02
	8-27	0.48	-0.56	-0.21	-0.19
B215M	2-27	0.88	-0.48	-0.01	-0.10
	2-19	0.93	-0.24	-0.10	-0.07
	2-7	0.83	-0.32	-0.21	-0.19
	2-10	0.61	-0.43	-0.01	-0.07
	2-13	0.53	-0.45	-0.12	-0.06
B13KM	15-07	0.87	-0.10	0.00	-0.07
	15-14	0.92	-0.01	0.05	0.02
	15-16	0.89	-0.02	0.04	0.05
	15-18	0.87	-0.15	-0.04	0.02
	15-29	0.82	0.01	0.09	0.09

It has been shown in, for example, Teunissen (1997) and Wang et al. (1998a), that the stochastic models have a significant influence on ambiguity resolution. The discrimination test is one of the critical steps. Both the classical F-ratio statistic and an alternative statistic proposed by Wang et al. (1998b) are considered here. The larger the values of these statistics, the more reliable the ambiguity resolution. For method B, all three baselines have small F-ratio values (Table 4.3). In the case of baseline B15M, both methods C and D produce larger F- and W-ratio than methods A and B. However, in the case of baselines B215M and B13KM, contrary results were obtained. These phenomena might be linked to the systematic errors existing in the measurements. But, in view of the fact that methods C and D generate random residuals for all the baselines,

the F-ratio and W-ratio statistics obtained by methods C and D could be considered to be more realistic than those obtained by methods A and B.

Table 4.3 F-ratio and W-ratio values for the ambiguity validation test.

Baseline	F-ratio statistics				W-ratio statistics			
	A	B	C	D	A	B	C	D
B15M	25.933	1.151	47.740	51.850	61.517	4.592	82.649	86.345
B215M	6.935	1.155	4.232	5.695	30.580	4.717	20.871	25.122
B13KM	38.080	1.765	7.287	9.211	76.642	9.968	29.981	34.189

The estimated baseline components and their *a-posteriori* standard deviations are presented in Table 4.4.   These results indicate that there is generally no significant difference in the horizontal components. However, it is important to note that in the case of baselines B215M and B13KM, the differences in estimated height components between methods A and C (or D) can be as large as 10 mm. This is a significant difference for high-precision applications, and thus, a realistic stochastic model is critical for such applications. For the baseline B215M, the estimated baseline lengths using methods C and D are slightly closer (4mm closer for the worst case) to the known baseline length than using methods A and B. In term of standard deviation, method B generally produces larger standard deviations than the other methods, and methods C and D produce slightly larger standard deviations than method A (except the B215M baseline). Although method B seemed to produce larger standard deviations, these standard deviations may not be realistic. This can be seen in the case of the B13KM baseline, method B produces the larger standard deviations in the horizontal components than the height component (it is well known that GPS gives the worst solution in the height component.). Hence, methods C and D tend to produce the most realistic standard deviations.

Table 4.4 Estimated baseline components and standard deviations.

Baselines	Methods	Estimated baseline components (m)			Baseline	Standard Deviations (mm)		
		North	East	Height	length (m)	North	East	Height
B15M	A	3.8509	14.4315	0.0305	14.9365	0.2	0.2	0.4
	B	3.8502	14.4315	0.0303	14.9363	3.1	3.1	6.7
	C	3.8510	14.4316	0.0301	14.9366	0.2	0.2	0.6
	D	3.8511	14.4316	0.0300	14.9366	0.2	0.2	0.5
B215M	A	-188.5110	105.2942	0.5034	215.9248	0.7	0.6	1.1
	B	-188.5097	105.2938	0.4996	215.9235	5.3	4.9	8.2
	C	-188.5139	105.2944	0.5120	215.9275	0.4	0.6	0.8
	D	-188.5122	105.2957	0.5143	215.9266	0.5	0.6	1.1
B13KM	A	7209.3677	-11173.7096	-30.0798	13297.6567	1.2	0.4	1.6
	B	7209.3659	-11173.7062	-30.0747	13297.6528	7.7	2.6	0.9
	C	7209.3698	-11173.7108	-30.0839	13297.6588	1.7	0.9	2.5
	D	7209.3689	-11173.7102	-30.0873	13297.6578	1.6	0.9	2.3

4.5   Concluding Remarks

A realistic stochastic model for GPS measurements is critical for reliable ambiguity resolution and precise baseline component estimation. With the aid of three static baseline data sets, some aspects of the misspecification in the stochastic model were analysed.

After reviewing the existing methods, an iterative stochastic modelling procedure has been proposed to directly estimate the time correlation coefficients, and the time-independent variance and covariance components of the GPS measurements. In the proposed procedure, the commonly used stochastic model is first used to estimate approximate values of the temporal correlation coefficients. Based on the estimated time correlation coefficients, the original DD observables are then transformed into a new set of measurements. These transformed measurements are free of time correlations, and thus have a block diagonal covariance matrix. The covariance matrix for the new measurements can be estimated using the MINQUE method (or the simplified MINQUE procedure). An advantage of the transformed DD carrier phase observables is

that the effects of systematic errors are largely eliminated, and thus the resulting residuals may be considered random. By removing the systematic errors from the measurements, as expected, the certainty of the estimated positioning results is improved. In addition, the quality of ambiguity resolution can be more realistically indicated.

Based on the development work in this Chapter, a practical stochastic modelling procedure will be proposed in the next Chapter. This will effectively deal with long observation period data sets, as well as reducing the computational load and memory usage of the iterative stochastic modelling procedure.

A SEGMENTED STOCHASTIC MODELLING PROCEDURE

5.1 Introduction

An iterative stochastic modelling procedure, which takes into account all of the error features, has been proposed in Chapter 4. This procedure is suitable for short observation periods as it assumes that the temporal correlation coefficients and the variance of GPS measurements are constant for the whole observation period. Initial experiments based on this procedure have demonstrated encouraging results in the case of short observation periods and for short baselines (see Chapter 4).

However, when this procedure is applied to long observation period data sets, several shortcomings of the procedure needed to be addressed. For example, the assumption that the temporal correlation coefficients and the variance of GPS measurements are constant for the whole observation period is not realistic. Furthermore, in practice, an observation period of several hours may be expected for some geodetic applications. Thus the memory usage and computational load can become unbearable when the standard MINQUE technique (or even the simplified MINQUE procedure) is applied. Hence, it is necessary to develop a new stochastic modelling procedure that addresses these shortcomings.

In this Chapter, a new procedure is proposed, that deals with long observation period data sets, with the aim of reducing the computational load. This procedure will also take into account the temporal correlations in the GPS measurements. The effectiveness of the new procedure is tested using both real data and simulated data sets for short to medium length baselines.

5.2   Segmented Stochastic Modelling Procedure

To process long observation session data sets, a three-step procedure has been proposed to estimate realistic stochastic models for the GPS measurements. The first step is to divide the whole session into short segments. Secondly, the inter-temporal correlation coefficients (for different satellite pairs) should be set to zero. In the third step, the MINQUE procedure for the estimation of variance-covariance components is replaced by an alternative method.

5.2.1   Step 1: Data Segmentation

Given that GPS measurements are contaminated by errors (e.g. atmospheric delays, multipath) whose characteristics change slowly with time, it is appropriate to divide the whole measurement session into short segments, in which each segment has the same number of satellites and all the measurements for the same satellite pairs have an invariant stochastic model. This is illustrated in Figure 5.1. During a long observation period the satellite geometry changes considerably, hence the use of fixed 'window' widths in order to segment the measurements is not advisable.

A method to circumvent this problem is proposed, in which a default window width is first selected. Then indices of when the satellite geometry has changed during the entire session are determined, and the number of observations between consecutive indices checked. If the number of observations between any pair of consecutive indices is larger than the default window width, the measurements are divided into short segments until the number of observations in the last segment is smaller than or equal to the default window width. In this case, the observations from the last segment will be combined with the ones from the previous segment. However, if the number of observations between the consecutive indices is not sufficient to form a new segment, the stochastic model estimated from the previous segment is applied to these observations.
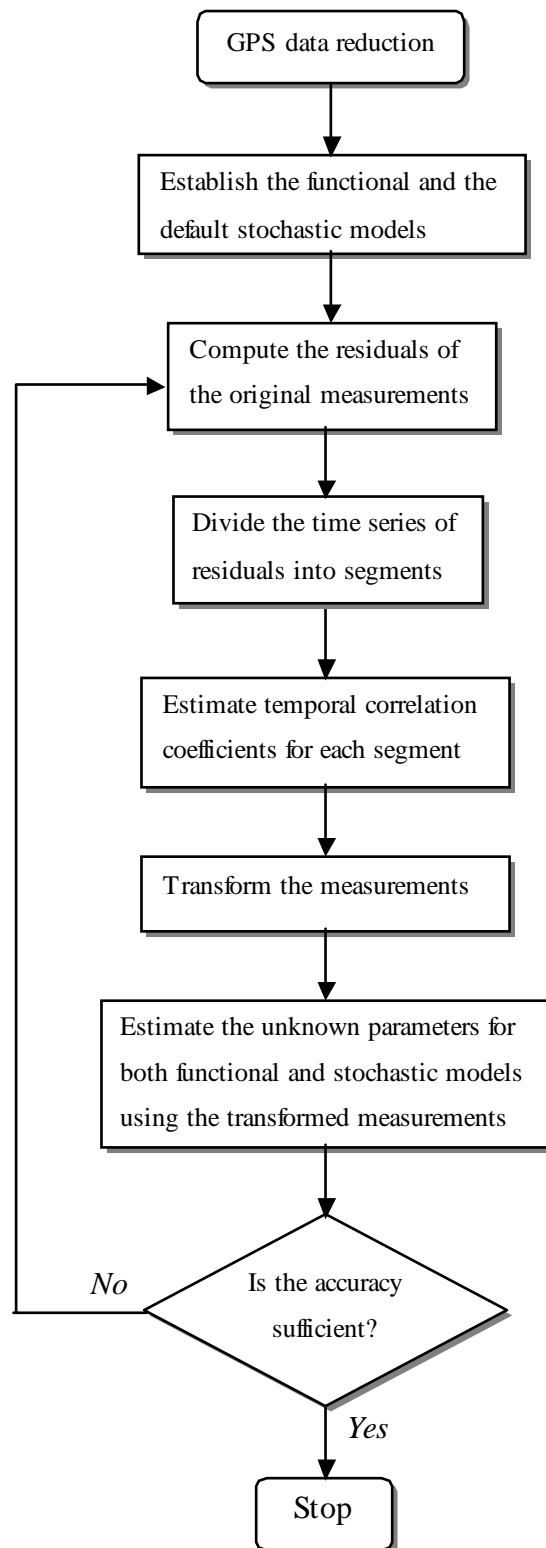
Figure 5.1 Flowchart of the segmented stochastic modelling procedure.

5.2.2   Step 2: Estimation of Temporal Correlation Coefficients

Assuming that the inter-temporal correlations are zero, the error specification is:

$$
\begin{bmatrix} e_1(t) \\ e_2(t) \\ . \\ . \\ e_n(t) \end{bmatrix} = \begin{bmatrix} \rho_{11} & 0 & . & . & 0 \\ 0 & \rho_{22} & . & . & 0 \\ . & . & & & . \\ . & . & & & . \\ 0 & 0 & . & . & \rho_{nn} \end{bmatrix} \cdot \begin{bmatrix} e_1(t-1) \\ e_2(t-1) \\ . \\ . \\ e_n(t-1) \end{bmatrix} + \begin{bmatrix} u_1(t) \\ u_2(t) \\ . \\ . \\ u_n(t) \end{bmatrix} \tag{5.1a}
$$

or

$$
e(t) = R \cdot e(t-1) + u(t) \tag{5.1b}
$$

where

ρ_{ii} is the temporal correlation within the ith satellite pair,

n is the number of satellite pairs forming the DD measurements, and

e is the vector of original residuals.

According to the Durbin-Watson statistic (Durbin & Watson, 1950), the temporal correlation coefficient is:

$$
\rho = 1 - d/2 \tag{5.2}
$$

with

$$
d = \frac{\sum_{k=2}^{m}(e_k - e_{k-1})^2}{\sum_{k=1}^{m}e_k^2} \tag{5.3}
$$

where m is the number of observation epochs in a segment.

The estimated temporal correlation coefficient is then used to transform the original measurements. Details of this transformation step can be found in Section 4.3.2.

5.2.3 Step 3: Estimation of Variance-Covariance Components

As previously stated, an observation period of several hours may be expected for some geodetic applications, and hence the memory usage and computational load can become unbearable when the standard (or even simplified) MINQUE procedure is applied. In this step, an alternative method of estimating variance-covariance components for the GPS measurements is proposed. Its performance has been tested using various experimental data sets.

5.2.3.1 The proposed method

The estimation of variance-covariance components can be performed using the classical definition of the variance-covariance matrix:

$$C = E[(v\text{-}\mu)\,(v\text{-}\mu)^T]\quad = E[vv^T]\text{-}\mu\mu^T \tag{5.4}$$

where μ is the mean value. The residuals obtained from the transformed measurements are random and have zero mean ($\mu=0$). Hence, the variance-covariance matrix can be obtained by averaging the residuals within the same segment:

$$C = \frac{1}{m}\sum_{k=1}^{m} v_k v_k^T \tag{5.5}$$

An iterative estimation procedure is required, as the estimation of the residuals is dependent on the variance-covariance matrix. Based on Equation (5.5), the implementation of the proposed method is relatively straightforward. Its performance has been evaluated using three data sets. Details of the three data sets are given in Table 5.1.

Table 5.1 Details of the three experimental data sets

Receivers	NovAtel Millennium	Leica system 300	CRS1000
Baseline length (m)	15	870(~1km)	2660(~2km)
Survey date	July 10, 2000	Nov 18, 1996	Oct 12, 1999
Satellites	02,08,11,13,27	04,14,18,19,24,27,29	04,05,07,08,09,24
Elevation angle (°)	63,68,16,54,49	41,25,61,71,26,36,30	64,29,35,32,55,40
Data interval (sec)	15	15	15
Data span (min)	30	30	30

For ambiguity discrimination, the difference between the best and second best ambiguity combination is crucial. The F-ratio (e.g. Euler & Landau, 1992) and the W-ratio (Wang et al., 1998b) are chosen for comparison (Table 5.2).

Table 5.2 Comparison of F-ratio and W-ratio statistics.

Baseline	Method	F-ratio	W-ratio
15m	Standard MINQUE	12.76	26.65
	Simplified MINQUE	12.77	26.67
	Proposed method	12.80	26.72
1km	Standard MINQUE	9.20	29.92
	Simplified MINQUE	9.16	29.87
	Proposed method	9.17	29.86
2km	Standard MINQUE	4.54	16.12
	Simplified MINQUE	4.59	16.25
	Proposed method	4.57	16.19

Remark: The observation period is 15 minutes,

and the sampling rate is 15 seconds.

From Table 5.2, there is no significant difference in the F-ratio and W-ratio statistics obtained from the three methods. In terms of the estimated baseline components and the positional standard deviations, the results obtained from the three methods are also essentially identical (less than 0.1 mm). A comparison of the computational load is presented in Table 5.3.

Table 5.3 Comparison of computational time and memory usage.

Baseline	Method	Computational time (s)	Memory usage (Kbytes)
15m (5 sats)	Standard MINQUE	263.4	450.0
	Simplified MINQUE	7.6	7.5
	Proposed method	1.2	*None*
1km (7 sats)	Standard MINQUE	1519.0	1012.5
	Simplified MINQUE	33.2	16.9
	Proposed method	1.9	*None*
2km (6 sats)	Standard MINQUE	700.6	703.1
	Simplified MINQUE	18.6	11.7
	Proposed method	1.5	*None*

Remark: All solutions computed using Matlab GPS baseline software on

a PentiumII-366MHz processor.

Interestingly, if the matrix R^* in the simplified MINQUE method (see Equation (3.17)) is assumed to be constant, the variance-covariance components obtained from the proposed method are identical to those obtained from the simplified method. The assumption that the matrix R^* is constant is reasonable for short observation periods. This is supported by the study described in Han & Rizos (1995), which established that the maximum difference in the matrix A is about 8% for a 15 minute observation span.

In summary, the proposed method can not only substantially reduce the computational load but also ease the memory usage. The proposed method is therefore appropriate for estimating variance-covariance components in the segmented stochastic modelling procedure.

5.3   Test Data

Both simulated and real data have been used in this study.

5.3.1   Simulations

There are two main advantages to using simulated data: (a) to evaluate the performance of the proposed algorithm (since it is very difficult to derive highly accurate GPS station

coordinates in practice), and (b) to study the impact of incorporating different systematic errors. The data simulation involves two parts.

5.3.1.1   Simulating the raw GPS observations

A simulation of the raw GPS observations was performed using the Bernese GPS software version 4.0. Different observation noises were assigned to different satellites varying from 1mm to 3mm. Two data sets, for a 9km and a 79km baseline, were simulated. Details of these data sets are given in Table 5.4.

Table 5.4 Details of the simulated data sets.

Baseline length (km)	9	79
Survey date	March 1, 2000	March 1, 2000
Satellites observed	15,21,17,3,31, 23,9,29	1,5,9,11,14,15, 16,18,21,22,23, 25,29,30
Data interval (sec)	15	15
Data span (hr)	5	5

5.3.1.2   The systematic error components

A wavelet-based technique (e.g. Chui, 1992; Wickerhauser, 1994) was applied to the GPS DD residuals in order to extract the systematic error component. The GPS DD ambiguity-fixed residuals obtained from two real data sets were decomposed into the low-frequency bias and the high-frequency noise components. Both data sets were processed using the standard GPS data processing. The baseline lengths of the first and second data sets are 215m and 11km respectively. The dominant error of the first data set is multipath (the details of the first data set are also given in Chapter 6) while the dominant errors of the second data set are the atmospheric delays. The extracted systematic error component was then added to the simulated GPS observations. Two different systematic error patterns, denoted E1 (from the first data set) and E2 (from the second data set), were extracted and are plotted in Figures 5.2 and 5.3. These systematic error patterns have been used in subsequent analyses.
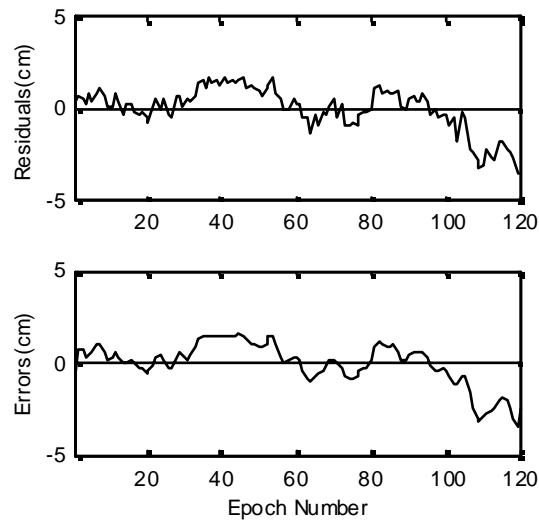
Figure 5.2 Signal extraction using wavelets. Top: Original DD residuals. Bottom: E1
error pattern.
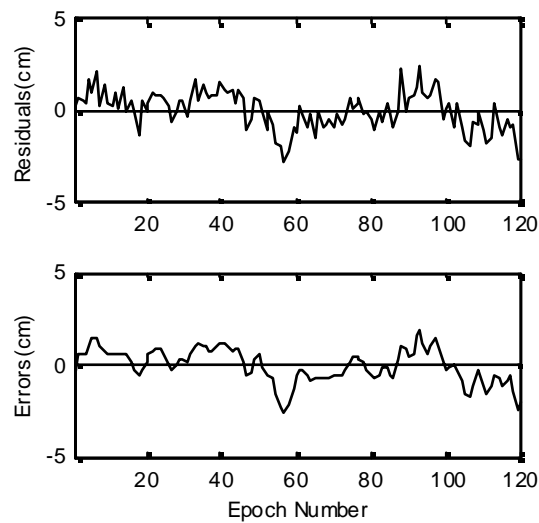
Figure 5.3 Signal extraction using wavelets. Top: Original DD residuals. Bottom: E2
error pattern.

5.3.2   Real Data Sets

Two data sets were downloaded from http://sopac.ucsd.edu/, collected by receivers of
the Southern California Integrated GPS Network (SCIGN). For demonstration purposes,

3-hr and 5-hr observation periods were considered for the 23km and 75km baseline data sets respectively (Table 5.5).

Table 5.5 Details of the real data sets.

Baseline length (km)	23	75
Survey date	Nov 23, 2000	Nov 23, 2000
Satellites observed	4,5,7,8,9,24,26	2,4,5,6,7,9,10, 17,30
Data interval (sec)	30	30
Data span (hr)	3	5

5.4   Results from Simulated Data Sets

In this Section the effectiveness of the proposed algorithm is demonstrated using both the short and medium length baseline data sets. For both data sets the impact of systematic errors on the GPS positioning results was analysed for two different cases. The first case involved varying the number of satellites but adding the same error pattern to the same satellite pair. In the second case, the two error patterns were added to the satellite pairs in an alternating fashion (see Tables 5.7 and 5.9). In this case, the approach consisted of the following steps: i) adding the error pattern E1 to different satellite pairs and obtaining a solution, ii) adding the error pattern E2 to different satellite pairs and obtaining a solution.

5.4.1   The Short Baseline

Matlab-coded GPS baseline processing software developed at The University of New South Wales was used to process the data sets. Only the L1 frequency data were used. To obtain more accurate baseline results for comparison purposes, the data set with observation noise was first processed using the MINQUE procedure and the results were used as reference values. Then, in both cases, the data set with intentionally added systematic errors was processed using the following two procedures:

A. The standard procedure with the simplified stochastic model (which includes only mathematical correlation), and assuming that temporal correlations are absent.

B. The segmented stochastic modelling procedure with a 20-epoch window width.

5.4.1.1   Case I – Varying the number of satellites

The number of satellites varied from 8 to 5 satellites, and the E1 error pattern was added to satellite pair PRN23-15 for every satellite geometry. The DD residuals for satellite pair PRN 23-15 are shown in Figure 5.4. The thick grey line denotes the post-fit residuals obtained using method A, while the thin line shows the residuals obtained from method B. It can be seen that the systematic errors of the transformed measurements are much smaller than those of the original measurements. Similar results from real data sets, for the short baseline case, were reported in Chapter 4.
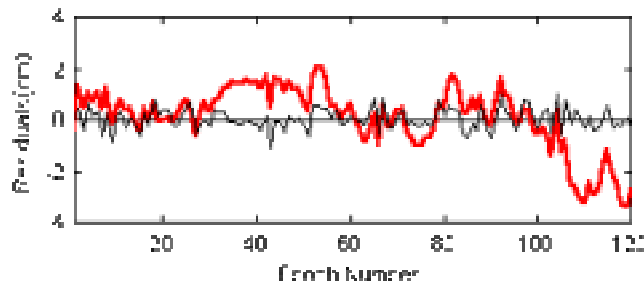
Figure 5.4 DD residuals obtained from the 9km baseline for satellite pair PRN 23-15.

The estimated baseline components obtained from both methods were compared with the reference values. The differences for each coordinate component and standard deviations are shown in Table 5.6. It can be seen that in all cases the proposed algorithm (B) produced more accurate results than the standard procedure (A).

Table 5.6 The differences between estimated baseline components and the reference values and standard deviations (Case I).

Sat used	Method	Difference in each component (mm)			Standard deviation (mm)		
		ΔN	ΔE	ΔH	N	E	H
8 sats	A	0.4	0.2	2.1	1.3	0.1	3.5
	B	0.0	0.0	0.0	1.7	0.1	5.6
7 sats	A	0.0	0.1	1.7	0.9	0.5	0.6
	B	0.0	0.0	0.0	0.9	0.4	2.3
6 sats	A	1.2	0.8	3.4	0.3	0.8	0.2
	B	0.0	0.0	0.0	1.5	0.0	3.2
5 sats	A	3.2	4.0	10.7	2.5	4.9	9.6
	B	0.0	0.0	0.0	0.7	0.9	1.1

Remark: E1 error pattern added to PRN23-15.

In addition, the impact of systematic errors on the positioning results tends to increase with a decrease in the number of satellites used in procedure A. In the case of 5 satellites, the difference in the height component is as large as 10.7mm.

5.4.1.2   Case II – Varying the error patterns and satellite pairs

The E1 and E2 error patterns were added to different satellite pairs for the geometry consisting of 5 satellites only. The DD residuals showed similar trends to those obtained for Case I. The differences in each coordinate component are shown in Table 5.7. It is evident that different error patterns and different satellites have a different influence on the positioning results using procedure A, but not for procedure B.

Table 5.7 The differences between estimated baseline components and the reference
values and standard deviations (Case II).

Error pattern /sat pair	Method	Difference in each component (mm)			Standard deviation (mm)		
		ΔN	ΔE	ΔH	N	E	H
E1/23-15	A	3.2	4.7	10.7	2.5	4.9	9.6
	B	0.0	0.0	0.0	0.7	0.9	1.1
E1/23-03	A	3.4	4.0	10.9	4.1	3.1	12.0
	B	0.0	0.0	0.0	0.7	0.9	1.1
E1/23-31	A	0.3	0.1	0.3	1.0	1.0	1.4
	B	0.0	0.0	0.0	0.7	0.9	1.1
E2/23-15	A	0.4	2.0	5.4	0.9	2.9	4.3
	B	0.0	0.0	0.0	0.7	0.9	1.1
E2/23-03	A	1.7	2.2	5.7	2.4	1.3	6.8
	B	0.0	0.0	0.0	0.7	0.9	1.1
E2/23-31	A	0.2	0.0	0.2	0.9	0.9	1.3
	B	0.0	0.0	0.0	0.7	0.9	1.1

5.4.2   The Medium Length Baseline

It is a common practice to process dual-frequency data in cases of medium length
baselines. The data processing consisted of three steps. The first and second steps were
carried out using the Bernese GPS software. The DD ambiguities were solved in the
first program run. These ambiguities were then introduced as fixed values in the next
program run. In this step, some information was output for further use with the Matlab-
coded GPS processing software. In the first and second program runs standard
parameters such as the Saastamoinen troposphere model and the IGS precise orbit were
used. In the third program run, the output information was processed using the proposed
procedure. Since the dual-frequency data were used, the initial coordinates applied to
simulate the GPS observations were used as true values for comparison purposes.
Similar to the short baseline case, in both cases the data set which contains systematic
errors was processed using procedures A and B.

5.4.2.1   Case I – Varying the number of satellites

The number of satellites varied from 14 to 11 satellites, and the E1 error pattern was added to the satellite pair PRN25-1 for every satellite geometry. The DD residuals for the satellite pair PRN25-1 are plotted in Figure 5.5. The thick grey line denotes the post-fit residuals obtained from procedure A, while the thin line shows the residuals obtained from procedure B. It is clear that the post-fit residuals obtained from procedure B are more random than those obtained using procedure A.
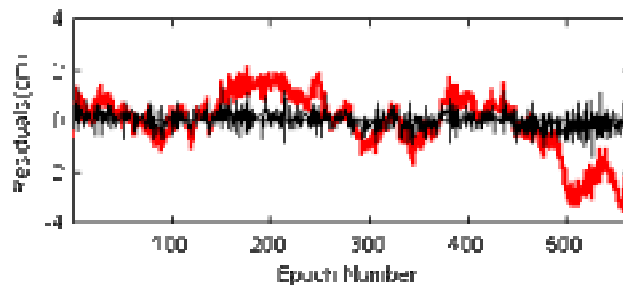
Figure 5.5 DD residuals obtained from the 79km baseline for satellite pair PRN25-1.

The estimated baseline components obtained from both methods were subsequently compared with the true values, and the differences in each coordinate component are shown in Table 5.8. The results are similar to the short baseline case. Therefore, it can be concluded that procedure B is a significant improvement over procedure A.

Table 5.8 The differences between estimated baseline components and the true values and standard deviations (Case I).

Sat used	Method	Difference in each component (mm)			Standard deviation (mm)		
		ΔN	ΔE	ΔH	N	E	H
14 sats	A	0.1	0.2	1.9	0.1	0.2	1.9
	B	0.0	0.0	0.0	0.0	0.0	0.0
13 sats	A	0.1	0.3	2.4	0.1	0.3	2.4
	B	0.1	0.0	0.1	0.1	0.0	0.1
12 sats	A	0.2	0.2	2.5	0.2	0.2	2.5
	B	0.1	0.0	0.1	0.1	0.0	0.1
11 sats	A	0.1	0.1	2.6	0.1	0.1	2.6
	B	0.1	0.0	0.2	0.1	0.0	0.2

Remark: E1 error pattern added to PRN25-1.

5.4.2.2   Case II – Varying the error patterns and satellite pairs

Once again the E1 and E2 error patterns were added to different satellite pairs for the geometry consisting of 11 satellites only. The DD residuals showed similar trends (for the sake of brevity, the residuals are not shown here). Table 5.9 shows the differences between the estimated baseline components and the true values. The results confirm that different error patterns and different satellites have a different influence on the positioning results for procedure A, but not for procedure B.

Table 5.9 The differences between estimated baseline components and the true values and standard deviations (Case II).

Error pattern /sat pair	Method	Difference in each component (mm)			Standard deviation (mm)		
		ΔN	ΔE	ΔH	N	E	H
E1/25-01	A	0.1	0.1	2.6	0.1	0.1	2.6
	B	0.1	0.0	0.2	0.1	0.0	0.2
E1/25-14	A	2.9	0.1	0.7	2.9	0.1	0.7
	B	0.0	0.0	0.0	0.2	0.0	0.1
E1/25-21	A	0.7	0.1	2.7	0.7	0.1	2.7
	B	0.1	0.0	0.3	0.1	0.0	0.3
E2/25-01	A	0.1	0.0	1.1	0.1	0.0	1.1
	B	0.1	0.1	0.2	0.1	0.1	0.2
E2/25-14	A	1.3	0.1	1.2	1.3	0.1	1.2
	B	0.1	0.0	0.1	0.1	0.0	0.1
E2/25-21	A	0.5	0.0	1.5	0.5	0.0	1.5
	B	0.1	0.0	0.2	0.1	0.0	0.2

5.5   Results from Real Data Sets

The data processing strategies used here are the same as in the medium length baseline case, except that systematic errors have not been added to the observations. The DD residuals obtained from all satellite pairs show similar trends. Selected residuals obtained from the 23km and 75km baselines are plotted in Figures 5.6 and 5.7 respectively. Again, the thick grey line denotes the post-fit residuals obtained from

procedure A, while the thin line shows the residuals obtained using procedure B. Clearly procedure B generates random residuals for both data sets.
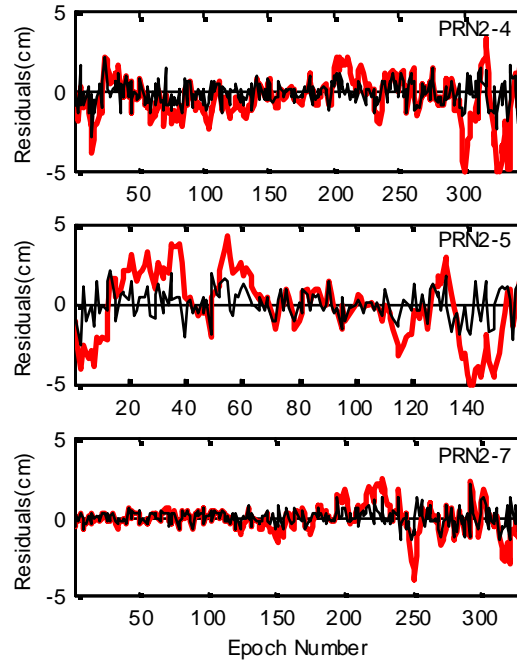
Figure 5.6 Selected DD residuals obtained from the 23km baseline for several satellite
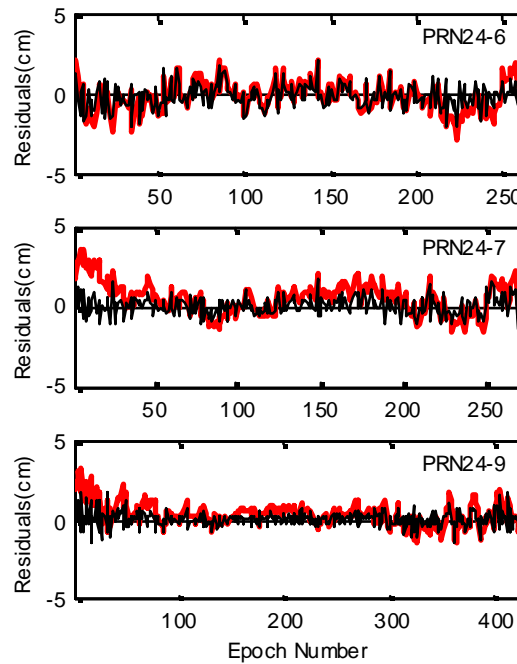
pairs.

Figure 5.7 Selected DD residuals obtained from the 75km baseline for several satellite

pairs.

The differences in estimated baseline components between procedures A and B are presented in Table 5.10. It can be seen that the differences are 1.2 mm and 1.9 mm for the 23-km and 75-km baselines consecutively. These discrepancies are certainly significant for high-accuracy applications.

Table 5.10 The differences in estimated baseline components between procedures A and B.

Baseline	Difference in each component (mm)		
	ΔN	ΔE	ΔH
23-km	0.8	0.2	1.2
75-km	1.9	1.9	0.1

5.6   Concluding Remarks

Based on a new framework of error analysis of GPS measurements, an improved stochastic modelling procedure, which takes into account the temporal correlations in the GPS measurements, has been introduced to effectively deal with long observation periods for high precision static positioning applications. It has been shown that any misspecification in the stochastic model may have a significant influence on the positioning results. The impact of temporal correlations was analysed using simulated and real data sets. The results indicate that there are significant biases in the positioning results when the temporal correlations are not taken into account in the stochastic model. By applying the proposed segmented stochastic modelling procedure, the residuals are more random and the accuracy of the estimated baseline components is improved to the millimetre level.

In summary, a segmented stochastic modelling procedure has been developed and its performance has been demonstrated in this Chapter. Furthermore, it was shown that the segmented stochastic modelling procedure could be applied not only to single-frequency data, but also to dual-frequency data (Sections 5.4 and 5.5). Hence, it is recommended that this method should be employed in the GPS data processing step for all precise static relative positioning applications.

As demonstrated in Section 5.3.1.2, wavelet decomposition has shown great potential in extracting a systematic error component from the GPS measurements. Therefore, it is interesting to further investigate the use of wavelet-based methods in GPS data processing. An approach to GPS analysis incorporating wavelet decomposition is presented in the next Chapter.

6.1   Introduction

The least-squares estimation method is usually employed for the processing of GPS measurements. The least-squares method is based on the formulation of a mathematical model consisting of the functional model and the stochastic model. If the functional model is adequate, the residuals obtained from the least-squares solution should be randomly distributed. However, the GPS measurements are contaminated by several kinds of errors or biases, such as orbital error, atmospheric biases, multipath disturbance and receiver noise. Dealing with such biases would be relatively straightforward if there were some apriori knowledge of the phenomena related to these errors. As this is not the case, the least-squares method generates residuals which contain the signature of both unmodelled systematic biases and random measurement noise. It is desirable to extract (or minimise) the systematic biases contained within the GPS measurements. Recently, some wavelet-based techniques have been introduced to the field of GPS data processing (e.g. Collin & Warnant, 1995; Fu & Rizos, 1997; Ogaja et al., 2001; Satirapod, 2001). The methods introduced have, for example, addressed some of the potential applications such as signal denoising, outlier detection, bias separation and data compression.

This Chapter proposes a new method based on a *wavelet* decomposition technique and a robust estimation of the VCV matrix. The wavelet technique is first applied to decompose the GPS double-differenced residuals into the low-frequency bias and high-frequency noise terms. The extracted bias component is then applied directly to the GPS measurements to correct for the trend introduced by this error component. The remaining terms, largely characterised by the GPS range measurements and high-frequency measurement noise, are expected to give the best linear unbiased solutions

from a least-squares process. The simplified MINQUE procedure (Satirapod et al, 2001b) is applied to formulate the stochastic model.

The content of this Chapter is organised as follows. First, the theory of wavelet decomposition and its application to GPS data processing is outlined. A discussion of the experimental results and analysis are then presented, followed by concluding remarks.

6.2   Wavelets

6.2.1   Theory

Wavelet theory provides a unified framework for a number of techniques which have been developed independently for various signal processing applications. It has potential applications in filtering, subband coding, data compression and multi-resolution signal processing. In particular, the Wavelet Transform (WT) is of interest for the analysis of *non-stationary* signals such as GPS measurements, because it provides an alternative to the classical Fourier Transform (FT), which assumes stationarity in signals. It can be viewed as an extension to Fourier analysis, which is well-suited for characterising signals whose spectral character change with time. Such signals are not well represented in time and frequency by the Fourier Transform methods. The method of wavelet analysis is closely related to time-frequency analysis based on the Wigner-Ville distribution (Olivier & Vetterli, 1991).

The WT involves representing general functions in terms of simple, fixed building 'blocks' at different scales and positions (Wickerhauser, 1994; Daubechies, 1990). These 'blocks' are actually a family of wavelet functions (or wavelet basis) generated from a prototype function, called a "mother" wavelet, by translation and scaling operations. That is, the signal is mapped to a time-scale plane that is analogous to the time-frequency plane used in the Fourier Transform.

Multi-resolution analysis provides a formal approach to constructing the wavelet basis. The idea of multi-resolution analysis is to write a function as a limit of successive approximations, each of which is a smoother version of the function. The sub-spaces contained within each other are meant to convey the notion of fine-to-coarse resolution, with the smoothness achieved through removal of some level of detail. For example, if the sub-space $V_{-1d}V_{0d}V_{1d}...$ and W_0 is the orthogonal compliment of $V_{0d}V_{-1}$, then

$$W_j \otimes V_j = V_{j+1}$$

The W_j contains the detailed information as the resolution goes from a finer (larger j) to a coarser (lower j) one. The sub-spaces, V_j each contain the best approximation at a particular resolution, that is:

$$\lim_{j \to \infty} V_j = \bigcup_{j \to -\infty}^{\infty} V_j$$

and there will be information loss as the resolution gets coarser (j = ..., -3, -2, -1, 0). That is, in the limit of the lowest resolution, the signal is approximated by 0:

$$\lim_{j \to \infty} V_j = \bigcup_{j \to -\infty}^{\infty} V_j = \{0\}$$

There are several types of Wavelet Transforms. For continuous signals, the time and scale parameters are continuous, leading to a Continuous Wavelet Transform (CWT). If the time and scale parameters are chosen to be discrete, this will give rise to a wavelet series expansion and hence a Discrete Wavelet Transform (DWT) for a discrete signal. As the scale parameter grows, the signal dilates more and, like a map, the image or Wavelet Transform gives a more 'global' or low-frequency view. The translation parameter serves to shift the function along the time axis. A special case is developed by discretization of the time-scale parameters. That is, if $a = 2^{-j}$ and $b = k2^{-j}$, the corresponding wavelets become a function of two integer parameters, j and k. For this case, the wavelets form a *dyadic series*.

Almost any function can be a prototype function, as long as it satisfies certain admissibility conditions. Daubechies (1990), for example, introduced a set of orthonormal wavelets and, more recently, a new family of non-orthogonal wavelets have been introduced by other authors. In general, the selection of the wavelet that best decomposes the data remains a research topic of its own.

6.2.2   Application of Wavelets to GPS Data Processing

A previous study by Fu & Rizos (1997) has outlined some of the applications of wavelets to GPS data processing. According to this study, the GPS bias terms such as multipath and ionospheric delay behave like low-frequency noise (between 0.00005 and 0.05 Hz) and the measurement noise as high-frequency noise (anything from DC to 10 Hz). Hence, the GPS bias terms are concentrated in the narrow low-frequency band and a high frequency resolution is needed to identify them. The Wavelet Transform can be used to achieve enough frequency resolution to discriminate these terms in the original GPS measurement. Figure 6.1 illustrates that process.

The key is to find or design the best *mother wavelet* to use in the transform. The mother wavelet is scaled in time (dilated or compressed) and also shifted in time to effectively scan across the time-domain signal. Compressing the mother wavelet's time duration (width) effectively creates a high-pass filter (HPF) for extracting the high-frequency components of the analysed signal, whereas dilating it creates a low-pass filter (LPF) for extracting the low-frequency components of the analysed signal.
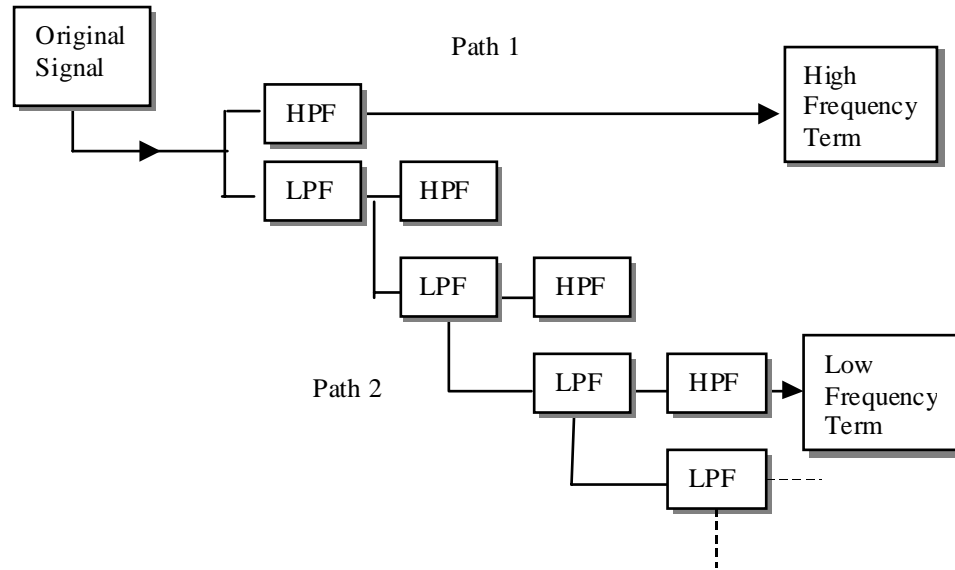
Figure 6.1 Applying a narrow daughter wavelet to the original signal is equivalent to applying a high-pass filter, which completes path 1. Extracting the leading low frequency requires applying a number of daughter wavelets that are wider than the signal you need to match, then applying a final daughter wavelet that becomes a high-pass filter, completing path 2.

A mother wavelet that approximates a bias term such as *multipath* is selected and dilated before performing the transform. To get the wavelet coefficients of sufficient magnitude to extract the bias term, the Wavelet Transform software has to process the wavelet a number of times, e.g. n times. For the first n-1 times the transform effectively passes the signal through a low-pass filter. On the nth time the transform would produce coefficients substantial enough to extract the remaining low-frequency signal through the high-pass filter. At that point the width of the wavelet becomes long enough for its frequency to be below that of the bias term, and thus the final stage is a high-pass filter. The combination of the n-1 low-pass filters and the final high-pass filter creates a *bandpass filter*.

Figure 6.2 is an example of results obtained after applying the process in Figure 6.1 to DD float ambiguity carrier phase residuals for a given pair of satellites. Path-1 indicates that the Wavelet Transform required just one high-pass filter to extract the high-frequency component of the residuals. Path-01, however, corresponds to two filter banks used to extract the corresponding high-frequency term at a different resolution

level. The zero indicates that the signal passed through one low-pass filter before the transform could apply a high-pass filter. Similarly, Path-00 corresponds to two filter banks of low-pass filters only for extracting the low-frequency component.
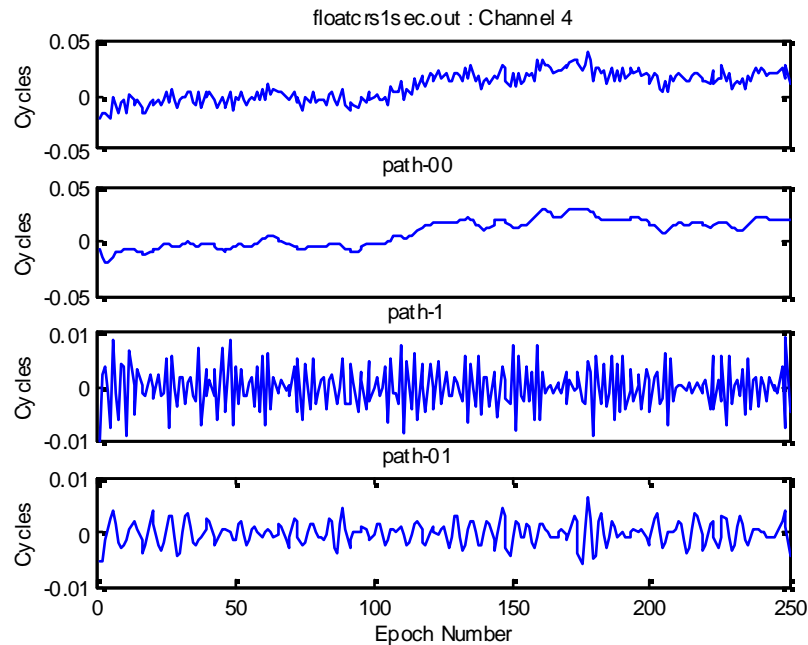
Figure 6.2 First row: DD float ambiguity carrier phase residuals (original signal); second row: low-frequency component; third row: high-frequency component; fourth row: high-frequency component (at higher resolution).

Once the wavelet application for extracting the low-frequency term corresponding to say *multipath* has been developed, it can be programmed to continuously process the GPS data affected by such biases.

6.3   Experimental Results

In this Section, results processed from real GPS data are presented, in order to demonstrate the usefulness of the proposed method of wavelet decomposition for extracting the low-frequency bias term. Static GPS data was analysed and the results from the processing are discussed.

6.3.1   Data Acquisition

The data set used here was collected on 7 June 1999 using two Ashtech Z-XII receivers at a sampling interval of 1 second. The receivers were mounted on pillars that are part of a first-order terrestrial survey network. The known baseline length between the two pillars is 215.929 ± 0.001m. This will be used as the ground truth to verify the accuracy of the results. A 30-minute span of data was extracted from the original data set and resampled every 15 seconds. Six satellites (PRNs 2, 7, 10, 13, 19, and 27) were selected, as they were visible during the entire selected observation period. All data were first processed using the standard GPS data processing method to check the data quality. In the data processing step, satellite PRN2 was selected as the reference satellite to form the double-differenced observables since it had the highest elevation angle. Double-differenced (DD) residuals for various satellite pairs are shown in Figure 6.3. The DD residuals indicate the presence of some significant multipath errors for satellite pairs PRN 2-7 and 2-19.
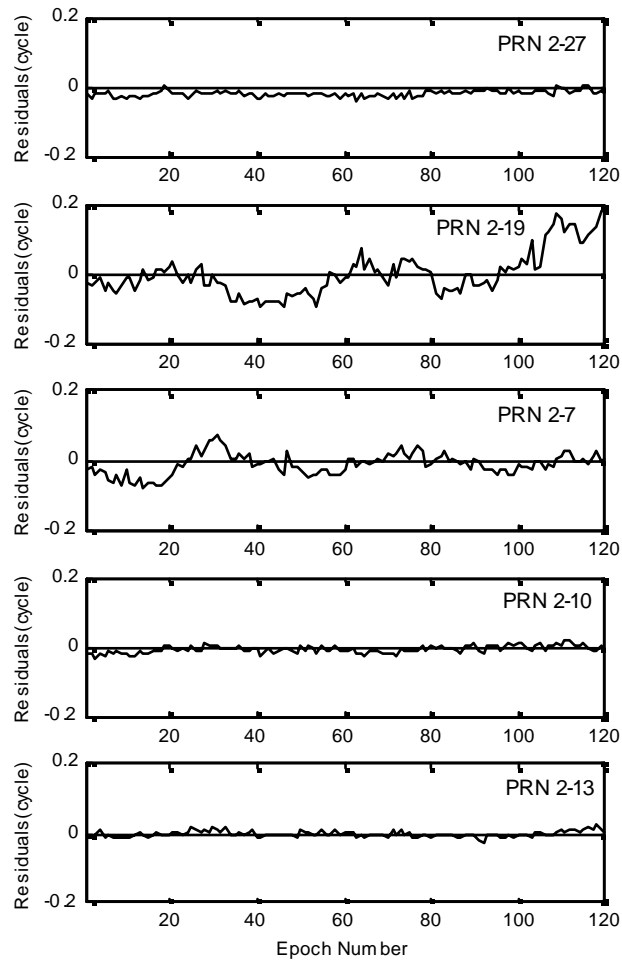
Figure 6.3 DD residuals obtained for the Ashtech receivers.

6.3.2   Data Processing Step

In data processing step, the data set was divided into three batches, each of ten minutes length. Each batch was first processed using the standard GPS data processing procedure and treated as an individual session. The wavelet technique was then used to decompose GPS double-differenced (ambiguity-free) residuals into the low-frequency bias and the high-frequency noise terms for each batch (see Figure 6.4, for example). The extracted bias component was applied directly to the GPS measurements to correct for this term, and the simplified MINQUE procedure was then employed to estimate the

variance-covariance matrix of the measurements. The results obtained from the standard procedure and the proposed procedure are discussed in the next Section.
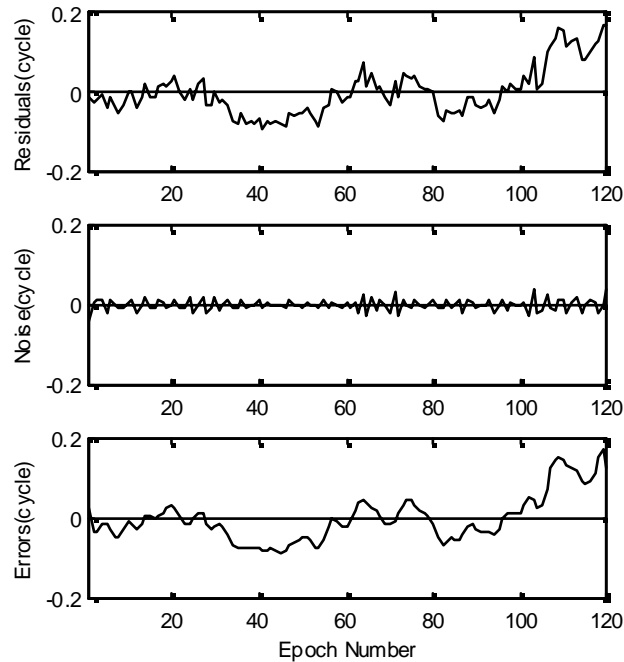
Figure 6.4 Signal extraction using wavelets for PRN 2-19. Top: Original DD residuals. Middle: Extracted noise component. Bottom: Extracted systematic component.

6.3.3   Analysis of Results

Results obtained from the processing described in the previous section have been analysed from two points of view: ambiguity resolution and the estimation of baseline components. For reliable ambiguity resolution, the difference between the best and second-best ambiguity combination is crucial for the ambiguity discrimination step. The F-ratio is commonly used as the ambiguity discrimination statistic, and the larger the F-ratio value the more reliable is assumed to be the ambiguity resolution. The critical value of the F-ratio is generally (arbitrarily) chosen to be 2.0 (e.g. Euler & Landau, 1992). The ambiguity validation test can also be based on an alternative statistic, the so-called W-ratio (Wang et al., 1998b). In a similar fashion, the larger the W-ratio value, the more reliable the ambiguity resolution is assumed. The values of these statistics obtained from the data processing step are shown in Figure 6.5. The top plot indicates

the F-ratio statistic, while the bottom plot represents the W-ratio statistic, where each group of columns represents the solution obtained from the three individual sessions. As can be seen, the F-ratio and W-ratio values obtained from the proposed procedure are larger compared to those from the standard procedure. This indicates that the certainty of the resolved ambiguities has been significantly improved.
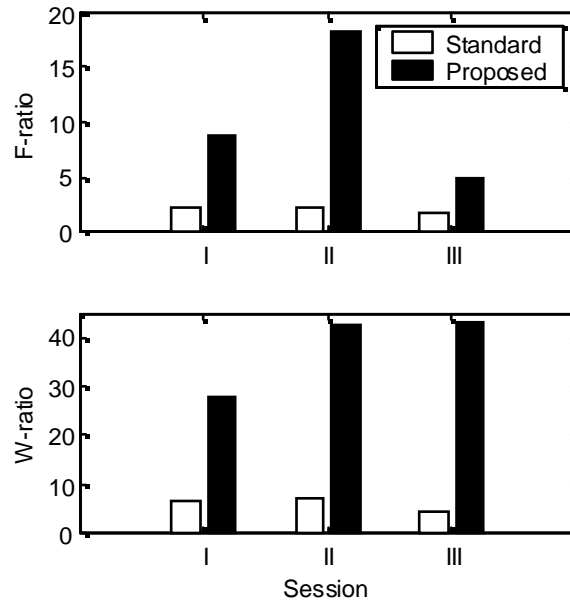
Figure 6.5 F-ratio (top) and W-ratio (bottom) statistics in ambiguity validation tests.

In the case of the estimated baseline components, the results are presented in Table 6.1. The results show that the proposed procedure generates more accurate estimated baseline components. This is confirmed by comparing the estimated baseline lengths obtained from both procedures to the known baseline length. The values of the estimated baseline length obtained from the proposed procedure are closer to the ground truth values than those obtained from the standard procedure. The maximum difference in the baseline length between sessions is 4.8 mm when the standard GPS data processing procedure is used. This is reduced to 0.2 mm when applying the proposed procedure. In addition, the maximum difference in the height component between sessions is up to 19.3 mm when the standard GPS data processing procedure is used. This is reduced to 9.3 mm when the proposed procedure is used.

Table 6.1 Estimated baseline components

Session	Procedure	Estimated baseline components(m)			Standard deviation (mm)			Baseline length (m)
		North	East	Height	North	East	Height	
I	Standard	-188.5131	105.2933	0.5107	0.9	0.8	1.4	215.9262
	Proposed	-188.5147	105.2933	0.5121	0.3	0.4	0.4	215.9276
II	Standard	-188.5135	105.2932	0.5075	0.9	0.8	1.3	215.9265
	Proposed	-188.5154	105.2925	0.5099	0.2	0.2	0.5	215.9278
III	Standard	-188.5068	105.2954	0.4914	1.4	1.3	2.2	215.9217
	Proposed	-188.5132	105.2961	0.5028	0.5	0.6	0.8	215.9276

In a further investigation, the DD (ambiguity-fixed) residuals were decomposed into their high and low-frequency components. The extracted systematic component was applied to the GPS measurements in the same way as in the above method. The results showed an improvement in statistics in ambiguity validation tests. However, the estimated baseline components obtained from this procedure exactly matched those obtained from the standard procedure.

6.4   Concluding Remarks

In this Chapter a procedure based on wavelet decomposition has been reviewed, and a new method of GPS data processing based on wavelet decomposition and the robust estimation of VCV matrix has been developed. Initial results from the proposed procedure indicate that both the ambiguity resolution and the accuracy of estimated baseline components are improved. In the worst data set, the statistics in the ambiguity validation test are improved by at least 2.83 times. The estimated baseline lengths obtained are much closer to the ground truth value than those obtained by the standard procedure. Furthermore, the variation in the height component between sessions is reduced by approximately a half when the proposed procedure is used.

In conclusion, the proposed procedure has been shown to produce encouraging results. However, due to the time limitation in conducting this research, the proposed procedure has not been fully tested using various data sets, over different baseline lengths. Before a solid conclusion can be drawn further tests will need to be conducted to validate the effectiveness of the proposed procedure.

AN IMPLEMENTATION OF THE SEGMENTED STOCHASTIC MODELLING PROCEDURE AND SOME CONSIDERATIONS

The investigations concerning the new stochastic modelling procedure were discussed in Chapters 3 to 5. The theoretical work basis of the procedure and the experimental results were presented in those chapters. In this Chapter the details of the segmented stochastic modelling procedure necessary to implement the proposed procedure are presented.

7.1   An Implementation of the Segmented Stochastic Modelling Procedure

The segmented stochastic modelling procedure can be conveniently divided into four steps, namely, *preparation*, *data segmentation*, *iteration*, and *final estimation*.

7.1.1   Preparatory Step

The Preparatory Step is the basic preparation procedure of standard GPS data processing, which can be summarised in Figure 7.1.

```
                            ╭─────────────╮
                            │    START    │
                            ╰─────────────╯
                                   │
                                   ▼
              ┌──────────────────────────────────────┐
              │ 1.1) Load observation files into the software │
              └──────────────────────────────────────┘
                                   │
                                   ▼
                   ┌──────────────────────────┐
                   │   1.2) GPS data reduction │
                   └──────────────────────────┘
                                   │
                                   ▼
                ┌─────────────────────────────────┐
                │ 1.3) Cycle slip detection and repair │
                └─────────────────────────────────┘
                                   │
                                   ▼
               ┌──────────────────────────────────┐
               │ 1.4) Form double-differenced observations │
               └──────────────────────────────────┘
                                   │
                                   ▼
               ┌──────────────────────────────────┐
               │ 1.5) Construct the standard stochastic model │
               └──────────────────────────────────┘
                                   │
                                   ▼
             ┌────────────────────────────────────────┐
             │ 1.6) Estimate the unknown parameters and residuals │
             └────────────────────────────────────────┘
                                   │
                                   ▼
                 ┌────────────────────────────┐
                 │  1.7) Estimate the VCV matrix │
                 └────────────────────────────┘
                                   │
                                   ▼
                  ╭───────────────────────────────╮
                  │   END OF PREPARATORY STEP     │
                  ╰───────────────────────────────╯
```
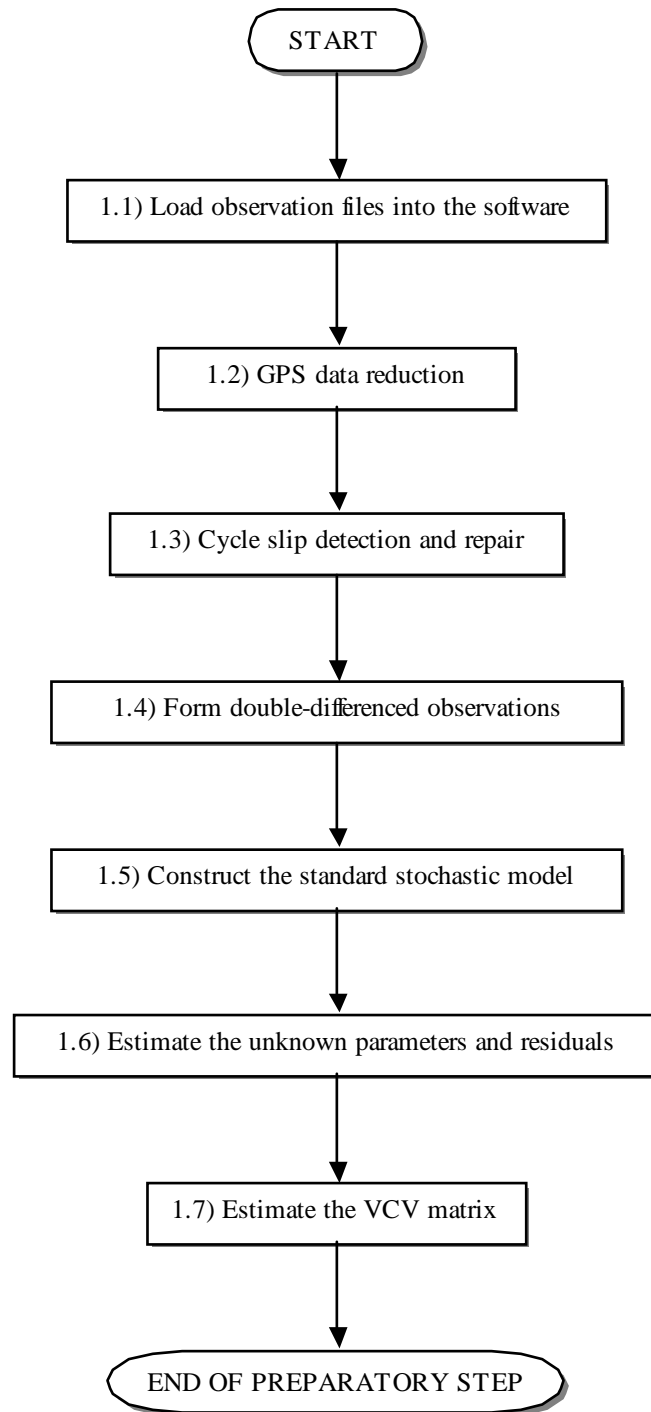
Figure 7.1 Flow chart for the Preparatory Step.

Step 1.1-- The observation files from both the reference and user receivers are loaded into the GPS data processing software.

Step 1.2 – Typically, the GPS observations are inserted into a database and receiver clock biases are calculated by using Single Point Positioning algorithms.

Step 1.3 -- The cycle slip detection and repair process is carried out in this step.

Step 1.4 -- The double-differenced observables are formed in this step.

Step 1.5 -- This step constructs the standard stochastic model represented by Equation (4.7). This standard stochastic model assumes that all observations have the same precision, and the mathematical correlation is taken into account in this stochastic model.

Step 1.6 -- This step estimates the unknown parameters (baseline components & ambiguity parameters) and residuals using Equations (4.8) and (4.9). The estimated parameters obtained from this step are the result of so-called *ambiguity-float solutions*.

Step 1.7 -- This step estimates the covariance matrix ($\hat{\Sigma} = \hat{\Omega}$) using Equation (4.10).

It can be seen that the Preparatory Step does not involve any iteration unless no good coordinates are known. In addition, if an ambiguity resolution step and an estimation of the baseline components (by introducing ambiguity parameters as known parameters) have been added before Step 1.7, this is essentially a standard GPS data processing procedure.

7.1.2   Data Segmentation Step

The basic process is to divide the whole measurement session into short segments, in which each segment there are the same number of satellites and all the measurements for the same satellite pairs have the same stochastic model. The Data Segmentation Step can be summarised in Figure 7.2.

```
                         ╭─────────────╮
                         │    START    │
                         ╰──────┬──────╯
                                │
                                ▼
              ┌─────────────────────────────────────┐
              │ 2.1) Define a default window width and│
              │    determine indices of measurements  │
              └─────────────────┬───────────────────┘
                                │
                                ▼
              ┌─────────────────────────────────────┐
              │ 2.2) Divide the time series of residuals│
              │          into short segments          │
              └─────────────────┬───────────────────┘
                                │
                                ▼
            ╭─────────────────────────────────────────╮
            │    END OF DATA SEGMENTATION STEP          │
            ╰───────────────────────────────────────────╯
```
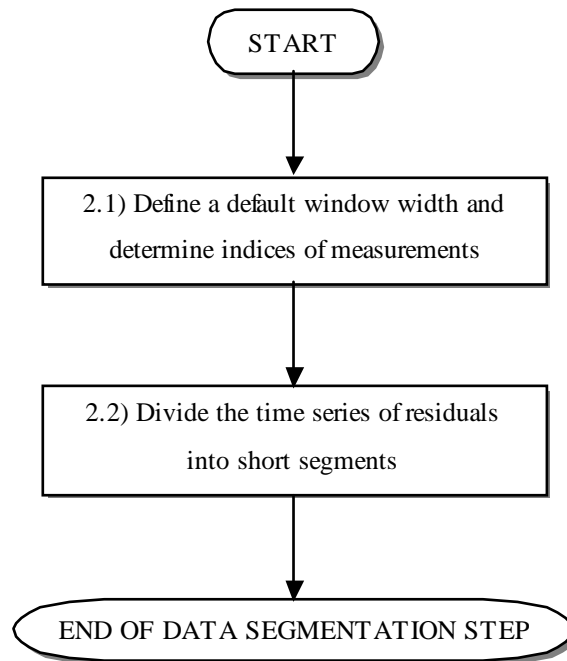
Figure 7.2 Flow chart for the Data Segmentation Step.

Step 2.1 -- A default window width is first selected. In this study a 20-epoch window width is used. Then, indices of when the satellite geometry has changed during the entire session are determined, and the number of observations between consecutive indices is stored.

Step 2.2 -- This step divides the data into short segments using the following criteria:

- If the number of observations between any pair of consecutive indices is larger than the default window width, the measurements are divided into short segments until the number of observations in the last segment is smaller than or equal to the default window width.

- If the number of observations from the last segment is smaller than the default window width, the observations from the last segment will be combined with the ones from the previous segment.

- However, if the number of observations between the consecutive indices is not sufficient to form a new segment, the stochastic model estimated from the previous segment is applied to these observations.

7.1.3 Iterative Step

The Iterative Step involves several phases, which may need iteration. The iterative step is illustrated in Figure 7.3.

Step 3.1 -- This step estimates the temporal correlation matrix $\hat{R}$ defined by Equation (5.1b) for each segment using Equations (5.2) and (5.3).

Step 3.2 -- This step constructs the transform matrix G using Equations (4.18), (4.19), (4.20) and (4.21) with the matrices $\hat{R}$ and $\hat{\Omega}$.

Step 3.3 -- The observation and design matrices are transformed using the following relationships $\bar{l} = Gl$ and $\overline{A} = GA$. It is also important to note that the integer nature of the double-differenced ambiguities still remains in the mathematical model as the transformation procedure only affects the design matrix A.

Step 3.4 -- This step estimates the variance-covariance matrix $\hat{\Omega}$ for the transformed measurements $\bar{l}$ using the proposed procedure defined by Equation (5.5).

Step 3.5 -- This step estimates the unknown parameters (baseline components and ambiguity parameters) using the transformed measurements and VCV matrix obtained from the previous step. The relationship between the unknown parameters and other matrices can be expressed as:

$$\hat{x} = [\overline{A}^T (\hat{\Omega}^{-1} \otimes I_s) \overline{A}]^{-1} \overline{A}^T (\hat{\Omega}^{-1} \otimes I_s) \bar{l}$$

Step 3.6 -- This step estimates the residuals of the original measurements $\hat{e}$ from Equation (4.9) using the estimated unknown parameters $\hat{x}$ obtained from the previous step.

```
                          ┌──────────┐
                          │  START   │
                          └──────────┘
                                │
                                ▼
    ┌──────────────────────────────────────────────────────────────┐
    │ 3.1) Estimate the temporal correlation coefficients for each segment │
    └──────────────────────────────────────────────────────────────┘
                                │
                                ▼
              ┌──────────────────────────────────┐
              │ 3.2) Construct the transform matrix │
              └──────────────────────────────────┘
                                │
                                ▼
              ┌──────────────────────────────────┐
              │ 3.3) Transform the measurements     │
              └──────────────────────────────────┘
                                │
                                ▼
    ┌──────────────────────────────────────────────────────────┐
    │ 3.4) Estimate the VCV matrix for the transformed measurements │
    └──────────────────────────────────────────────────────────┘
                                │
                                ▼
              ┌──────────────────────────────────┐
              │ 3.5) Estimate the unknown parameters │
              └──────────────────────────────────┘
                                │
                                ▼
          ┌────────────────────────────────────────────┐
          │ 3.6) Estimate the residuals of the original measurements │
          └────────────────────────────────────────────┘
                                │
                                ▼
  ┌────────────────────────────────────────────────────────────┐
  │ 3.7) Estimate the temporal correlation coefficients for each segment │
  └────────────────────────────────────────────────────────────┘
                                │
                                ▼
              ╱──────────────────────────────╲
     No      ╱      3.8) Is the accuracy         ╲
  ◄─────────◄              sufficient?             ►
             ╲                                    ╱
              ╲──────────────────────────────╱
                                │
                               Yes
                                ▼
                    ┌────────────────────────┐
                    │  END OF ITERATIVE STEP  │
                    └────────────────────────┘
```

Figure 7.3 Flow chart for the Iterative Step.

Step 3.7 -- This step estimates the temporal correlation matrix $\hat{R}$ for each segment using Equations (5.2) and (5.3) with the estimated residuals obtained from the previous step.

Step 3.8 -- This step checks the variations of the estimated elements of matrices $\hat{R}$ and $\hat{\Omega}$. In this study, the critical value for the variation of the estimated elements of matrix $\hat{R}$ is set as 0.01 while the critical value for the variation of the estimated elements of matrix $\hat{\Omega}$ is set as 0.0000005 cycle^2. If the variations of the estimated elements of matrices $\hat{R}$ and $\hat{\Omega}$ are less than the critical values, the iterative process will be terminated.

7.1.4   Final Estimation Step

The Estimation Step involves two simple steps, as illustrated in Figure 7.4.
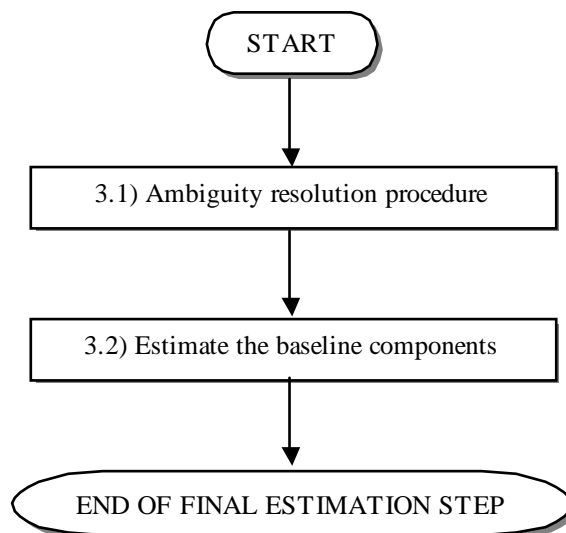

Figure 7.4 Flow chart for the Estimation Step.

Step 3.1 -- This step tries to resolve integer numbers of ambiguity parameters. In this study, the *LAMBDA* method (Tiberius and De Jonge, 1995) is used as an ambiguity resolution procedure.

Step 3.2 -- The ambiguity parameters obtained from the previous step are first introduced as the known parameters. Then, the baseline components are estimated using the following relationship:

$$\hat{x} = [\overline{A}^T (\hat{\Omega}^{-1} \otimes I_s) \overline{A}]^{-1} \overline{A}^T (\hat{\Omega}^{-1} \otimes I_s) \overline{l}$$

7.2   Some Considerations

Based on experience gained in the processing of GPS data with the segmented stochastic modelling procedure, the following comments can be made:

- The proposed procedure tends to show an improvement over the standard procedure when the observations are highly correlated.

- In the case of long observation period data sets, ambiguity resolution is not a critical issue. It is therefore recommended that the ambiguity resolution procedure be carried out before the iterative process begins.

- It is important to emphasise that the proposed procedure is restricted to the relative static GPS positioning mode. However, this procedure can be applied to any baseline length. In addition, it can be applied to single-frequency data as well as dual-frequency data.

8.1   Conclusions

In the case of GPS, two types of measurements, the pseudorange and the carrier phase, can be made with the aid of the incoming signals. Carrier phase measurements are much more precise than pseudorange measurements, and thus they are extensively used in precise static relative positioning applications. The GPS carrier phase measurements are generally processed using the least-squares method, for which both the functional and stochastic models need to be carefully defined. Whilst the functional model for precise GPS positioning is sufficiently well known, realistic stochastic modelling for the GPS carrier phase measurements is still both a controversial topic and a difficult task to accomplish in practice. Therefore, substantial investigations concerning the stochastic modelling issue have been conducted in this study.

8.1.1   Quality Indicators for GPS Carrier Phase Observations

Recently investigators have used two types of external information, namely Signal-to-Noise Ratio (SNR) and satellite elevation angle, as quality indicators for GPS carrier phase observations. These two data quality indicators are widely used for generating the stochastic model of the GPS observations. In this study, these indicators have been compared. Single-differenced residuals were used to analyse the validity of the quality indicators, on a satellite-by-satellite basis. Based on the results obtained from a series of tests, it can be concluded that these two quality indicators do not always indicate the same quality trend. In general, both SNR values and satellite elevation angle information can be used as quality indicators, but they do not always reflect reality.

Therefore, the challenge was to develop more rigorous quality indicators for high-accuracy positioning applications.

8.1.2   A Simplified MINQUE Procedure for the Estimation of Variance-Covariance Components for GPS Observables

Minimum Norm Quadratic Unbiased Estimation (MINQUE) is one of the commonly used methods for the estimation of variance-covariance components and in this study has been successfully used to estimate the variance-covariance components of the GPS observables. However, the MINQUE procedure imposes a big computational burden, and the requirement of having an equal number of variance-covariance components in the estimation step is a major limitation. It is therefore difficult to implement this procedure when the number of observed satellites has changed during an observation period. In this study, a simplified MINQUE procedure is proposed, for which the computational load and time are significantly reduced. The quality of the results obtained is very similar to those from the rigorous procedure. Furthermore, the effect of a changing number of satellites on the computations is effectively dealt with.

8.1.3   An Iterative Stochastic Modelling Procedure

As previously stated, the GPS measurements have a heteroscedastic, space- and time-correlated error structure. In this study, an iterative stochastic modelling procedure has been proposed to directly estimate the time correlation coefficients, and the time-independent variance and covariance components of the GPS observables. The basic idea behind the iterative stochastic modelling procedure is that the double-differenced (DD) carrier phase observables are transformed into a set of new observables using estimated temporal correlation coefficients. The transformed observables are free of temporal correlations and thus have a block diagonal variance-covariance matrix. Consequently, the immense memory usage and computational load for the inversion of a fully populated variance-covariance matrix can be avoided, and the variance-covariance matrix for the transformed observables can be estimated using a rigorous statistical method such as the MINQUE. An iterative process is performed until

sufficient accuracy is achieved. Test results indicate that by applying the stochastic assessment procedure developed here, the certainty of the estimated positioning results is improved. In addition, the quality of ambiguity resolution can be more realistically evaluated.

8.1.4   A Segmented Stochastic Modelling Procedure

As demonstrated in Chapter 4, the iterative stochastic modelling procedure is suitable for short observation periods as it assumes that the temporal correlation coefficients and the variance of GPS measurements are constant for the whole observation period. In practice, an observation period of several hours may be expected for some geodetic applications. The assumption that the temporal correlation coefficients and the variance of GPS measurements are constant for the whole observation period is therefore not realistic. In addition, the memory usage and computational load can become unbearable when the standard MINQUE technique (or even the simplified MINQUE procedure) is applied to long observation period data sets. Thus, it was necessary to develop a new stochastic modelling procedure that addressed these shortcomings.

Based on the iterative stochastic modelling procedure developed in Chapter 4, a segmented stochastic modelling procedure has been proposed that deals with long observation period data sets, and at the same time reduces the computational load. This procedure also takes into account the temporal correlations in the GPS measurements. The effectiveness of the new procedure is tested using both real and simulated data sets for short to medium length baselines. By applying the proposed segmented stochastic modelling procedure it has been found that the residuals are more random and the accuracy of the estimated baseline components is improved to the millimetre level. More importantly, the segmented stochastic modelling procedure can be used not only with single-frequency data, but also dual-frequency data.

8.1.5   GPS Analysis with the Aid of Wavelets

Classical least-squares processing of GPS measurements generates residuals which contain the signature of both unmodelled systematic biases and random measurement noise. It is desirable to extract (or minimise) the systematic biases contained within the GPS measurements. This would be relatively straightforward if there were some apriori knowledge of the phenomena related to these errors. Common ways of dealing with this problem include: (i) changes to the stochastic modelling, and (ii) redefinition of the functional model.

In this study, a method based on *wavelets* is applied to decompose GPS double-differenced residuals into a low-frequency bias term and a high-frequency noise term. The extracted bias component is then applied directly to the GPS measurements to correct for this term. The remaining terms, largely characterised by the GPS range measurements and high-frequency measurement noise, are expected to give the best linear unbiased solutions from a least-squares process. A robust VCV estimation, using the simplified MINQUE procedure, controls the formulation of the stochastic model. The results indicate that this method can improve both the ambiguity resolution and the accuracy of the estimated baseline components.

8.2   Recommendations

Based on both the theoretical studies and experimental results obtained in this research, the following recommendations are made for future research work.

1)   As demonstrated in Chapter 5, initial experiments have shown promising results. However, there are some challenges in implementing the segmented stochastic modelling procedure for precise positioning in geodetic applications. These are summarised as follows:

   • The optimal length of the segments to be used in the stochastic modelling procedure needs to be investigated in more detail. This is to ensure that a robust

performance can be achieved. A possible criterion for this purpose is the degree of stationarity of the time series of residuals. Appropriate measures will need to be developed and tested to check for stationarity of data on-line.

- The significance of the inter-temporal correlations (for different satellite pairs) should be statistically tested. Although extensive experiments have confirmed that there are significant temporal correlations within the residuals for the same satellite pairs, the inter-temporal correlations between the time series for the different satellite pairs are not well understood. If some of the inter-temporal correlation coefficients are small, or insignificant, they could be considered as zero, and then removed from the unknown parameter set. This will improve the certainty of the estimation of the other unknown parameters since the geometry of the solution is strengthened.

2) As demonstrated in Chapter 6, a new method based on the wavelet decomposition technique and a robust estimation of the variance-covariance matrix has been shown to improve the certainty of ambiguity resolution and the accuracy of estimated baseline components. However, there are some challenges in implementing the proposed procedure. These are summarised as follows:

- In order to optimise the effectiveness of the proposed method, an optimal degree of wavelet coefficients for different types of systematic errors (i.e. multipath error, ionospheric delay, tropospheric delay etc.) needs to be investigated.

- Before a firm conclusion can be made, the effectiveness of this method should be tested and evaluated with various data sets, especially for medium and long baselines. Future work will focus on comparing the segmented stochastic modelling procedure and the proposed method based on a combination of the wavelet decomposition technique and a robust estimation of the variance-covariance matrix.

- This method may be further developed for other applications (for example, dual-frequency multi-reference stations for a small area network). The wavelet

decomposition may be applied to reduce the noise level of the correction terms generated by a network of multi-reference stations for various applications (e.g. Chen et al., 2000; Janssen et al., 2001; Rizos et al., 2000).

REFERENCES

Barnes, B.J., Ackroyd, N. and Cross, P.A. (1998) Stochastic modelling for very high precision teal-time kinematic GPS in an engineering environment, *FIG XXI International Conference*, Brighton, U.K., 21-25 July, Commission 6, 61-76.

Blewitt, G., Lindqwister, U.J. and Hudnut, K.W. (1989) Densification of continuously operating GPS arrays using rapid static surveying techniques, *Eos, Transaction of American Geophysics Union*, 70(43), 1054.

Borre, K. and Tiberius C.C.J.M. (2000) Time series analysis of GPS observables, *13th International Technical Meeting of the Satellite Division of the Institute of Navigation, ION GPS-2000*, Salt Lake City, Utah, 19-22 September, 1885-1894.

Brunner, F.K., Hartinger, H. and Troyer, L. (1999) GPS signal diffraction modelling: The stochastic SIGMA-Δ model, *Journal of Geodesy*, 73, 259-267.

Brunner, F.K. and Welsch, W.M. (1993) Effect of the troposphere on GPS measurements, *GPS World*, 4(1), 42-51.

Cannon, M.E. (1998) Dynamic real time precise positioning, *ION GPS-98 tutorial notes*, Nashville, Tennessee, 15 September, 5-7.

Cannon, M. E. and Lachapelle, G. (1995) Kinematic GPS trends: equipment, methodologies and applications, In: Beutler, Hein, Melbourne & Seeber (Ed.): *GPS Trends in Precise Terrestrial, Airborne, and Space-borne Applications, IAG Symposium No. 115*, Springer-Verlag, Berlin Heidelberg New York, 161-169.

Chen, D. S. (1994) *Development of a Fast Ambiguity Search Filtering (FASF) Method for GPS Carrier Phase Ambiguity Resolution,* Ph.D thesis, Department of Geomatics Engineering, University of Calgary, Canada, 98pp.

Chen, X., Han, S., Rizos, C. and Goh, P.C. (2000) Improving real-time positioning efficiency using the Singapore Integrated Multiple Reference Station Network (SIMRSN), *13ᵗʰ International Technical Meeting of the Satellite Division of the Institute of Navigation, ION GPS-2000*, Salt Lake City, Utah, 19-22 September, 9-18.

Chui C.K. (1992) *An Introduction to Wavelets,* Academic Press, Inc., Boston, 264pp.

Clarke, B. (1994) *Aviator's Guide to GPS*, McGraw-Hill, Inc., 235pp.

Collin, F. and Warnant, R. (1995) Applications of the wavelet transform for GPS cycle slip correction and comparison with Kalman filter, *Manuscripta Geodaetica*, 20, 161-172.

Comp, C.J. and Axelrad, P. (1996) An adaptive SNR-based carrier phase multipath mitigation technique, *9ᵗʰ International Technical Meeting of the Satellite Division of the Institute of Navigation, ION GPS-96*, Kansas City, Missouri, 17-20 September, 683-697.

Counselman, C.C. and Shapiro, I.I. (1979) Miniature interferometric terminals for earth surveying, *Bulletin Geodesique*, 53, 139-163.

Crocetto, N., Gatti, M. and Russo, P. (2000) Simplified formulae for the BIQUE estimation of variance components in disjunctive observation groups, *Journal of Geodesy*, 74, 447-457.

Cross, P.A., Hawksbee, D.J. and Nicolai, R. (1994) Quality measures for differential GPS positioning, *The Hydrographic Journal*, 72, 17-22.

Daubechies, I. (1990) The wavelet transform, time-frequency localisation and signal analysis, *IEEE trans. IT*, 36(5).

Dodson A., Shordlow, P., Hubbard, L., Elgered, G. and Jarlemark, P. (1996) Wet tropospheric effects on precise relative GPS height determination, *Journal of Geodesy*, 70, 188-202.

Durbin, J. and Watson, G.S. (1950) Testing for serial correlation in least squares regression I, *Biometrika*, 37, 409-428.

El-Rabbany, A.E-S. (1994) *The effect of Physical Correlations on the Ambiguity Resolution and Accuracy Estimation in GPS Differential Positioning*, Ph.D. thesis, Department of Geodesy and Geomatics Engineering, University of New Brunswick, Canada, 161pp.

Enge, P.K. and Van Dierendonck, A.J. (1996) Wide Area Augmentation System, In *Global Positioning System: Theory and Applications (Vol. 2)*, Edited by Parkinson & Spilker, American Institute of Aeronautics and Astronautics, Inc., Washington D.C., 117-142.

Erickson, C. (1992) *Investigation of C/A Code and Carrier Measurement and Techniques for Rapid Static GPS Surveys*, UCGE Report Number 20044, The University of Calgary, 180pp.

Estey, L.H. and Meertens, C.M. (1999) TEQC: The multi-purpose toolkit for GPS/GLONASS data, *GPS Solutions*, 3(1), 42-49.

Euler, H.J. and Goad, C.C. (1991) On optimal filtering of GPS dual-frequency observations without using orbit information. *Bull Geod*, 65, 130-143.

Euler, H.J. and Landau, H. (1992) Fast GPS ambiguity resolution on-the-fly for real-time applications, *6th International Symposium on Satellite Positioning*, Columbus, Ohio, 17-20 March, 650-659.

Euler, H.J., Sauermann, K. and Becker, M. (1990) Rapid ambiguity fixing in small scale networks, *Second International Symposium on Precise Positioning with the Global Positioning System*, Ottawa, Canada, 3-7 September, 508-523.

Euler, H.J. and Schaffrin, B. (1990) On a measure of the discernibility between different ambiguity solutions in the static-kinematic GPS-mode, *IAG International Symposium No. 107 on Kinematic Systems in Geodesy, Surveying and Remote Sensing*, Springer Verlag, New York, 10-13 September, 285-295.

Frei, E. and Beulter, G. (1990) Rapid static positioning based on the Fast Ambiguity Resolution Approach FARA: Theory and first results, *Manuscripta Geodaetica*, 15, 325-356.

Fu, W.X. and Rizos, C. (1997) The applications of wavelets to GPS signal processing, *10th International Technical Meeting of the Satellite Division of the Institute of Navigation, ION GPS-97*, Kansas City, Missouri, 16-19 September, 1385-1388.

Georgiadou, Y. and Doucet, K.D. (1990) The issue of Selective Availability, *GPS World*, 1(5), 53-56.

Georgiadou, Y. and Kleusberg, A. (1989) On carrier signal multipath effects in relative GPS positioning, *Manuscripta Geodaetica*, 14, 143-148.

Gerdan, G.P. (1995) A comparison of four methods of weighting double-difference pseudo-range measurements. *Trans Tasman Surveyor*, Canberra, Australia, 1, 60-66.

Gianniou, M. and Groten, E. (1996) An advanced real-time algorithm for code and phase DGPS. *Paper presented at DSNS'96 Conference*, St. Petersburg, Russia, 20-24 May.

Goad, C.C. (1987) Precise positioning with the GPS, *In Applied Geodesy, Lecture Notes in Earth Sciences*, Edited by Turner, Springer-Verlag, Berlin, 12, 17-30.

Gourevitch, S. (1996) Measuring GPS receiver performance: A new approach. *GPS World*, 7(10), 56-62.

Guilkey, D.K. and Schmidt, P. (1973) Estimation of seemingly unrelated regressions with vector autoregressive errors, *Journal of the American Statistical Association*, 68, 642-647.

Han, S. (1997) Quality control issues relating to instantaneous ambiguity resolution for real-time GPS kinematic positioning, *Journal of Geodesy*, 71, 351-361.

Han, S. and Rizos, C. (1995) Standarization of the variance-covariance matrix for GPS rapid static positioning, *Geomatics Research Australasia*, 62, 37-54.

Hartinger, H. and Brunner, F.K. (1998) Attainable accuracy of GPS measurements in engineering surveying, *Proceedings of FIG XXI International Conference*, Brighton, UK, 21-25 July, Commission 6, 18-31.

Hatch, R. (1986) Dynamic differential GPS at the centimetre level, *Fourth International Geodetic Symposium on Satellite Positioning*, Austin, Texas, 28 April-2 May, 1287-1298.

Hatch, R. and Euler, H.-J. (1994) Comparison of several AROF kinematic techniques, *7th International Technical Meeting of the Satellite Division of the Institute of Navigation, ION GPS-94*, Salt Lake City, Utah, 20-23 September, 363-370.

Hofmann-Wellenhof, B., Lichtenegger, H. and Collins, J. (1997) *Global Positioning System: Theory and Practice*, 4th edition, Springer-Verlag, Berlin Heidelberg New York, 389pp.

Howind, J., Kutterer, H. and Heck, B. (1999) Impact of temporal correlations on GPS-derived relative point positions, *Journal of Geodesy*, 73, 246-258.

IGS (2001) The International GPS Service web site: http://igscb.jpl.nasa.gov/components/prods.html.

Janssen, V., Roberts, C., Rizos, C. and Abidin, H. (2001) Experiences with a mixed-mode GPS-based volcano monitoring system at Mt. Papandayan, Indonesia, *Geomatics Research Australasia*, 74, 43-58.

Jin, X. (1996) *Theory of Carrier Adjusted DGPS Positioning Approach and Some Experimental Results*, Ph.D. thesis, Delft University Press, Technical University of Delft, The Netherlands, 162pp.

JPS (1998) A GPS Tutorial: Basics of High Precision Global Positioning Systems, Javad Positioning Systems, Inc., http://www.topconps.com

Kaplan, E. (ed.) (1996) *Understanding GPS: Principles & Applications*, Artech House Publishers, Boston London, 554pp.

Kee, C. (1996) Wide Area Differential GPS, In *Global Positioning System: Theory and Applications (Vol. 2)*, Edited by Parkinson & Spilker, American Institute of Aeronautics and Astronautics, Inc., Washington D.C., 81-115.

Kim, D. and Langley, R.B. (2001) Estimation of the stochastic model for long-baseline kinematic GPS applications, *The Institute of Navigation 2001 National Technical Meeting*, Long Beach, CA, 22-24 January, 586-595.

King, R.W., Masters, E.G., Rizos, C., Stolz, A. and Collins, J. (1987) *Surveying with GPS*, Dümmler, 128pp.

Klobuchar, J.A. (1987) Ionospheric time-delay algorithm for single-frequency GPS users, *IEEE Transactions on Aerospace and Electronic Systems*, AES-23(3), 325-331.

Klobuchar, J.A. (1991) Ionospheric effects on GPS, *GPS World*, 2(4), 48-51.

Lachapelle, G. (1990) GPS observables and error sources for kinematic positioning, *IAG International Symposium No. 107 on Kinematic Systems in Geodesy, Surveying and Remote Sensing*, Springer Verlag, New York, 10-13 September, 17-26.

Lamons, W. (1990) A program status report on the Navstar Global Positioning System (GPS), *Second International Symposium on Precise Positioning with the Global Positioning System*, Ottawa, Ontario, 3-7 September, 3-8.

Langley, R.B. (1993) The GPS observables, *GPS World*, 4(4), 52-59.

Langley, R.B. (1997) GPS receiver system noise, *GPS World*, 8, 40-45.

Langley, R.B. (1998) RTK GPS, *GPS World*, 9(9), 70-76.

Lau, L. and Mok, E. (1999) Improvement of GPS relative positioning accuracy by using SNR, *Journal of Surveying Engineering,* 125(4), 185-202.

Leick, A. (1995) *GPS Satellite Surveying,* 2nd edition, John Wiley & Sons, Inc., New York, 560pp.

Lin, L.S. (1997) *Real-Time Estimation of Ionospheric Delay Using GPS Measurements*, Ph.D. thesis, School of Geomatic Engineering, The University of New South Wales, Sydney, Australia, 198pp.

NGS (2001) National Geodetic Survey web site: http://www.ngs.noaa.gov/ANTCAL/

NIMA (1997) *Department of Defense World Geodetic System 1984: Its Definition and Relationships with Local Geodetic Systems*, NIMA TR8350.2, 3rd edition, National Imagery and Mapping Agency, St. Louis, MO, 170pp.

Ogaja, C., Rizos, C., Wang, J. and Brownjohn, J. (2001) Towards the implementation of on-line structural monitoring using RTK-GPS and analysis of results using the wavelet transform, *10th FIG Int. Symp. on Deformation Measurements*, Orange, California, 19-22 March, 284-293.

Olivier, R. and Vetterli, M. (1991) Wavelets and signal processing, *IEEE Sig. Processing*, October, 14-38.

Parkinson, B.W. (1979) Global Positioning System (NAVSTAR), *Bulletin Geodesique*, 53, 89-108.

Parkinson, B.W. (1994) GPS eyewitness: the early years, *GPS World*, 5(9), 32-45.

Parkinson, B.W. (1996) GPS Error analysis, In *Global Positioning System: Theory and Applications (Vol. 1)*, Edited by Parkinson & Spilker, American Institute of Aeronautics and Astronautics, Inc., Washington D.C., 469-483.

Parkinson, B.W. and Enge, P.K. (1996) Differential GPS, In *Global Positioning System: Theory and Applications (Vol. 2)*, Edited by Parkinson & Spilker, American Institute of Aeronautics and Astronautics, Inc., Washington D.C., 3-50.

Parkinson, B.W. and Spilker Jr., J.J. (eds.) (1996) *Global Positioning System: Theory and Applications (Vol. 1)*, American Institute of Aeronautics and Astronautics, Inc., Washington D.C., 793pp.

Qiu, W. (1993) *An Analysis of Some Critical Error Sources in Static GPS Surveying*, UCGE Report Number 20054, The University of Calgary, 102pp.

Rao, C.R. (1970) Estimation of heterogeneous variances in linear models, *Journal of American Statistical Association*, 65, 161-172.

Rao, C.R. (1971) Estimation of variance and covariance components- MINQUE, *Journal of Multivariate Analysis*, 1, 257-275.

Rao, C.R. (1979) MINQUE Theory and its relation to ML and MML estimation of variance components, *Sankhya*, 41, Series B, 138-153.

Remondi, B.W. (1985) Performing centimetre accuracy relative surveys in seconds using carrier phase, *First International Symposium on Precise Positioning with the Global Positioning System*, Rockville, Maryland, 15-19 April, 1, 789-797.

Rizos, C. (1997) *Principles and Practice of GPS Surveying*, Monograph 17, School of Geomatic Engineering, The University of New South Wales, 555pp.

Rizos, C., Han, S. and Hirsch, B. (1997) A high precision real-time GPS surveying system based on the implementation of a single-epoch ambiguity resolution algorithm, *38th Australian Surveyors Congress*, Newcastle, Australia, 12-18 April, 20.1-20.10.

Rizos, C., Han, S., Ge, L., Chen, H.Y., Hatanaka, Y. and Abe, K. (2000) Low-cost densification of permanent GPS networks for natural hazard mitigation: first tests on GSI's Geonet network, *Earth, Planets & Space*, 52(10), 867-871.

Rizos C. and Satirapod C. (2001) GPS with SA off: How Good Is It? *Measure & Map*, 12, 19-21.

Roberts, C. and Rizos, C. (2001) Mitigating differential troposphere for GPS-based volcano monitoring, *5th International Symposium on Satellite Navigation Technology & Applications*, Canberra, Australia, 24-27 July, paper 38.

Rothacher, M., Beulter, G., Gurtner, W., Schneider, D., Wiget, A., Geiger, A. and Kahle, H.G. (1990) The role of atmosphere in small GPS networks, *Second International Symposium on Precise Positioning with the Global Positioning System*, Ottawa, Ontario, 3-7 September, 581-598.

Sargan, J.D. (1961) The maximum likelihood estimation of econometric relationships with autoregressive residuals, *Econometrica*, 29, 414-426.

Satirapod, C. (1999) The effect of a new stochastic model on GPS epoch-by-epoch solutions, *presented at the 27th Annual Research Seminars*, School of Geomatic Engineering, The University of New South Wales, Sydney, Australia, 8-9 November.

Satirapod, C. (2001) Improving the accuracy of static GPS positioning with a new stochastic modelling procedure, *to be presented at 14th International Technical Meeting of the Satellite Division of the Institute of Navigation, ION GPS-2001*, Salt Lake City, Utah, 11-14 September.

Satirapod, C. and Wang, J. (2000) Comparing the quality indicators of GPS carrier phase observations, *Geomatics Research Australasia*, 73, 75-92.

Satirapod, C., Wang, J. and Rizos, C. (2000) Stochastic modelling in GPS data processing, *presented at the 28th Annual Research Seminars*, School of Geomatic Engineering, The University of New South Wales, Sydney, Australia, 20-21 November.

Satirapod, C., Ogaja, C., Wang, J. and Rizos, C. (2001a) GPS analysis with the aid of wavelets, *5th International Symposium on Satellite Navigation Technology & Applications*, Canberra, Australia, 24-27 July, paper 39.

Satirapod, C., Wang, J. and Rizos, C. (2001b) A simplified MINQUE procedure for the estimation of variance-covariance components of GPS observables, *Submitted to Survey Review*.

Sauer, D. B., Frei, E. and Beulter, G. (1992) The importance of code measurements in relative positioning and navigation, *5th International Technical Meeting of the Satellite Division of the Institute of Navigation, ION GPS-92*, Albuquerque, New Mexico, 22-24 September, 1043-1051.

Seeber, G. (1993) *Satellite Geodesy: Foundations, Methods & Applications,* Walter de Gruyter, Berlin New York, 531pp.

Sleewaegen, J.M. (1997) Multipath mitigation, benefits from using the Signal-to-Noise Ratio, *10th International Technical Meeting of the Satellite Division of the Institute of Navigation, ION GPS-97*, Kansas City, Missouri, 16-19 September, 531-540.

SNAP (2001) The SNAP group website: www.gmat.unsw.edu.au/snap/staff/ chalermchon_satirapod.htm

Spilker Jr., J.J. (1978) GPS signal structure and performance characteristics, *Navigation*, Journal of The (U.S.) Institute of Navigation, 25(2), 121-146.

Spilker, Jr., J.J. (1996a) Tropospheric effects on GPS, In: Parkinson, B.W. et al. (eds.), *Global Positioning System: Theory and Applications*, Progress in Astronautics & Aeronautics, 163, 517-546.

Spilker, Jr., J.J. (1996b) GPS signal structure and theoretical performance, In: Parkinson, B.W. et al. (eds.), *Global Positioning System: Theory and Applications*, Progress in Astronautics & Aeronautics, 163, 57-119.

Strang, G., and Borre, K. (1997) *Linear Algebra, Geodesy, and GPS*, Wellesley-Cambridge Press, Wellesley, Mass., 624pp.

Talbot, N. (1988) Optimal weighting of GPS carrier phase observations based on the signal-to-noise ratio, *International Symposium on Global Positioning Systems*, Brisbane, Australia, October, 4.1-4.17.

Talbot, N.C. (1993) Centimetre in the field, a user's perspective of real-time kinematic positioning in a production environment, *6th International Technical Meeting of the Satellite Division of the Institute of Navigation, ION GPS-93*, Salt Lake City, Utah, 22-24 September, 1049-1057.

Teunissen, P.J.G. (1997) On the sensitivity of the location, size and shape of the GPS ambiguity search space to certain changes in the stochastic model, *Journal of Geodesy*, 71, 541-551.

Teunissen, P.J.G. (1998) Quality Control and GPS, In: Kleusberg, A. and Teunissen, P.J.G. (eds), *GPS for Geodesy* (2nd edition), Springer-Verlag, Berlin Heidelberg New York, 271-318.

Teunissen, P.J.G. and Kleusberg, A. (1998) *GPS for Geodesy*, Springer-Verlag, Berlin Heidelberg New York, 650pp.

Tiberius, C.C.J.M. and De Jonge, P.J. (1995) Fast positioning using the LAMBDA method, *4th International Conference on Differential Satellite Navigation Systems,* Bergen, Norway, 24-28 April, Paper No. 30.

Tiberius, C.C.J.M. and Kenselaar, F. (2000) Estimation of the stochastic model for GPS code and phase observables, *Survey Review*, 35, 441-454.

Tralli , D. and Lichten, S. (1990) Stochastic estimation of tropospheric path delays in Global Positioning System geodetic measurements, *Bulletin Geodesique*, 64, 127-159.

Vanicek, P., Beutler, G., Kleusberg, A., Langley, R.B., Santerre, R. and Wells, D.E. (1985) *DIPOP: Differential Positioning Program Package for the Global Positioning System*, Technical Report No. 115, Department of Surveying Engineering, University of New Brunswick, Canada.

Wang, J. (1998) Stochastic assessment of the GPS measurements for precise positioning, *11ᵗʰ International Technical Meeting of the Satellite Division of the Institute of Navigation, ION GPS-98*, 15-18 September, Nashville, Tennessee, 81-89.

Wang, J. (1999) *Modelling and Quality Control for Precise GPS and GLONASS Satellite Positioning*, Ph.D. thesis, School of Spatial Sciences, Curtin University of Technology, Perth, Australia, 171pp.

Wang, J, Stewart, M.P. and Tsakiri, M. (1998a) Stochastic modelling for static GPS baseline data processing, *Journal of Surveying Engineering*, 121(4), 171-181.

Wang, J., Stewart, M.P. and Tsakiri, M. (1998b) A discrimination test procedure for ambiguity resolution on-the-fly, *Journal of Geodesy*, 72, 644-653.

Wang, J., Satirapod, C., and Rizos, C. (2001) Stochastic assessment of GPS carrier phase measurements for precise static relative positioning, *Accepted for publication in Journal of Geodesy*.

Wells, D.E., Beck, N., Delikaraohlou, D., Kleusberg, A., Krakiwsky, E.J., Lachapelle, J., Langley, R.B., Nakiboglu, M., Schwarz, K.P., Tranquilla, J.M. and Venicek, P. (1987) *Guide to GPS Positioning*, 2ⁿᵈ edition, Canadian GPS Associates, Fredericton, New Brunswick, Canada, 503pp.

Wickerhauser, M. (1994) *Adapted Wavelet Analysis from Theory to Software*, AK Peters Ltd., Wellesley, Massachusetts, 486pp.

Williams J. Hughes Technical Center (2001) *Global Positioning System (GPS) Standard Posistioning Service (SPS) Performance Analysis Report*, Report No. 32 (submitted to Federal Aviation Administration), January, 47pp.

Wooden, W.H. (1985) Navstar Global Positioning System: 1985, *First International Symposium on Precise Positioning with the Global Positioning System*, Rockville, Maryland, 15-19 April, 1, 23-32.

Zumberge, J.F. (1999) Automated GPS data analysis service, *GPS Solutions*, 2(3), 76-78.

Zumberge, J.F., Heflin, M.B., Jefferson, D.C., Watkins, M.M. and Webb, F.H. (1997) Precise point positioning for the efficient and robust analysis of GPS data from large networks, *Journal of Geophysical Research*, 102(B3), 5005-5017.

Define r as the number of double-differenced measurement at epoch i, the accompanying matrices are:

$$T_{1i} = \begin{bmatrix} 1 & 0 & . & 0 \\ 0 & 0 & . & 0 \\ . & . & . & . \\ 0 & 0 & . & 0 \end{bmatrix}, \quad T_{2i} = \begin{bmatrix} 0 & 0 & . & 0 \\ 0 & 1 & . & 0 \\ . & . & . & . \\ 0 & 0 & . & 0 \end{bmatrix}, \dots\dots\dots, \quad T_{ri} = \begin{bmatrix} 0 & 0 & . & 0 \\ 0 & 0 & . & 0 \\ . & . & . & . \\ 0 & 0 & . & 1 \end{bmatrix}$$

$$T_{(r+1)i} = \begin{bmatrix} 0 & 1 & 0 & . & . & 0 & 0 \\ 1 & 0 & 0 & . & . & 0 & 0 \\ 0 & 0 & 0 & . & . & 0 & 0 \\ . & . & . & . & . & . & . \\ 0 & 0 & 0 & . & . & 0 & 0 \\ 0 & 0 & 0 & . & . & 0 & 0 \end{bmatrix}, \quad T_{(r+2)i} = \begin{bmatrix} 0 & 0 & 1 & . & . & 0 & 0 \\ 0 & 0 & 0 & . & . & 0 & 0 \\ 1 & 0 & 0 & . & . & 0 & 0 \\ . & . & . & . & . & . & . \\ 0 & 0 & 0 & . & . & 0 & 0 \\ 0 & 0 & 0 & . & . & 0 & 0 \end{bmatrix}, \quad T_{ki} = \begin{bmatrix} 0 & 0 & 0 & . & . & 0 & 0 \\ 0 & 0 & 0 & . & . & 0 & 0 \\ 0 & 0 & 0 & . & . & 0 & 0 \\ . & . & . & . & . & . & . \\ 0 & 0 & 0 & . & . & 0 & 1 \\ 0 & 0 & 0 & . & . & 1 & 0 \end{bmatrix}$$

where $k = r(r+1)/2$ is the number of unknown variance and covariance components. For a session solution with m epochs of data, the covariance matrix of all measurements is

$$C = \sum_{j=1}^{k} \theta_j T_j$$

where $T_j = \text{diag}(T_{ji})$, $i = 1,2,\dots,m$ and $j = 1,2,\dots,k$

VITA

Biodata

Full name: Chalermchon Satirapod

Gender: Male

Date of birth: August 12, 1973

Nationality: Thai

Marital status: Single

Religion: Buddhism

Work address: Department of Survey Engineering

                          Faculty of Engineering

                          Chulalongkorn University

                          Phyathai Road, Bangkok, Thailand 10330

University attended and degrees obtained:

1998-present: Ph.D Candidate

                          School of Surveying and Spatial Information Systems

                          (formerly School of Geomatic Engineering)

                          The University of New South Wales

                          Sydney, Australia (on study leave)

1994-1997:   Master of Engineering (Surveying)

                          Department of Survey Engineering

                          Chulalongkorn University, Bangkok, Thailand

1990-1994:   Bachelor of Engineering (Surveying)

                          Department of Survey Engineering

                          Chulalongkorn University, Bangkok, Thailand

Awards and Prizes

1998-present: Scholarship from Chulalongkorn University, Bangkok, Thailand to undertake PhD. studies at the School of Geomatic Engineering, The University of New South Wales, Sydney, Australia.

2001: The best student paper at the 5th International Symposium on Satellite Navigation Technology & Applications, Canberra, Australia, 24-27 July.

2001: The best student prize from U.S. Institute of Navigation (ION) to present the paper at the 14th International Technical Meeting of the Satellite Division of the U.S. Institute of Navigation, Salt Lake City, Utah, 11-14 September.

Academic Contributions (1999-2001)

List of Publications

1. **Satirapod, C.**, Rizos, C. and Han, S. (1999) GPS single point positioning: An attractive alternative?, *4th International Symposium on Satellite Navigation Technology & Applications*, Brisbane, Australia, 20-23 July, paper 47.

2. Rizos, C., **Satirapod, C.**, Chen, H. and Han, S. (1999) GPS with multiple reference stations: surveying scenarios in metropolitan areas, *6th South East Asian Surveyors Congress*, Fremantle, Australia, 1-6 November, 37-49.

3. **Satirapod, C.**, Wong, K. and Rizos, C. (2000) A web-based automated GPS processing system, *2nd Trans Tasman Survey Congress*, Queenstown, New Zealand, 20-26 August, 131-140.

4. **Satirapod, C.** and Wang, J. (2000) Comparing the quality indicators of GPS carrier phase observations, *Geomatics Research Australasia*, 73, 75-92.

5. **Satirapod, C.**, Rizos, C. and Wang, J. (2000) GPS single point positioning with SA off: How accurate can we get?, *Survey Review*, 36(282), 255-262.

6. **Satirapod, C.**, Wang, J. and Rizos, C. (2001) A simplified MINQUE procedure for the estimation of variance-covariance components of GPS observables, *Submitted to Survey Review*.

7. Rizos, C. and **Satirapod, C.** (2001) GPS with SA off: How good is it?, *Measure & Map*, 12, 19-21.

8. Wang, J., **Satirapod, C.**, and Rizos, C. (2001) Stochastic assessment of GPS carrier phase measurements for precise static relative positioning, *Accepted for publication in Journal of Geodesy*.

9. **Satirapod, C.** (2001) Improving the accuracy of static GPS positioning with a new stochastic modelling procedure, *14th International Technical Meeting of the Satellite Division of the U.S. Inst. of Navigation*, Salt Lake City, Utah, 11-14 September.

10. **Satirapod, C.,** Wang, J. and Rizos, C. (2001) A new stochastic modelling procedure for precise static GPS positioning, *ZFV,* 126(6), 365-373.

11. **Satirapod, C.**, Ogaja, C., Wang, J. and Rizos, C. (2001) GPS analysis with the aid of wavelets, *5th International Symposium on Satellite Navigation Technology & Applications*, Canberra, Australia, 24-27 July, paper 39.

12. Rizos, C. and **Satirapod, C.** (2001) Differential GPS: How good is it now?, *Measure & Map*, 15, 28-30.

13. **Satirapod, C.**, Ogaja, C., Wang, J. and Rizos, C. (2001) An approach to GPS analysis incorporating wavelet decomposition, *Artificial Satellites*, 36(2), 27-35.

List of Presentations

1. **Satirapod, C.** (1998) GPS Single Point Positioning with post mission information, *presented at the 26th Annual Research Seminars*, School of Geomatic Engineering, The University of New South Wales, Sydney, Australia, 16-17 November.

2. **Satirapod, C.** (1999) Prospects for single point GPS positioning, *presented at the BHPE Seminars*, Wollongong, Australia, 25 June.

3. **Satirapod, C.** (1999) GPS single point positioning: An attractive alternative?, *presented at 4th International Symposium on Satellite Navigation Technology & Applications*, Brisbane, Australia, 20-23 July.

4. **Satirapod, C.** (1999) The effect of a new stochastic model on GPS epoch-by-epoch solutions, *presented at the 27th Annual Research Seminars*, School of Geomatic Engineering, The University of New South Wales, Sydney, Australia, 8-9 November.

5. **Satirapod, C.** (1999) A new stochastic model of GPS epoch-by-epoch solutions, *presented at GPS/GIS showcase*, Nanyang Technological University, Singapore, 19-20 November.

6. **Satirapod, C.** (1999) GPS with multiple reference stations: surveying scenarios in metropolitan areas, *presented at a special meeting of the Thai surveying and mapping society*, Chulalongkorn University, Bangkok, Thailand, 23 November.

7. **Satirapod, C.** (2000) A web-based automated GPS processing system, *presented at 2nd Trans Tasman Survey Congress*, Queenstown, New Zealand, 20-26 August.

8. **Satirapod, C.** (2000) Stochastic modelling in GPS data processing, *presented at the 28th Annual Research Seminars*, School of Geomatic Engineering, The University of New South Wales, Sydney, Australia, 20-21 November.

9. **Satirapod, C.** (2001) GPS on the Internet & recent trends in GPS, *presented at the 6th Special Lectures on Advances in Spatial Information Technology*, Chulalongkorn University, Bangkok, Thailand, 3 May.

10. **Satirapod, C.** (2001) GPS analysis with the aid of wavelets, *presented at the 5th International Symposium on Satellite Navigation Technology & Applications*, Canberra, Australia, 24-27 July.

11. **Satirapod, C.** (2001) Improving the accuracy of static GPS positioning with a new stochastic modelling procedure, *presented at the 14th International Technical Meeting of the Satellite Division of the U.S. Inst. of Navigation*, Salt Lake City, Utah, 11-14 September.